THESIS

IMPROVED FUNCTIONAL AND STRUCTURAL OUTCOMES IN POST-TRAUMATIC OSTEOARTHRITIS WITH IMMUNE LICENSED MESENCHYMAL STROMAL CELL THERAPY

Submitted by

Cody Plaisance

Department of Clinical Sciences

In partial fulfillment of the requirements

For the Degree of Master of Science

Colorado State University

Fort Collins, Colorado

Summer 2026

Master's Committee:

Advisor: Lynn Pezzanite
Co-Advisor: Steven Dow

Kelly Santangelo

Copyright by Cody Louis Plaisance 2026

All Rights Reserved

ABSTRACT

IMPROVED FUNCTIONAL AND STRUCTURAL OUTCOMES IN POST-TRAUMATIC OSTEOARTHRITIS WITH IMMUNE LICENSED MESENCHYMAL STROMAL CELL THERAPY

Osteoarthritis is a painful and debilitating condition, impacting 655 million people worldwide and 33 million individuals in the US, particularly those >65 years of age. When measured in years lived with disability, knee OA was the 11th largest contributor to disability of 291 diseases evaluated[1,2]. OA is also common in companion animal species; in horses for example, osteoarthritis (OA) represents one of the most common conditions treated by equine practitioners, estimated to affect up to 2/3 of Thoroughbred racehorses and 80% of horses over 15 years of age[3,4]. Despite this high prevalence, no approved pharmacological intervention, biological therapy, or procedure prevents or reverses progressive destruction of the degenerative joint. Intra-articular administration of mesenchymal stromal cells (MSC) has demonstrated anti-inflammatory and chondroprotective activity in both preclinical models and in randomized clinical trials in patients with osteoarthritis (OA). Nonetheless, precedent from MSC studies in non-OA models suggests that the overall anti-inflammatory effectiveness of MSC can be improved by prior immune activation through cytokines or innate immune pathways. Therefore, in these studies, we determined whether activation of MSC by two different innate immune pathways (Toll-like receptor 3 (TLR3) pathway or Stimulator of Interferon Genes (STING) pathway) could improve their effectiveness for intra-articular treatment of OA, using a murine destabilization of the medial meniscus (DMM) model. Outcome parameters included voluntary

gait activity, joint histology and RNA transcriptomic analyses of synovial tissues. We found that activation of MSC via either of the two innate immune pathways improved functional voluntary movement outcomes compared to treatment with non-activated MSC. Moreover, cartilage integrity, including cartilage preservation, was significantly improved in mice receiving activated MSC, with greater benefits observed in animals treated with STING pathway-activated MSC compared to animals treated with non-activated MSC alone. Transcriptomic analysis of joint tissues revealed that treatment with activated MSC upregulated pathways associated with tissue remodeling, angiogenesis, and wound healing compared to tissues from animals treated with non-activated MSC. Importantly, the transcriptomic analysis also revealed important differences in pathways activated by TLR3 activation and STING activation. These findings indicate therefore that innate immune activation of MSC prior to intra-articular delivery for treatment of OA can significantly improve functional gait activity and chondroprotective effects compared to non-activated MSC and suggest that both strategies could be evaluated clinically.

ACKNOWLEDGMENTS

First, I would like to thank my graduate committee and advisors: Dr. Lynn Pezzanite, Dr. Steven Dow, and Dr. Kelly Santangelo for believing in me, taking a chance with me, and allowing me the opportunity to develop and become my true self. Their expertise and guidance helped flourish the professional confidence and abilities needed to begin my rigorous scientific research journey. Dr. Pezzanite – thank you so much for all of the support and guidance over the last few years in your lab. It has truly been such a wonderful experience and an honor to be a part of your research and surgical team as a new PI. Your lessons and assistance in the lab, surgeries, writing, public speaking, conferences, and more became the critical foundation that I will be building upon for the rest of my career. Dr. Dow – thank you for your trove of knowledge and expertise that has allowed for all of this to be possible. Dr. Santangelo – thank you for your career development expertise, as the quality of our conversations truly got to the core of what I want out of a career, and in life, in a way that made me think much deeper on these topics than I ever have before.

Importantly – I would also like to thank members of my research team, Renata Impastato, Jacob Singer, Peter Linde, and Isabella Sabino for the continued help, education, and support throughout these years with the Pezzanite and Dow labs. Renata – thank you for teaching me how to be a member of a lab and for all of your animal expertise over the last few years. Jacob & Peter – thank you for sitting down with me and teaching me cell culture and other lab techniques for the first time. It was/is great to be directly taught by such talented and knowledgeable students.

My parents, Laura & Jeffrey Plaisance, my brother, Jared Plaisance, and my grandparents, Judy & Richard Holmes, all deserve endless thanks and appreciation for their continued unconditional love and support that has nurtured me since my formative years. My parents and grandparents – I am forever grateful for the hard work and sacrifices you have all made so that I can be here writing this today.

Additionally, thank you to my friends Cameron Quelle, Cody Quelle, Jonathan & Haylie McLain, Chase Lane, and Lauren Hazel for their love, loyalty, and support in life. It was not easy, and I could not have done this without you all. Also, for all the late nights talking about the universe and the natural world. They say you are a combination of the people closest to you, and I could not think of better people for that to be from. Cameron Quelle – thank you for joining me on this journey by taking a sizeable risk with dropping everything and moving to Colorado in hopes of starting our career as scientists from the very bottom.

Lastly, this career got its start thanks to the Colorado State University Post-Baccalaureate Research Education Program (PREP) committee for accepting me into the pilot program here at CSU. That acceptance was everything I could have possibly hoped for, and more, to allow me to develop the skills, abilities, and confidence to pursue graduate school and a career as a research scientist. I cannot thank you all enough, especially Dr. John Gilbert, Dr. Mark Zabel, and Dr. Vanessa Selwyn for managing and orchestrating the program.

I gratefully acknowledge the Colorado State University Department of Clinical Sciences and the Graduate Department for acceptance into the program; as well as the Graduate Research Scholarship Award, PREP, NIH, and the Pezzanite/Dow lab for their financial support of this work.

TABLE OF CONTENTS

CHAPTER 1: Introduction and Literature Review of Mesenchymal Stromal Cell Usage in Osteoarthritis

1.1 Summary

Mesenchymal stromal cells (MSCs) are multipotent, stem-like, cells that may be derived from a variety of tissues and inherently possess the potential to differentiate into mesodermal lineages, including chondrocytes, osteoblasts, and adipocytes. These cells garnered attention due to their high abundance, ease of access, and limited spontaneous differentiation. Additionally, MSCs possess an expansive repertoire of secretion factors with an intrinsic range of immunomodulatory functions. These immunomodulatory properties of MSCs are the primary focus of this review, with minimal focus on their proliferation and differentiation potential. After injection into joints or tissues, these cells will rapidly undergo apoptosis – indicating that the primary influence of MSCs is from their secretome and immunomodulatory effect on adjacent tissues, and not due to their proliferation or differentiation to replace resident tissue types. The secretome of MSCs includes various cytokines, chemokines, extracellular vesicles, and growth factors. This review will expand upon MSCs, their activation and subsequent secretion profile, and how these activated cells can be exploited to advance their usage in alleviating inflammatory conditions, such as osteoarthritis (OA) – as OA therapy critically needs advanced therapeutics that lack the risk of adverse side effects.

1.2 Historic usage of mesenchymal stromal cells

Discovered in 1976 by Dr. Alexander Friedenstein, these cells were recognized for their regenerative capacity and ability to differentiate into fibroblastic colonies (chondrocytes) – with subsequent studies revealing the potential to differentiate into adipocytes, myocytes, and osteocytes. Originally derived from bone marrow, it was soon discovered these cells reside in

and can be derived from various tissue types – with common sources including adipose tissue, bone marrow, and peripheral blood[5,6]. Aside from adipose tissue MSCs and bone marrow MSCs having a distinct origin within their respective tissues, the cellular source of MSCs in peripheral blood and other tissues is uncertain and remains a source of debate. The primary current suspected sources are few and include pericytes, which typically reside embedded in blood vessel membranes (inner most layer) and regulate blood flow and vascular stability – and perivascular adventitial cells, which are found external to the smooth muscle layer and embedded within the loose connective tissue of the adventitia (outer most layer) and contribute to vascular homeostasis and repair[5].

The first MSC clinical trials for humans reportedly occurred in 1995 and focused on demonstrating the safety and feasibility of *ex vivo* expansion followed by subsequent intravenous infusion as a potential treatment for graft-versus-hose-disease in patients receiving bone marrow transplants[7,8]. Since then, our understanding and usage of these enigmatic cells in regenerative medicine has increased exponentially. To date, various forms of MSC cellular therapy treatments have been investigated for hundreds of diseases across over 1500 studies. In the three decades since the first human MSC clinical trial – it was not until December 2024, that the FDA approved the first MSC cellular therapy for application in human patients. The drug, Ryoncil, is an allogeneic mesenchymal cell therapy intended for use in pediatric steroid-refractory acute graft-versus-host disease[9].

MSCs exert their influence on the wound repair process by enhancing the individual's immune response and directing the localized inflammatory microenvironments towards favorable healing conditions. However, an expansive literature review of MSC cellular therapy studies revealed mixed results in terms of efficacy regarding beneficial outcomes in osteoarthritis

treatment. Heterogeneity among these stromal cell populations has been proposed to be in part responsible for the inconsistent therapeutic outcomes observed with MSC cellular therapy[10]. MSCs are notoriously sensitive to external and internal stimuli and have the potential to present different phenotypes as a result of the environmental conditions to which they are exposed[11]. Improved standardization of MSC's culture conditions could more uniformly commit MSCs to a particular gene expression pathway, potentially improving their therapeutic efficacy, expanding their therapeutic potential, and advancing the field of MSC cellular therapy and regenerative medicine.

1.3 Rationale for the activation of specific MSC immune receptors in osteoarthritis

Pattern recognition receptors (PRRs) are essential immune receptors that bridge the innate immune system and adaptive immune system by recognizing endogenous damage associated molecular patterns (DAMPs) and exogenous pathogen associated molecular patterns (PAMPs)[12]. The binding of PRRs to their DAMP and PAMP ligands initiates downstream gene expression pathways that establish an appropriate immune response. The best-known subset of these PRRs includes the Toll-like receptor (TLR) group. These TLRs are transmembrane receptors responsible for detecting and initiating various immune responses against the wide range of potential microbial exposures[13]. Among mammals, there are a total of 13 different TLRs, each with their own respective functional immune outcomes in terms of activating immune responses. There is considerable TLR variability among different species; examples of this include the presence of 9 known functional TLRs in humans, 12 in rodents, and 10 in horses, sheep, dogs, and cats[14]. These 13 mammal-specific TLRs can be further classified into five groups by their functions and specific microbial ligands:

Table 1.1: Summary of all mammalian Toll-like receptors (TLRs).

Microbial Ligand / Location	Receptor	Presence
Viral nucleic acids / Endosome	TLR3, TLR7, TLR8, TLR9	All mammals
Bacterial lipopeptides / Plasma membrane	TLR1, TLR2, TLR6, TLR10	All mammals (TLR10 is non-functional in rodents)
Lipopolysaccharide (Gram-negative bacteria) / Plasma membrane	TLR4	All mammals
Bacterial flagellin / Plasma membrane	TLR5	All mammals
Protozoa & rRNA / Endosome	TLR11, TLR12, TLR13	Rodent specific

Importantly – MSCs express most of the TLRs respective to that species, and reside in most tissues, as both of their suspected cellular progenitor sources, pericytes and adventitial perivascular cells, are abundantly present wherever there are blood vessels[5]. Therefore, these cells act as important signaling cells due to their systemic presence and diverse secretome. However, as previously mentioned, a thorough literature review of MSC cellular therapy in a therapeutic clinical context, especially for orthopedic diseases, yields mixed results in terms of efficacy. A proposed reason for these mixed results is that the MSC injections utilized in these treatments are comprised of heterogeneous stromal cell populations instead of the desired homogenous populations. To address this problem - immune licensing, or 'activation', of MSCs via stimulation of specific immune receptors with their respective ligands has recently been proposed as a means to generate more homogenous MSC populations for usage in cellular therapy applications *in vivo*. Previous research from our lab has demonstrated enhanced immunomodulatory properties of MSCs stimulated via their endosomal Toll-like receptor 3 (TLR3) with the synthetic ligand analog, polyinosinic:polycytidylic acid (pI:C). Our lab has performed various *in vivo* animal models that directly support the usage of TLR3-MSCs as an

effective therapeutic option and began as a methodology to enhance the antimicrobial properties of MSCs[15–25]. For example, in a rodent model of chronic Staphylococcus aureus biofilm infections, the TLR3-pIC-MSCs was the sole treatment that significantly reduced the bacterial load compared to antibiotics and naïve MSCs, or a combination of antibiotics and naïve MSCs[16]. Additionally, in a clinical study evaluating chronic drug-resistant Staphylococcus pseudointermedius and Escherichia coli infections in dog – it was revealed that canine MSCs activated via TLR3-pIC produce and secrete antimicrobial peptides that synergize with common antibiotics and trigger rapid bactericidal activity[17]. Furthermore, in an equine model of multidrug resistant Staphylococcus aureus septic arthritis, intra-articular TLR-3 activated MSC therapy produced positive results to reduce joint inflammation, specifically neutrophilic infiltration – indicating progressive resolution of the infection and protection of the joint space with improved osteoarthritis histologic scoring[15,25].

The work described in this thesis expands upon these findings to further evaluate immune activated cellular therapy in the context of diseases other than chronic infections. Specifically, this work investigated the effectiveness of innate immune activation of MSC as a strategy to improve their effectiveness for treatment of musculoskeletal diseases such as osteoarthritis.

Additionally, the immunomodulatory properties of activated MSCs include the potential to create more robust healing outcomes when compared to non-activated MSCs. Our positive findings with TLR-3 agonist polyI:C activated cell therapy led to investigation of alternate agonists that activate interferon pathways more potently, including the cGAS-STimulator of Interferon Genes (STING) pathway. Since there are a limited number of unique TLRs among vertebrates, and an even smaller amount with shared MSC expression between different species, it is essential to probe other highly conserved immune receptors that may provide similar

beneficial therapeutic outcomes[26,27]. Therefore, the STING-2'3'-cGAMP pathway was selected as a candidate due to its powerful anti-tumorigenic properties that induce apoptosis or senescence in damaged cells via various mechanisms, such as the release of type I interferons and modulation of resident immune cell behavior[28]. The inclusion of the STING pathway agonist, 2'3'-cGAMP, in cellular therapy expands the functional receptor repertoire while simultaneously increasing our understanding of how to most effectively utilize activated MSC therapy and maximize patient therapeutic outcomes.

The overarching functional outcome of these activated MSCs is not to differentiate directly into the damaged tissue types, but to direct the immune system through secreted factors to a pro-regenerative state. One method in which the immunomodulatory MSCs are hypothesized to achieve this is through secreted factors that, while over-simplified, induce a phenotypical transition of macrophages from the pro-inflammatory phenotype (M1) to the anti-inflammatory phenotype (M2)[29]. Some notable examples of these macrophage polarizing cytokines include interleukin-6 (IL-6), IL-10, IL-13, and indoleamine 2,3-dioxygenase (IDO).While M1 directed inflammation is essential to initiate and maintain the early wound immune response – excessive, prolonged, inflammation has deleterious effects on local tissues and reduces overall repair quality. To resolve this inflammatory cycle, the M2 macrophages modulate the wound repair process via secretion of anti-inflammatory cytokines and by enhancing extracellular matrix (ECM) deposition, cell migration, cell proliferation and differentiation, angiogenesis, and efferocytosis[30]. Aside from macrophage polarization – these activated MSCs also exert their influence via secretion of various growth factors and extracellular vesicles/exosomes, supportive organelle transfer, and modulate the behavior of other immune cells such as T cells, dendritic cells, and monocytes[31–33].

An example of this behavior modulation is the effect of TLR3-MSCs to promote the generation of regulatory T (Treg) cells and suppress other types of T cells, such as cytotoxic T cells (CD8+ T cells) or the various inflammatory subsets of T helper cells (CD4+ T cells). This increase in Treg cell count can directly enhance immune homeostasis and wound repair regulation *in vivo*[34]. Several days following injury, the localized infiltration of CD4+/CD8+ T cells begins and initiates the pro-inflammatory environment necessary for the initiation of wound repair mechanisms. However, while necessary for wound repair – dysregulation of these pro-inflammatory mechanisms is often responsible for chronic inflammation that results in comparatively worse healing outcomes. Interestingly, MSCs suppress this chronic inflammatory response with a similar mechanism that many cancers and tumors use to evade the immune system, and that is by expressing PD-L1, which binds to T-cell PD1 receptors to inhibit their activation and differentiation[35,36].

The selection of TLR3-pIC was initially based on results of prior studies involving the screening of different MSC immune receptor agonists and their subsequent antimicrobial properties – as TLR3 is a pattern recognition receptor (PRR) responsible for detecting endosomal double-stranded RNA, which is a pathogen associated molecular pattern (PAMP) indicating the presence of certain viruses[19,29,37]. For comparison – the cGAS-STING-2’3’-cGAMP receptor is specialized in detecting cytosolic DNA, which is DNA that accumulates in the cytosol due to microbial infection or cellular damage. Upon binding with the appropriate ligand – the downstream expression pathway of cGAS-STING-2’3’-cGAMP activation shares striking similarities, but also important differences, with the TLR3-pIC activation expression pathway. The notable differences include the inclusion of signal transducer and activator of transcription-1, 2, 6 (STAT-1,2,6), Janus activated kinase-1 (JAK1), and tyrosine kinase (TYK) – which

further enhances the stimulation of the desired interferon genes. The activation of both TLR3-pIC and STING-2'3'-cGAMP induces significant upregulation of various immunomodulatory cytokines, which notably includes the type I interferons: IFN-α, IFN-β, IFN-κ[38]. As essential inflammatory mediators, these type I interferon cytokines are secreted by nearly all nucleated cells, including immune cells (except for IFN-a) and sensory neurons following tissue injury or infection[39–44] – which has demonstrated the potential to be both anti- or pro-inflammatory, and/or antinociceptive, depending on the disease processes[40,44].

Figure 1: Schematic overview of the cGAS-STING and TLR3 expression pathways.

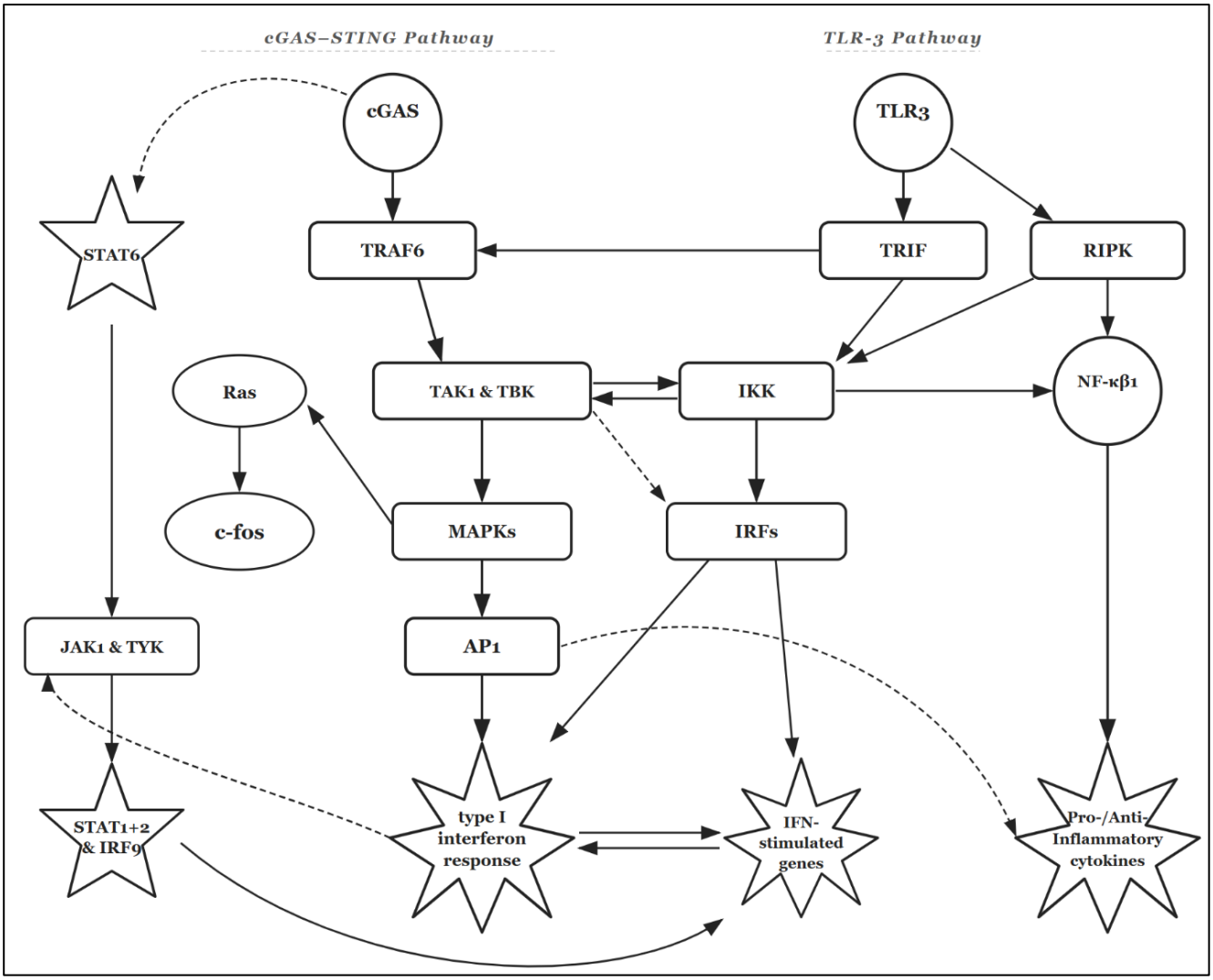

This paradoxical behavior for type I interferons (this is mainly attributed to IFN-b) can be attributed to the context, cell type, and duration of signaling. These type I interferon cytokines are more pro-inflammatory during acute early infections, and are more anti-inflammatory during chronic sustained signaling, such as chronic infections or during therapeutic usage. In addition to these type I interferons, MSCs possess an impressive repertoire of secretion factors that enhance the wound repair process via different mechanisms. These additional secretion factors include cytokines/chemokines, growth factors, extracellular matrix remodeling enzymes, extracellular vesicles, and microRNAs. These secreted cytokines notably include IL-6, IL-10, tumor necrosis factor (TNF), and monocyte chemoattractant protein-1 (MCP-1). These additional secretion factors have the potential to enhance cell survival and directly regulate the phenotype of endogenous chondrocytes and their ECM production[32].

Considering the multiple MSC tissue sources, receptors, dosing strategies, and routes of administration – the following literature review will discuss published reports of MSC usage from *in vivo* cell therapy models in the context of osteoarthritis; specifically, their efficiency within clinical settings and conclude with a comparative analysis of current treatment models involved in MSC wound repair augmentation. Aside from surgical interventions, the current therapeutics that are comparatively relevant to MSC cellular therapy are injections involving one or more of the following: platelet rich plasma (PRP), corticosteroids, hyaluronic acid, bone marrow concentrate (BMAC), and platelet lysate.

To begin the review, it is important to understand the TLR framework among various species. Among vertebrates, there are 15 unique Toll-like receptors, with mammals possessing 13 of these 15 TLRs. However, extensive research into these receptors has revealed that TLR2-4 are the most functionally relevant regarding immunomodulation and enhancing wound repair

outcomes. The other TLRs are not significantly utilized – either due to their niche and limited applications, lack of intraspecies conservation, potential to exacerbate the treated condition(s), or due to a critical lack of functional information about those TLRs. To begin – a literature search with Pubmed and ClinicalTrials.gov was performed and included a mixture of the search terms 'osteoarthritis', 'intraarticular', 'TLR3', 'polyinosinic:polycytidylic acid', 'cGAS-STING', 'STING', 'MSC', 'cell therapy', 'treatment', 'therapy', 'stifle', 'knee', 'meniscus', 'human', 'equine', 'ovine', and 'canine' with no date restrictions on search queries.

1.4 Review of MSC cellular therapy usage in osteoarthritis

Skeletal muscle tissue and the avascular connective tissues, such as cartilage, tendons, and ligaments possess low regenerative potential naturally – however, this repair potential can be augmented with targeted MSC cellular therapy, which has been the subject or prior investigation in multiple models. Critical aspects of MSC cellular therapy to consider include ease of access to tissue source, proliferative capabilities, secretome profile, migratory potential, cost, practicality, and viability. Regarding functionality, bone marrow MSCs (bmMSCs) may possess superior osteogenic and chondrogenic capabilities – but are more challenging to exploit *in vivo* due to their lower abundance and poor ability to target damaged tissues; as these cells have been found to primarily return to the bone marrow or sequester in the lungs, spleen, and lymph nodes following injection[32,45–47]. While bone marrow derived MSCs are commonly utilized in equine clinical practice, the pain associated with invasive bmMSC aspiration may limit their practical usage in human clinical settings. On the contrary – peripheral blood MSCs (pbMSCs) can be isolated with relative ease but are relatively less abundant compared to bmMSCs and far less abundant compared to adipose-derived MSCs (adMSCs), however, pbMSCs can be easily

expanded into the higher cellular quantities needed for therapeutic doses[48]. As such, adMSCs are an ideal MSC source due to their large quantities, ease of access, and enhanced immunomodulatory cytokine secretion – potentially being the superior option regarding practicality versus functionality in human models[49,50].

Table 1.2: Summary of primary MSC sources and their respective characteristics.

Attribute	Bone marrow	Adipose	Peripheral blood
Cell harvest yields	Low	Very high	Very low
Osteogenic & chondrogenic differentiation	Strong potential	Good, but frequently reported as lower	Comparable to bone marrow, especially if administered intraarticularly or IV
Proliferation	Moderate	High	Moderate to high
Homing potential	Limited	Low	High
Clinical practicality	Standard in bone/cartilage repair	Easily harvested and expandable	Convenient source but low yield, though culture expansion is feasible

This review takes these aspects into consideration while comparatively analyzing and discussing literature for tissue-derived MSC cellular therapy, with a focus on adMSC usage as a treatment for osteoarthritis. The goal is to utilize this activated MSC therapy in both human and veterinary patients. Considering the expansive literature in murine models and the intention to use this therapy in larger animal models – the focus of this review will primarily involve the usage of these cells in humans and animals larger than rodents and rabbits.

Cellular therapy with mesenchymal stromal cells has exponentially increased over the last few decades – with little increase in terms of clinical usage. This is important to address as current treatment and management options currently include one or more of the following: PRP, BMAC, platelet lysate, systemic injectables (such as pentosan polysulfate sodium, polysulfated

glycosaminoglycans, and hyaluronate sodium), intra-articular injectables (such as corticosteroids, hyaluronic acid, and polyacrylamide hydrogels), or symptom modifiers such as painkillers or over the counter non-steroidal anti-inflammatory drugs (NSAIDs).

Clinical osteoarthritis studies using human patients **(Table 1.3) –** Clinical reports involving investigations of MSC therapy for OA in human patients revealed that the vast majority involved the knee, including a few studies on hip OA and no available studies on hand or spine arthritis at the time of this writing. This was noteworthy considering that the global prevalence of OA diagnosed cases primarily involves the knee (60%), hand/wrist (~25%), and hip (~5%)[51].

Table 1.3: Summary of human *in vivo* clinical studies investigating adipose derived mesenchymal stromal cells for human knee osteoarthritis.

Table 1.3a: Summary of study type, source of adipose derived MSCs, sample size, sex, controls/placebo, study duration, age, and body mass index (BMI) in the human *in vivo* clinical studies investigating adipose derived mesenchymal stromal cells for human knee osteoarthritis.

Table 1.3b: Summary of dose, optimal dosing if more than one dose was administered as a treatment, number of injections, scoring assessments, and rates of adverse events in the human *in vivo* clinical studies investigating adipose derived mesenchymal stromal cells for human knee osteoarthritis.

Table 1.3a

Author	Study type	adipose MSCs	Sample size & sex	Control/Placebo	Study duration	Age (MSC vs Control) [subgroup]	BMI (MSC / Control) [subgroup]
Lee et al.	Treatment comparison study	Autologous	n=24, 18F+6M	Saline	6 months	62.2 ± 6.5 / 63.2 ± 4.2	25.3 ± 4.9 / 25.4 ± 3.0
Lu et al.	Treatment comparison study	Allogeneic	n=52, 46F+6M	HA/2xSham injection for MSCs	12 months	55.03 ± 9.19 / 59.64 ± 5.97	24.27 ± 3.04 / 24.26 ± 2.59
Kim et al.	Treatment comparison study	Autologous	n=60, 38F+22M	HA	12 months	63.0 ± 3.2 / 63.2 ± 3.8	26.4 ± 1.5 / 26.6 ± 1.5
Freitag et al.	Treatment comparison study	Autologous	n=30, 14F+16M	Sham injection	12 months	54.6 ± 6.3 [1] / 54.7 ± 10.2 [2] / 51.5 ± 6.1	31.6 ± 5.9 [1] / 30.4 ± 5.6 [2] / 25.2 ± 3.4
Koh and Choi	Treatment comparison study	Autologous	n=50, 34F+16M	PRP (no stem cells)	12 months	54.2 ± 9.3 / 54.4 ± 11.3	NA
Kuah et al.	Dose comparison study	Allogeneic	n=20, 8F+12M	CCM and cryopreservative	12 months	50.8 ± 7.29 [3.9M] / 55.0 ± 5.15 [6.7M] / 55.0 ± 10.42	27.7 ± 2.05 [3.9M] / 26.8 ± 2.98 [6.7M] / 25.5 ± 2.84
Lu et al.	Dose comparison study	Allogeneic	n=22, 19F+3M	None	11 months	59.29 ± 4.14 [low] / 57.30 ± 7.84 [med] / 57.20 ± 5.61 [high]	27.77 ± 1.93 [low] / 26.69 ± 2.63 [med] / 24.51 ±2.49 [high]
Jo et al.	Dose comparison study	Autologous	n=18, 15F+3M	None	6 months	63 ± 8.6 [low] / 65 ± 6.6 [med] / 61 ± 6.2 [high]	26 ±1.0 [low] / 28 ± 2.1 [med] / 26 ± 2.1 [high]
Pers et al.	Dose comparison study	Autologous	n=18, 10F+8M	None	6 months	63.2 ± 4.1 [low] / 65.5 ± 8.1 [med] / 65.2 ± 2.3 [high]	28.8 ± 1.5 [low] / 26.96 ± 3.1 [med] / 27.1 ± 2.4 [high]
Song et al.	Dose comparison study	Autologous	n=18, 14F+4M	None	22 months	52.1 ± 11.6 [low] / 59.6 ± 10.2 [med] / 52.7 ± 8.7 [high]	25.6 ± 1.9 [low] / 23.7 ± 2.9 [med] / 24.1 ± 1.4 [high]
Spasovski et al.	Interventional treatment trial	Autologous	n=9, 6F+3M	None	18 months	63 ± 10.4 (all)	29.5 ± 3.97 (all)
			---	---	---	---	---
			n=321: 222F(69%) + 99M (31%)		mean = 11.7 mont	Pooled mean: 56.05 for MSCs, 58.87 else	Pooled mean: 26.66 for MSCs, 25.46 else
			214 are treatment groups				Healthy BMI = 18.5-24.9; so overall only slightly overweight

Table 1.3b

Author	Dose ($x10^6$)	Optimal dosing (if more than 1)	# of injections	SCORING ASSESSMENTS	Imaging	Rate of Adverse Events
Lee et al.	100	NA	1	W, KL, V, KO	MRI	No adverse events
Lu et al.	50	NA	HA(x4), MSCs(x2), control(x2)	W, KL, V	MRI	19/26 (73.1%) experienced minor adverse events
Kim et al.	7	NA	1	KL, V, TL, IK, EQ	MRI	2/60 (3.3%) (mild swelling)
Freitag et al.	100	NA (also no difference between 1 or 2 injections)	1 or 2	KL, W, N, KO, M	MRI, baseline x-ray	Mild transient adverse events
Koh and Choi	2	NA	1	KL, V, TL	None	1/50 (2%) (pain & swelling)
Kuah et al.	3.9 or 6.7	Higher dose	1	KL, W, V	MRI	20/20 (100%) (althralgia, effusion, stifness, upper respiratory infection)
Lu et al.	10 or 20 or 50	Lower dose	2	KL, W, V, S	MRI, worms	19/22 (86.4%) (pain & edema)
Jo et al.	10 or 50 or 100	Higher dose	1	KL, W, KS	MRI, x-ray, arthroscropy	No adverse events
Pers et al.	2 or 10 or 50	Lower dose	1	KL, W, KO, SA, P	MRI	15/18 (83.3%) (effusion, joint pain)
Song et al.	10 or 20 or 50	Higher dose	3	KL, W, S, N	MRI	16/18 (88.9%) (swelling, joint pain)
Spasovski et al.	5-10	No signifcant difference	1	W, TV, L, KS, H, M	MRI	No adverse events

Abbreviations: Western Ontario and McMaster Univerisities Arthritis Index (W/WOMAC); Visual Analog Scale (V/VAS); Knee Injury and Osteoarthritis Outcome Score (KO/KOOS); Kellgren-Lawrence (KL); Numeric Pain Rating Scale (N/NPRS); Tegner-Lysholm (TL); Short Form-36 (S); International Knee Documentation Committee (IK/IKDC); MRI Osteoarthritis score (M/MOAKS); Knee Society Clinical Rating System (KS/KSS); Short Arthritis Assessmemt Scale (SA/SAS); Patient Global Assessment (P/PGA); Numerical Pain Rating Scale (N/NRS-11); Hospital for Special Surgery Knee Score (H/HSS-KS); Body Mass Index (BMI); Magntic Resonance Observation of Cartilage Repair Tissue (M/MOCART); Magnetic Resonance Imaging (MRI); EuroQol Group – 5 dimensions (EQ/EQ-5D); Mesenchymal stromal cell (MSC); Hyualuronic Acid (HA); Platelet-Rich Plasma (PRP); Cell Culture Media (CCM); Whole-Organ Magnetic Resonance Imaging Score (WORMS)

Importantly, no serious adverse effects were reported for any of the MSC injections from any of the reviewed clinical trials – aside from swelling and pain around the injection and liposuction sites. This demonstrates the inherent safety of MSC therapy injections. Although autologous MHC-I matched MSCs are typically regarded as 'immune evasive' with minimal immunogenicity, the usage of allogeneic MSC cell therapy does theoretically carry increased risk of serious adverse events, at least with repeated injections[52]. However, the rate of adverse events may be attributed to a number of factors such as route of administration, dose, injection number, cell culture quality, and/or underlying patient conditions – as underlying medical conditions can augment systemic and local inflammation levels, which may compromise MSC quality and reduce their homing and therapeutic efficacy. Therefore, patient-specific levels of systemic and local inflammatory mediators may modulate the MSC's treatment response and secretome. The likelihood of these adverse reactions is greater when administering subsequent injections of allogeneic MHC-I, and sometimes MHC-II, mismatched MSCs – therefore repeated dosing is ideally performed only for autologous MSCs and MHC matched allogeneic MSCs, however studies have demonstrated the inherent safety of allogeneic MSCs, which rarely cause significant side effects. The specific purpose of this literature review is to review and compare clinical studies involving human adipose-derived MSCs used for treatment in knee osteoarthritis. The

objective of this review is not to distinguish whether allogeneic or autologous cells are more beneficial; rather, it is to distinguish if adipose derived MSCs are an appropriate therapeutic for the attenuation of bothersome osteoarthritic symptoms. This literature search revealed 11 studies that fit within the desired parameters. Of those 11 studies, 8 of them utilized autologous adMSCs and the remaining 3 utilized allogeneic adMSCs. Directly comparing study outcomes is difficult due to the low abundance of controlled studies; however, general trends can still be observed among the groups.

The studies mentioned in Table 1.3 revealed promising results in terms of improving patient clinical outcomes. None of these studies utilized immune receptor activated MSCs prior to injection – using only minimally manipulated naïve MSCs in the treatment groups. While there were no reported severe adverse events from any of the reported studies, these MSC injections are overall yielding mixed results in terms of efficacy, especially regarding the ideal treatment dosage. Regarding structural improvement outcomes for the dose comparison studies, 2/5 of the studies reported the most significant improvements in cartilage quality with a high dose (>50 million cells)[53,54], 2/5 for a low dose (<10 million cells)[55,56], and 0/5 for a medium dose (10-50 million cells) – with the remaining study comparing the outcomes of two separate low doses, at 3.9 and 6.7 million cells[57]. These dosing outcomes are an accurate representation of the saying, “sometimes less is more”. While all the reviewed studies did in fact report significant improvements for the MSC treatment groups – this emphasizes the need for enhanced standardization of MSC preparation, and closer assessment of patient age, sex, weight, and disease conditions prior to usage as a therapeutic intervention.

The mean study duration among the studies was 11.7 months. This fits into the 6 to 12 months seemingly required for MSCs to begin significantly performing better than the

conventional therapies, such as intra-articular injections of hyaluronic acid (HA) and platelet rich plasma (PRP). Multiple randomized trials and meta-analyses report that while MSC treatments (with or without PRP) may not provide superior relief at ≤ 3 months compared to HA or PRP, they consistently demonstrated significantly better outcomes at 6 months and maintain durable benefit through 12+ months[58–60]. Generally, these conventional therapies present faster, short term relief, and trend downwards in efficacy around 6 to 12 months following injection when compared to MSCs, while the MSC treatment groups begin trending upwards, indicating a more lasting beneficial outcome for the MSC treatment groups. Additionally, the pooled mean age among the studies is 56.05 years for the MSC treatment groups, and 58.87 for the other groups, which are the HA, PRP, and placebo control groups. Body mass index (BMI) was reported in 10/11 studies (excluding Koh et al.) – with the pooled mean BMI among these studies being 26.66 for the MSC treatment groups, and 25.46 for the other groups. The recommended healthy BMI is 18.5-24.9, therefore the pooled mean BMI in this study indicates the patients were only slightly overweight, overall. Among the 11 studies, 321/337 (95%) patients completed their study and subsequent follow-up appointments. These 321 patients were comprised of 222 females (69%) and 99 males (31%), with 214 (67%) receiving MSC injections and 107 (33%) receiving either HA, PRP, or placebo. The treatments were generally well-received with minimal adverse events. The patients (16/337, 5%) that did not complete the study were due to a variety of causes. The adverse events related to treatment withdrawal include an iodophor allergy during liposuction, two separate cases of injection associated infection, and two separate cases of withdrawal due to a lack of noticeable benefits. The unrelated adverse events included two patients withdrawing for knee arthroplasty surgery, one for a vertebral fracture, and one for gallbladder carcinoma. Additionally, there were a considerable amount of mild transient events

such as effusion, swelling, and joint pain – which was readily resolved. Lastly, there were six withdrawals reported for unknown reasons.

Cartilage outcomes from human clinical knee osteoarthritis treatment trials **(Table 1.4)** **–** All of the studies mentioned in Table 1.4 analyzed and collected imaging data using magnetic resonance imaging (MRI). An analysis of cartilage outcomes can be found in Table 1.4. Overall – these studies reported significant improvements regarding function and/or pain for patients experiencing knee osteoarthritis. The controlled studies all reported significant improvements regarding pain and function by the end of the study protocols.

Table 1.4: Summary of cartilage outcomes in human clinical knee osteoarthritis trials.

Author	Adipose MSC Type	Dose (x 10^6)	Number Injections	Cartilage Assessment	Cartilage Findings	Notes
Lee *et al.*[61]	Autologous	100	1	MRI (WORMS scoring)	↓ degeneration in treated vs control	WORMS showed cartilage deterioration in controls but not in MSC group
Lu *et al.*[62]	Allogeneic	50	HA(x4), MSCs(x2), control(x2)	MRI + second-look arthroscopy + biopsy	↑ cartilage volume in high dose group	High dose: regeneration visible on MRI; biopsy showed hyaline-like repair
Kim *et al.*[63]	Autologous	7	1	Clinical outcome only (no cartilage-specific imaging)	Not reported	Study focused on comparing adMSCs to PRP and HA; not cartilage structure
Freitag *et al.*[64]	Autologous	100	1 or 2	Arthroscopy (ICRS cartilage grade)	↑ ICRS cartilage quality (mostly Grade I/II)	Clear arthroscopic signs of regeneration post-MSC treatment
Koh and Choi [65]	Autologous	2	1	MRI (volumetrics)	No cartilage volume ↑	Structural changes were not observed despite clinical benefits
Kuah *et al.*[57]	Allogeneic	3.9 or 6.7	1	MRI (quantitative)	No significant ↓ in cartilage volume vs Significant ↓ for HA	Short follow-up (6 mo) may limit detection of structural changes
Lu *et al.*[55]	Allogeneic	10 or 20 or 50	2	MRI (cartilage segmentation)	↑ cartilage volume in adMSC vs HA	High dose (50 million) showed better cartilage thickness
Jo *et al.*[53]	Autologous	10 or 50 or 100	1	MRI (volumetrics)	Trend toward ↑ cartilage volume	Small phase I pilot, underpowered for structural outcomes
Pers *et al.*[56]	Autologous	2 or 10 or 50	1	Not assessed	N/A	Phase I study focused on safety; not imaging or cartilage change
Song *et al.*[54]	Autologous	10 or 20 or 50	3	MRI segmentation + 3D analysis	↑ cartilage volume in femur, patella, tibia	High dose group showed significant increase at 48–96 weeks
Spasovski *et al.*[66]	Autologous	5-10	1	MOCART score (MRI)	MOCART ↑ from 43 to 63 in 18 months	Indicates improved integration, repair, and surface continuity

Abbreviations: Magnetic Resonance Imaging (MRI); Whole-Organ Magnetic Resonance Imaging Score (WORMS); Adipose-Derived Mesenchymal Stromal Cells (adMSCs); Platelet-Rich Plasma (PRP); Hyaluronic Acid (HA); International Cartilage Research Society (ICRS); Magnetic Resonance Observation of Cartilage Repair Tissue (MOCART).

Pers *et al*. (2016) conducted a Phase I dose-escalation trial evaluating intra-articular injections of adMSCs in patients with severe knee OA[55]. The study found that all doses led to functional improvements in Western Ontario and McMaster Universities Arthritis Index (WOMAC), and Knee Injury and Osteoarthritis Outcome Score (KOOS) in 6 months, with the highest dose group also showing signs of cartilage repair with magnetic resonance imaging (MRI) using the Magnetic Resonance Observation of Cartilage Repair Tissue (MOCART) scoring system.

A phase I pilot study conducted by Lu *et al*. (2020) in which patients with bilateral knee osteoarthritis received intra-articular injections of adMPCs in one knee, and placebo in the other, found that adMPC-treated knees showed greater improvements in pain, function, and stiffness regarding WOMAC and Short Form-36 (SF-36) scores over 6 months when compared to the placebo-treated control knees[56]. This study found no significant improvements towards cartilage volume; however, they hypothesize that a type II error may have occurred due to low subject count.

A phase I/IIa, randomized, double-blind, placebo controlled clinical trial by Kuah *et al*. (2018) found that a single intra-articular injection of adMSCs resulted in significant improvements for pain and function, particularly at the highest tested dose (60 x 10^6 cells), in patients with knee OA[57]. The improvements were reflected in reductions in Visual Analog Scale (VAS) and WOMAC scores over 24 weeks when compared to the placebo; of which contained only cell culture medium and cryopreservative. This study found significant decreases for the HA

control group regarding lateral tibial cartilage volume when compared to no decreases in the MSC treatment (3.9 million cells) group.

A Phase I/II dose-escalation trial by Jo *et al*. (2014) evaluating intra-articular injections of adMSCs for knee OA and found that the high-dose group (100 million cells) showed the greatest improvements in pain, function (WOMAC), and cartilage volume on MRI over 6 months. Lower dose groups showed minimal change, suggesting a dose-dependent therapeutic effect[53].

A phase IIb randomized, double-blind, controlled clinical trial by Lee *et al*. (2019) found that a single injection of adMSCs significantly improved the patients' WOMAC score at 26 weeks; indicating functional and pain improvement outcomes. Although MRI analysis revealed no cartilage improvements, the treatment groups did not worsen while the control groups did[61].

In another phase IIb randomized, double-blind, active-controlled trial – Lu *et al*. (2019) demonstrated that intra-articular injection of adipose derived mesenchymal progenitor cells (adMPCs) significantly improved pain, stiffness, and function in patients with knee OA compared to hyaluronic acid (HA) over a 12-month period[62]. MRI evaluation also showed stabilization and/or improvements of cartilage defects, including regeneration of articular cartilage, in the adMPCs group when compared to the HA group. Additionally, the HA group observed an overall decrease in cartilage volume for the femur, tibia, and patella.

A randomized controlled trial by Freitag *et al*. (2019) evaluated the usage of adMSCs as a treatment for knee osteoarthritis. They evaluated and demonstrated the administration of adMSCs with two treatment groups consisting of either one or two injections with the same dose (100 million cells) and a control group consisting of conservative management[64]. For the two-injection treatment group, the second injections were administered at 6 months post-baseline. By the end of the 12-month study follow-up, radiological imaging revealed that 67% of the control

group had further loss of cartilage, which is quite significant when compared to both treatment groups (one injection = 30%, two injections = 11%). Additionally, further progression of osteophytic growth was significantly reduced only for the two-injection treatment group (11%) when compared to the one injection treatment group (50%) and control group (56%).

In a matched-pair cohort study, Kim *et al*. (2020) found that intra-articular injections of adMSCs provided significantly greater improvements in pain, function, and quality of life according to VAS, WOMAC, and EQ-5D (EuroQol Group – 5 Dimensions) scores when compared to HA or platelet-rich plasma (PRP) over a 12-month follow-up period[63]. However, this study also found that at one-year post-injection, there were no radiological significant differences between the treatment and control groups.

Koh and Choi (2012) reported that arthroscopic injection of adMSCs derived from the infrapatellar fat pad led to significant improvements in pain and function in patients with knee OA, as measured by International Knee Documentation Committee (IKDC) and Tegner scores over a 2-year period. Second-look arthroscopy at 12-18 months, postoperatively, showed improved cartilage appearance in the treatment group compared to the PRP (no stem cells) control group[65].

Song *et al*. (2018) conducted a pilot study involving repeated intra-articular injections of adMSCs for knee OA and found sustained improvements in pain, function (WOMAC and VAS scores), and quality of life (SF-36) over a 96-week follow-up period. MRI analysis indicated stabilization of cartilage defects, supporting potential long-term benefits of repeated adMSC treatment[54]. Additionally, a significant increase in bilateral knee cartilage volume was found in the 24-, 48-, and 72-week time points.

Finally – Spasovski *et al*. (2018) reported that a single intra-articular injection of adMSCs in patients with knee OA led to significant improvements in pain and function (VAS and KOOS scores) over a 12-month period. MRI evaluation also showed reduced cartilage defects and bone marrow lesions post-treatment[66]. Additionally, radiology revealed no continued improvements or degradation to the knee during the study follow-up, while the MOCART score assessment revealed significant restoration of cartilage within the joint space.

One of the puzzling aspects to consider when administering MSCs as a therapeutic is the dosage. Among the studies that investigated the usage of more than one dosage, there were glaring differences for which dosage had the most beneficial outcome. The dosages are commonly referred to as low dose (<10 million cells), moderate dose (10-50 million cells), and high dose (>50 million cells) per injection. Importantly, as Pers *et al.* reported in 2016, the response to treatment dosing may be closely linked to disease state[56]. The study noted an inverse dosing effect where the low dose group (2 million cells) experienced the greatest therapeutic outcomes. Being that the low dose group in this study reported the highest pain levels at baseline, it is likely that this inverse effect is due to these injected MSCs becoming increasingly polarized towards their immunomodulatory phenotype from the higher levels of pre-existing inflammatory cytokines. Interestingly, as Dell'Isola *et al.* noted in a system review, these chronic inflammatory phenotypes are seemingly responsible for only 12-22% of knee OA diagnoses[67]. However, as Jo *et al.* reported in 2014, when investigating articular cartilage lesions – the most significant improvements were a result of the high dose group (100 million cells), with milder improvements in the low (10 million cells) and moderate (50 million cells) dosing groups. Although this study had no control, it further supports the need to analyze the disease condition when determining the proper dosage for treatment, as beneficial therapeutic outcomes have been

seen with as few as 2 million cells and as many as 100 million cells in OA treatments – with most studies observing beneficial outcomes with doses greater than 40 million cells[32,53]. However, MSC immune priming can mitigate this by polarizing these cells into their enhanced immunomodulatory phenotype prior to injection, thus dampening the effects that the patient's pre-existing inflammatory condition has on the therapeutic behavior of these cells.

Clinical MSC osteoarthritis studies using animal patients **(Table 1.5) –** This section reviews clinical reports involving investigations of MSC therapy for OA in animal patients including canine, equine, and ovine. These 15 studies include eight canine models (n = 471), five equine models (n = 104), and two ovine models (n = 23).

Table 1.5: Summary of clinical OA studies using large animal models.

Table 1.5a: Summary of species, joint assessed, study type, MSC type, and sample size in the clinical OA studies using large animal models.

Table 1.5b: Summary of control and treatment groups, study duration, age, and weight in the clinical OA studies using large animal models.

Table 1.5a and 1.5b: Summary of clinical OA studies using large animal models.

Table 1.5a

Author	Species	Joint	Study Type	MSC Type	Sample Size (Sex)
Armitage et al.	Canine	Multiple	Retrospective clinical study	Autologous MSCs (with PRP, some IV/epidural)	245 (109F, 136M)
Harman et al.	Canine	Multiple	Randomized, placebo-controlled trial	Allogeneic adMSCs	74 (46F, 36M)
Barrachina et al.	Equine (pony)	Radiocarpal	Controlled experimental study	Allogeneic bmMSCs (naïve vs pro-inflammatory primed)	18
Ferris et al.	Equine	Stifle (femorotibial)	Prospective case series	Autologous bmMSCs	33
Joswig et al.	Equine	Metacarpophalangeal	Controlled experimental study	bmMSCs (autologous vs allogeneic)	18F
Kearney et al.	Equine	Radiocarpal	Controlled experimental study	Allogeneic bmMSCs	8 (6F, 2M)
Kriston-Pál et al.	Canine	Multiple	Clinical long-term follow-up	Allogeneic adMSCs	58
Lei et al.	Ovine	Knee	Controlled experimental study	Human adMSCs (xenogeneic)	11M
Yun et al.	Canine	Knee	Controlled OA model	Allogeneic adMSCs	24
Maki et al.	Canine	Hip	Randomized, double-blind, placebo-controlled pilot	Allogeneic adMSCs	20
Luque et al.	Equine	Carpus & fetlock	Prospective, single-blinded, randomized	Umbilical cord blood	27(10F, 17M)
Delling et al.	Ovine	Knee	Prospective, controlled, longitudinal preclinical	Autologous bmMSCs	12F
Muir et al.	Canine	Stifle	Prospective, controlled, exploratory	Autologous bmMSCs	12 (7F, 5M)
Beerts et al.	Canine	Stifle	Prospective, controlled, preclinical + translational	Equine pbMSCs (xenogeneic)	32 (16F, 16M)
Li X et al.	Canine	Stifle	Prospective, controlled preclinical translational study	Allogeneic adMSCs	6F

Table 1.5b

Author	Control & Treatment Groups	Study Duration	Age	Weight (lbs)
Armitage et al.	No control group; clinical follow-up post-MSC + PRP	2 years	Median: 6.3 (range: 6mo - 14 years)	Not reported
Harman et al.	Saline control(n=36) vs Single MSC injection(n=38)	60 ± 4 days	Treated, mean: 7.98 ± 3.56y / Control, mean: 8.59 ± 3.53y	Treated, mean: 69.29 ± 23.70 / Control, mean: 64.79 ± 26.08
Barrachina et al.	LRS control(n=4), MSC-naïve(n=7), MSC-primed(n=7)	6 months	Not reported (but standardized)	220 - 365
Ferris et al.	No control; horses received MSCs post-operatively	Mean follow-up 24 months	Median: 5 (no range available)	Not reported
Joswig et al.	Autologous (n=6), Autologous + FBS(n=6), Allogeneic (n=6)	Mean follow-up 24 months	Median: 11.5 (range: 3-17)	Not reported
Kearney et al.	MSC secretome vs medium (Phase 1); MSCs vs secretome (Phase 2)	7 days	Mean: 14.6 ± 2.4	816.59 ± 60.84
Kriston-Pál et al.	No control; MSC-treated only	4–5 years	Variable due to long term nature of study	Not reported
Lei et al.	Saline vs hAD-MSC	21 weeks post-surgery	15-18 months	165.35 ± 22.05
Yun et al.	MSC, PRP, PBS	90 days	2-3 years	16.98 ± 2.43
Maki et al.	Saline (n=4), MSC 5M (n=5), 25M (n=6), 50M (n=5)	90 days	10.03 ± 1.74 years	28.005 ± 4.293 kg
Luque et al.	eCB-MSCs vs HA efficacy comparison	18 weeks	10.81 ± 1.75 years	Not reported
Delling et al.	Colateral knee as negative control	12 weeks	24-30mo	Mean: 166
Muir et al.	No control; MSC-treated only	8 weeks	4.93 ± 0.7 years (range: 1.6-9.6)	92.15 ± 12.13 (range: 36.16-176.37)
Beerts et al.	Saline vs ePB-MSCs	42 ± 4 days	16-19mo	16.09 - 32.19
Li X et al.	PBS vs adMSCs	6 weeks	8mo	Not reported

Table 1.5c: Summary of dose, injections, and scoring in the clinical OA studies using large animal models.

Author	Dose (x 10^6)	Number & Timing of Injections	Scoring Assessments
Armitage et al.	>2.5(lesions), >10(LSD), 1 per kg(IV)	1–2 injections; second at 12 weeks if needed	Stance/gait analysis, ROM, pressure, HRQL, pain/QoL scores
Harman et al.	12	Single injection	CSOM (owners), vet pain, vet/owner global scores
Barrachina et al.	10	2 injections, 4 months apart, in both RC joints	Clinical signs, synovial cytology, gross anatomy, histology, gene expression
Ferris et al.	13.2 ± 5.6	Single injection post-surgery	Return to work (owner/trainer reports)
Joswig et al.	10	2 injections at weeks 0 and 4	Pain on manipulation, synovial cytology
Kearney et al.	10	Single injection, 2 hrs post-LPS induction	Clinical scores, synovial biomarkers
Kriston-Pál et al.	12 ± 3.2	Single injection	Owner-reported lameness (4-5 years)
Lei et al.	100	2 injections at weeks 6 and 9, post-surgery	Histology, immunohistochemistry
Yun et al.	10	Multiple injections (1x week/month)	Histology, inflammatory markers
Maki et al.	5, 25, or 50	Single injection	Lameness score, IL-10 levels
Luque et al.	10 or 20	Single injection	Joint effusion (0-4), lameness (0-5)
Delling et al.	10	Single injection	Movement, swelling, heat, general appearance/behavior, vital signs, histology
Muir et al.	2 or 5 per kg	Single injection	Radiographs, VAS, synovitis, osteophytes
Beerts et al.	0.06 or 0.3 or 1.5	Single injection	Histology, gross pathology, gait data
Li X et al.	10	3 injections at weeks 2, 4, and 6	Lameness, stifle thickness and width

Table 1.5d: Summary of key findings in the clinical OA studies using large animal models.

Author	Key Findings
Armitage et al.	Significant and sustained improvements in objective and subjective outcomes. Imaging showed resolution of tendinopathies.
Harman et al.	Statistically significant improvements in pain and function in MSC group vs placebo control.
Barrachina et al.	MSC-treated joints had reduced inflammation and better gross cartilage appearance; primed MSCs (TNFa & IFNg) showed enhanced anti-inflammatory gene expression.
Ferris et al.	75% of horses with meniscal injury returned to work; improved outcome vs historical controls.
Joswig et al.	Adverse joint reaction after 2nd allogeneic injection; autologous was better tolerated.
Kearney et al.	MSC secretome demonstrated similar outcomes to whole MSC therapy.
Kriston-Pál et al.	83% of dogs improved or maintained improvement; safe long-term outcome with minimal adverse events.
Lei et al.	Human adMSCs improved cartilage thickness and repaired chondral defects in sheep KOA model.
Yun et al.	Multiple adMSC injections reduced inflammation and repaired cartilage damage.
Maki et al.	All doses improved clinical lameness, some as early as 5 days.
Luque et al.	Return to exercise rates (89%) in the 10 million MSC group; (78%) in the 20 million MSC group; (56%) in the HA group.
Delling et al.	MSCs improved MRI scores, controls did not.
Muir et al.	Significant reduction in post-treatment synovial inflammatory cytokines when compared to pre-treatment.
Beerts et al.	Demonstrated efficacy and safety for xenogenic equine MSCs for treatment in canines.
Li X et al.	Demonstrated efficacy and safety for repeated allogenic MSC injections in reducing inflammatory expression.

Table 1.5e: Summary of adverse event rates and imaging in the clinical OA studies using large animal models.

Author	Rate of Adverse Events	Imaging
Armitage et al.	<1%	Radiographs, musculoskeletal ultrasound (diagnosis)
Harman et al.	6/93 (6.5%)	Radiographs (diagnosis)
Barrachina et al.	No major adverse events	Radiology, ultrasound, MRI (scoring)
Ferris et al.	3/33 (10%) (transient joint flares)	Arthroscopy
Joswig et al.	No major adverse events	None
Kearney et al.	No adverse events	None
Kriston-Pál et al.	2/58 (3.5%) (local inflammation)	None
Lei et al.	Not reported	MRI, micro-CT (scoring)
Yun et al.	Not reported	None
Maki et al.	No major adverse events	Radiographs (diagnosis)
Luque et al.	No major adverse events	Radiographs (diagnosis)
Delling et al.	Not reported	MRI (scoring), radiographs (diagnosis)
Muir et al.	No major adverse events	Radiographs (scoring)
Beerts et al.	No major adverse events	Radiographs (scoring)
Li X et al.	No major adverse events	X-ray

Abbreviations: Mesenchymal stromal cell (MSC); Hyualuronic Acid (HA); Platelet-Rich Plasma (PRP); Osteoarthritis (OA); Peripheral Blood MSCs (pbMSCs); Equine Peripheral Blood (ePB); Bone-Marrow MSCs (bmMSCs); Adipose-Deived MSCs (adMSCs); Phosphate Buffer Solution (PBS); Lipopolysaccharide (LPS); Magnetic Resonance Imaging (MRI).

This retrospective study involving 245 canines, performed by Armitage *et al*. (2023), demonstrated significant improvements for autologous-adMSC-treated groups at all time points[70]. The measured parameters include stance analysis, shoulder and hip range of motion (ROM), lumbosacral pressure algometry, and carpus and elbow ROM from weeks 49-78. This study utilized canines that were unresponsive to conventional treatments and therefore acted as their own controls. Diagnostic imaging confirmed tendinopathy resolution including restoration of proper mineralization and fiber patterns, as well as enhanced fibrosis resolution. The treatment was accepted well with less than 1% suffering from transient joint flare-ups, which were quickly resolved.

This prospective, randomized, masked, placebo-controlled, clinical study from Harman *et al*. (2016) utilized 74 canines to observe whether a single intraarticular allogeneic-adMSC injection is significantly more effective than a saline control[71]. This study enrolled dogs possessing up to two osteoarthritic joints, which included the hips, elbows, stifles, and/or shoulders. This study found significant improvements towards pain resolution and function in the allogeneic-adMSC group when compared to the saline control. Both the treatment and control groups experienced similar rates of adverse events, which demonstrates the inherent safety of single injection allogeneic-adMSC treatments.

This controlled, experimental study from Barrachina *et al*. (2018), utilized 18 ponies and their radiocarpal joints to observe the outcomes comparing repeated administration of naïve bone

marrow MSCs (bmMSC) and bmMSCs stimulated with the inflammatory cytokines, tumor necrosis factor (TNF) and interferon-γ (IFN-γ) against a lactated ringer solution (LRS) control[72]. Acute osteoarthritis was induced in these animals via intraarticular injection of amphotericin-b, an anti-fungal agent that causes pore formation, ion leakage, and cell lysis in chondrocytes and synoviocytes. Radiology and imaging revealed no significant differences between either MSC groups or the control group, however, ultrasonography indicated a reduction in synovial effusion in ponies receiving MSC treatments. Clinical and synovial inflammatory signs resolved more rapidly in the MSC treatment groups when compared to the LRS control group. Though transient, mild local inflammation was observed after the second dose in the cytokine-primed MSC group. Benefits were observed in the MSC groups as early as one week indicated by decreased joint effusion and capsulitis. Additionally, gene expression analysis for the MSC treated groups revealed significant upregulation of type II collagen, inducible nitric oxide synthase (iNOS), and transforming growth factor (TGF), as well as significant downregulation of tumor necrosis factor (TNF), matrix metalloproteinase-13 (MMP13), cyclooxygenase-2 (COX-2), and interleukin-1β (IL-1β).

This prospective case series from Ferris *et al*. (2014) investigated the usage of intraarticular autologous-bmMSCs as a treatment for equine femorotibial lesions (meniscal, cartilage, or ligamentous) [73]. This study did not have a control group; however, they compared their findings to the results from two other studies, including Walmsley *et al*. and Cohen *et al.*[68,69]. These studies investigated the return to function in horses following stifle arthroscopy and bmMSC intraarticular bmMSCs; with the goal of this study being the observation of long-term outcomes for horses treated with intraarticular bmMSCs and arthroscopic surgery. As such, Ferris et al. included 39 horses, with 33 available for outcome analysis at end-term. Additionally,

the study's goal included horses presenting an overall poor prognosis. Regardless of the varying levels of equine health, these treatments were overall received well with 75% of treated horses returning to at least some level of work at two years – this is significantly increased when compared to their control comparison studies treated with arthroscopy alone (60-63%). There were minimal treatment-related adverse events in the study, that included three cases of transient joint inflammation, which were resolved within 24 hours of treatment.

This controlled, experimental study by Joswig *et al*. (2017) evaluated the clinical response of autologous bmMSCs, allogeneic bmMSCs, and autologous bmMSCs containing fetal bovine serum (FBS) as a xeno-contaminate in an equine metacarpophalangeal model[74]. This study included 18 female quarter horses, with six assigned per group. The three groups included receiving intraarticular injections of 1) autologous bmMSCs depleted of FBS, 2) allogeneic cells depleted of FBS, and 3) autologous cells not depleted of FBS. This study found that even autologous bmMSC treatments containing xeno-contaminates (FBS) and repeated injections of allogeneic bmMSCs are significantly more likely to induce adverse effects when compared to a single injection autologous bmMSCs depleted of FBS; however, none of these treatment-related adverse events required any horse to withdraw from the study and were quickly resolved within a few days of treatment injection. This study did not analyze functional or mechanistic improvements, as this study sought only to observe treatment-related adverse effects to determine the safety and efficacy of cell therapy containing xeno-contaminates such as FBS.

This randomized, controlled, study by Kearney *et al*. (2022) investigated the usage of allogeneic-bmMSCs as a treatment for equine radiocarpal inflammation[75]. Prior to injection – these allogeneic-bmMSCs were stimulated with the inflammatory cytokines, TNF and IFN-γ, similarly to Barrachina *et al.* (2018)[72]. Both radiocarpal joints were induced for joint

inflammation, and the contralateral limb served as the negative control and received the cell culture medium as treatment. This study included six female and two male horses, with three females and one male assigned to each group. The treatment was received well with no adverse events for either the bmMSC group or the control group. Overall, the joint circumference was significantly reduced for the bmMSC treatment group when compared to the control group at the 24-hour timepoint. Additionally, the bmMSC group experienced significantly increased synovial glycosaminoglycans (GAG) values at the same 24-hour timepoint. Glycosaminoglycans are significant for their high water content, providing lubrication, preventing joint desiccation, and acting as a shock absorber.

This clinical long-term follow-up study performed by Pál É *et al*. (2020) investigated the usage of allogeneic adMSCs as a treatment for canines suffering from OA[76]. This study investigated the adMSC usage in multiple joints (elbow = 42, knee = 8, hip = 5, ankle = 2, and hock = 1) and included a total of 58 dogs. During the study, 16 dogs died due to unrelated reasons, including four to cancer and 12 to other diseases. This study did not utilize a control group as it was a long-term follow-up study aimed at observing the efficacy of allogeneic adMSC treatments. Overall, the study indicates that treatment with allogeneic adMSCs can potentially reduce lameness in the long-term. Only two of the 58 dogs suffered from treatment related adverse events, which only included transient local inflammation.

This controlled, experimental study by Lei *et al*. (2025) is unique in that it sought to investigate the usage of human ad-MSCs as a treatment for ovine knee OA[77]. This study included 11 male sheep who underwent anterior cruciate ligament (ACL) and medial meniscectomy to induce OA and subsequently received an injection into the right knee containing the human adMSCs treatment group or the saline control group. The injections occurred at 6- and 9-weeks

post-surgery. Overall, the sheep treated with the xenogeneic human-adMSCs displayed significantly improved MOCART scores based on magnetic resonance imaging (MRI). Additionally, histology, micro-CT, and MRI combined revealed a significant reduction in collagen X expression and a significant increase in collagen II expression. A reduction in collagen X expression is ideal as this collagen type is directly associated with the pathology of OA, and an increase in collagen II is ideal due to being the primary collagen type for hyaline and articular cartilage. Additionally, an increase in cartilage thickness of the femoral condyles was significantly increased when compared to the sterile saline control group.

This controlled study by Yun *et al*. (2016) investigated the usage of allogeneic adMSCs as a treatment for canine stifle osteoarthritis[78]. This study utilized 24 dogs in four distinct groups: 1) allogeneic ad-MSC treatment group, 2) platelet rich plasma (PRP) treatment group, 3) adMSCs+PRP, and 4) phosphate buffered solution (PBS) control group. Osteoarthritis was induced via cranial cruciate ligament transection and was subsequently treated once per week for four weeks. Overall, the MSC treatment group was more efficient at reducing lameness score at 2 months and 3 months after treatment, with the PRP group also performing better than the adMSC+PRP group; however, no significant improvements were found when comparing PRP to the adMSC+PRP group.

This randomized, double-blind, placebo-controlled pilot study from Maki *et al*. (2020) investigated the usage of allogeneic adMSCs to treat hip osteoarthritis in a canine model[79]. This pilot study included 20 canines in four different groups, including MSCs at three separate doses (5, 25, and 50 million) as well as a saline control group. Overall, the treatments were received well, with no major adverse events recorded. Importantly, 65% of dogs in the MSC treatment

groups demonstrated improved lameness scores at 90 days post-administration, with all doses presenting significant improvements when compared to the saline control group.

This prospective single-blinded, randomized study from Luque *et al*. (2025) is unique in that it investigated the safety and efficacy of equine umbilical cord-derived MSCs combined with HA compared to HA alone as a control group[80]. This study utilized 27 client-owned horses with fetlock or carpus osteoarthritis, and the MSC treatments contained either 10 (10M) or 20 million cells (20M) as the two separate treatment groups. Throughout the 18 weeks dedicated to the study there were no significant improvements for the MSC groups when compared to the control group. The authors contribute this to unexpectedly high success rates in the HA groups, which they believe underpowered the study. This study utilized 27 horses, and the authors believe the proper power would have been achieved with the enrollment of 30 horses. This study reports improvements to all three group's lameness scores by 6 weeks post-treatment. At week 18, the quantity of participants that were able to return to exercise included 8/9 for the 10M cells + HA group, 7/9 for the 20M + HA group, and only 5/9 or the HA-only control group. No significant differences were observed between the separate dosing treatment groups; however, these findings suggest substantial improvements to the MSCs + HA group – revealing lasting improved outcomes when MSCs are used as a treatment combined with HA.

This prospective, controlled, longitudinal preclinical study by Delling *et al*. (2015) investigated the usage of autologous bmMSCs as a treatment for ovine knee osteoarthritis[81]. Osteoarthritis was induced in one knee via lateral meniscectomy. This study utilized 12 female sheep to analyze the treatment outcomes, including the contralateral limb as the negative control. This study reported no treatment-related adverse effects. Additionally, this study reports significantly reduced lameness, as well as a significant increase in the volume of the meniscus

for the MSC treatment group when compared to the control group. Following the study end term at 12 weeks post-treatment, the knee joint tissues were then collected and analyzed for histological grading. However, radiographic imaging results revealed no major significant differences between any of the treatment groups or the control groups at 12 weeks post-treatment, except MRI scoring revealing significant improvements for treatment group MRI scores when compared to the controls at 6 weeks post-treatment. However, this study reported no overall treatment-related significant improvements for OA stage grading utilizing MRI, radiographs, and macroscopic/histologic observations by the study's 12-week end term.

This prospective, controlled, exploratory study by Muir *et al*. (2016) investigated the usage of autologous bmMSCs as a strategy to modulate inflammatory markers in canine stifle joints[82]. This study included 12 female canines with no control group, with the treatment groups including autologous bmMSCs at two different doses: lower dose (2 million cells per kilogram of bodyweight) and a higher dose (5 million cells per kilogram of bodyweight). Upon study completion – a significant reduction in inflammatory cytokines was observed when compared to the pre-treatment levels. Additionally, there were no reported major adverse events, which indicates the inherent safety of utilizing autologous MSCs in the context of inflammatory resolution.

This prospective, controlled, preclinical plus translational study by Beerts *et al*. (2023) investigated the usage of equine peripheral blood MSCs (pbMSCs) as a treatment in canine stifle arthritis[83]. The study included 32 canines, half female and half male, and included dogs with naturally occurring OA. The study utilized sterile saline as a control and three separate doses of equine pbMSCs were prepared for treatment, which included 60,000 cells, 300,000 cells, or 1.5 million cells. These treatments were received well with no reported major adverse events. The

treatment group with the most significant improvements is the 300,000 equine pbMSC group. Interestingly, this study found that the equine pbMSCs homed towards the injury in a canine model – thus demonstrating a treatment strategy that is both effective and safe.

This prospective, controlled, preclinical translational study by Li *et al*. (2025) investigated the usage of allogeneic adMSCs as a treatment in canine stifle arthritis[84]. This study utilized three injections over six weeks as the treatment and PBS as the control. Although this was a small study including only six dogs, it demonstrated efficacy and safety for repeated allogeneic MSC injections in reducing inflammatory expression. Being that this has not been the case for all the allogeneic MSC studies listed in this literature review, this serves as another example of MSC cellular therapy yielding mixed results in terms of efficacy when compared to other allogeneic MSC studies.

A 2018 study performed by Barrachina et al. was the sole study in this literature review that investigated the usage of immune primed MSCs in an equine (pony) model of radiocarpal osteoarthritis[72]. These MSCs were stimulated with both tumor necrosis factor (TNF) and interferon-gamma (IFN-γ). In early (2 month) cytokine and gene assessments, the MSC-primed treatment group showed significant upregulation of cartilage matrix genes (COL2A1 and TGF-β1) and suppression of inflammatory mediators (IL-1β, COX-2) when compared to naïve MSC treatment group. Additionally, there were significant reductions in TNF and IL-1β levels within the synovium. By the six-month assessment – several beneficial patterns persisted, including the upregulation of ECM genes, the downregulation of TNF, and sustained suppression of MMP-13 regarding MSC-primed vs MSC-naïve. However, the upregulation of TNF and MMP-13 for MSC-naïve reflects the more potent immunomodulatory benefits that were observed in the MSC-primed treatment group. The results from this study directly demonstrate the enhanced anti-

inflammatory, anti-catabolic, and regenerative promoting environment induced as a result of treatment with primed MSCs compared to naïve MSCs.

A controlled study by Yun *et al*. (2016) investigated mRNA outcomes using real-time PCR and measured the extracellular matrix and chondrogenic genes in both the femoral and tibial cartilage in a canine stifle osteoarthritis model[78]. Additionally, this cartilage was stained utilizing immunohistochemistry for the levels of specific cytokines and inflammatory proteins, such as TNF, COX-2, IL-1β, IFN-γ, iNOS, and caspase-3. Both aggrecan and SOX9 were significantly increased by all treatment groups (MSC, PRP, and MSC+PRP) when compared to the control group – with the MSC+PRP treatment group demonstrating the largest increase, followed by PRP, then the MSC treatment group. Additionally, all of the screened inflammatory cytokines were downregulated in the treatment groups with the greatest reductions again being the MSC+PRP treatment group. Therefore, these results reveal the inherent synergistic effects that combining MSC and PRP exert on the microenvironment of the osteoarthritic joint.

The study by Muir *et al*. (2016) utilized a canine model and investigated circulating T cell subset populations via flow cytometry and utilized a multiplex magnetic-bead assay to screen for the levels of serum and synovial cytokine concentrations for IFN-γ, TNF, CXCL1/8/10, CCL2, IL-2/6/7/10/15/18, and GM-CSF for a canine stifle joint osteoarthritis model[82]. The study found at each time-point that serum levels of IFN-γ, IL-6/10/15/18, CCL2, CXCL1, and GM-CSF were not significantly affected by the bmMSC treatment. However, the study found reductions of IFN-γ and IL-6 in the synovial fluid by 8 weeks with the bmMSC treatment group, as well as minimal detection of TNF. An important caveat to this study is that the passage number of MSCs varied among the dogs, which can potentially greatly alter the properties, behavior, and quality among various MSC cell populations.

In the 2020 pilot study by Maki *et al*., intra-articular administration of allogeneic adMSCs in dogs with hip osteoarthritis was associated with immunomodulatory effects reflected in serum cytokine changes[79]. Dogs treated with MSCs who showed clinical improvement exhibited increased serum IL-10, an anti-inflammatory cytokine, which persisted through 90 days, while placebo dogs did not show this elevation. Interleukin-1 receptor antagonist protein (IL1RA,) also increased in dogs with improved lameness, but this change was observed in both MSC-treated and placebo dogs, indicating it may reflect general improvement rather than a specific MSC effect. The study was relatively brief yet found trends suggesting higher MSC doses produced greater IL-10 elevations, although these were not statistically significant due to small sample sizes. Cytokine measurements were limited to serum and did not include synovial fluid, so localized joint changes remain unclear, and pro-inflammatory cytokines were not assessed. Overall, the results suggest that MSCs may reduce pain and lameness, with IL-10 serving as a potential biomarker of MSC-specific effects.

Lastly, Li *et al*. (2025) investigated the effects of multiple intra-articular injections of adMSCs on canine osteoarthritis[84]. OA modeling increased inflammatory cytokines TNF and IL-6, as well as matrix-degrading enzymes MMP-13 and ADAMTS-5, while suppressing cartilage formation markers COL II and aggrecan. Treatment with adMSCs normalized TNF and IL-6 expression by week 4, with IL-6 also reduced in circulation, indicating anti-inflammatory effects. MMP-13 and ADAMTS-5 were downregulated, reducing cartilage catabolism, while COL II and aggrecan expression increased, supporting tissue regeneration. Some rebound of TNF and IL-6 occurred after treatment cessation, thus demonstrating the importance of treatment timing and frequency. Overall, adMSCs appear to modulate inflammation and promote cartilage repair, demonstrating both immunomodulatory and regenerative effects in canine OA.

Overall – these studies emphasized the inherent safety and therapeutic potential of MSCs derived from a variety of sources, including adipose, bone marrow, peripheral blood, and umbilical cord as a therapeutic intervention for osteoarthritis. Induction of OA among studies indicates individual variability, which may be attributed to differences in surgical technique among various surgeons. This surgical variability has been theorized to be partially responsible for differences in outcomes in both human and animal models. No large animal models, in this literature review, other than Barrachina *et al*. (2018) utilized injections of immune primed MSCs in the context of OA[72]. This is important as we propose stimulating these cells as a means to generate homogenous populations of therapeutic MSCs. Additionally, this Barrachina *et al*. (2018) study revealed improved MSC cytokine expression; including upregulation in inflammatory resolving cytokines, enhanced immunomodulation and immune privilege, and a downregulation in pro-inflammatory cytokines[72]. Priming of these MSCs with tumor necrosis factor (TNF) and interferon-gamma (IFN-γ) demonstrated enhanced immunomodulatory properties when compared to the same MSCs lacking stimulation with TNF and IFN-γ. These studies further support our intention of using these inflammatory primed MSCs in a large animal model of osteoarthritis of which is discussed further in chapter three of this thesis. The therapeutic scenarios which induced the highest rate of adverse events were that of allogeneic MSCs, with a higher rate for repeat allogeneic injections, and the highest rate containing xeno-contaminate MSCs, proteins, or cells. Overall, the studies presented in this literature review confirm the inherent benefits and safety of utilizing MSCs as a therapeutic intraarticular injection for bothersome symptoms of osteoarthritis, but careful consideration remains important to evaluate the source of these cells, eliminate contamination, and frequency of injections. These decisions will be dependent on the species of animal, the stage of pathologic OA progression,

pre-existing conditions, and the overall vitality of the treated animal.

1.5 Conclusions

A literature review of intra-articular administration of non-activated MSCs demonstrated enhanced patient outcomes with MSC therapy even with a singular injection; however, findings were inconsistent between studies which has been attributed, in part, to heterogeneity between reported cell populations. Negative side effects when injected via intra-articular route of injection are minimally reported with the primary symptoms including local pain and swelling around the site of injection and liposuction if adipose tissue is harvested for cell isolation. However, although MSCs have been investigated for usage in osteoarthritis for over two decades (2002), these cells are still not readily available for usage in clinical settings. Cellular therapy with immune licensed MSCs has the potential to significantly increase the quality of life for those suffering from osteoarthritis by improving homogeneity and subsequent functionality of cellular populations. The data we present in this thesis indicates that activating MSC immune receptors, such as TLR3-pIC and STING-2’3’-cGAMP, is a reliable strategy to produce homogenous MSC populations for their subsequent usage in intra-articular cellular therapy with minimal risk of adverse side effects in a rodent model. This technique will allow for further development and standardization of clinically relevant MSCs with potential to improve clinical outcomes for patients with OA or other degenerative conditions.

References

1. Qin, J. *et al.* Lifetime risk of symptomatic hand osteoarthritis: The Johnston County Osteoarthritis Project. *Arthritis Rheumatol.* **69**, 1204–1212 (2017).

2. Hunter, D. J., March, L. & Chew, M. Osteoarthritis in 2020 and beyond: A lancet commission. *Lancet* **396**, 1711–1712 (2020).

3. Wang, Y. *et al.* Knee effusion volume assessed by magnetic resonance imaging and progression of knee osteoarthritis: data from the Osteoarthritis Initiative. *Rheumatology (Oxford)* **58**, 246–253 (2019).

4. Ireland, J. L. *et al.* Disease prevalence in geriatric horses in the United Kingdom: veterinary clinical assessment of 200 cases: Veterinary clinical assessment of disease prevalence in geriatric horses. *Equine Vet. J.* **44**, 101–106 (2012).

5. Murray, I. R. *et al.* Natural history of mesenchymal stem cells, from vessel walls to culture vessels. *Cell. Mol. Life Sci.* **71**, 1353–1374 (2014).

6. Bianco, P., Robey, P. G. & Simmons, P. J. Mesenchymal stem cells: revisiting history, concepts, and assays. *Cell Stem Cell* **2**, 313–319 (2008).

7. Galipeau, J. & Sensébé, L. Mesenchymal stromal cells: Clinical challenges and therapeutic opportunities. *Cell Stem Cell* **22**, 824–833 (2018).

8. Lazarus, H. M., Haynesworth, S. E., Gerson, S. L., Rosenthal, N. S. & Caplan, A. I. Ex vivo expansion and subsequent infusion of human bone marrow-derived stromal progenitor cells (mesenchymal progenitor cells): implications for therapeutic use. *Bone Marrow Transplant.* **16**, 557–564 (1995).

9. Kurtzberg, J., Burke, E., Hayes, J., Rose, D. E. & Itescu, S. Ryoncil (remestemcel-L) for third-line treatment of SR-aGVHD in adolescents and adults. *Transplant. Cell. Ther.* **31**, S288–S289 (2025).

10. Ouzin, M. & Kogler, G. Mesenchymal stromal cells: Heterogeneity and therapeutical applications. *Cells* **12**, 2039 (2023).

11. Lyamina, S. *et al.* Mesenchymal stromal cells as a driver of inflammaging. *Int. J. Mol. Sci.* **24**, 6372 (2023).

12. Li, D. & Wu, M. Pattern recognition receptors in health and diseases. *Signal Transduct. Target. Ther.* **6**, 291 (2021).

13. El-Zayat, S. R., Sibaii, H. & Mannaa, F. A. Toll-like receptors activation, signaling, and targeting: an overview. *Bull. Natl. Res. Cent.* **43**, 1–12 (2019).

14. Jann, O. C. *et al.* Comparative genomics of Toll-like receptor signalling in five species. *BMC Genomics* **10**, 216 (2009).

15. Pezzanite, L. M. *et al.* TLR-activated mesenchymal stromal cell therapy and antibiotics to treat multi-drug resistant Staphylococcal septic arthritis in an equine model. *Ann. Transl. Med.* **10**, 1157 (2022).

16. Johnson, V. *et al.* Activated mesenchymal stem cells interact with antibiotics and host innate immune responses to control chronic bacterial infections. *Sci. Rep.* **7**, 9575 (2017).

17. Johnson, V., Chow, L., Harrison, J., Soontararak, S. & Dow, S. Activated mesenchymal stromal cell therapy for treatment of multi-drug resistant bacterial infections in dogs. *Front. Vet. Sci.* **9**, 925701 (2022).

18. Plaisance, C. *et al.* Innate immune pathway activated mesenchymal stromal cells improve function and histologic outcomes in a rodent osteoarthritis model. *Front. Bioeng. Biotechnol.* **13**, 1525969 (2025).

19. Pezzanite, L. M. *et al.* Toll-like receptor activation of equine mesenchymal stromal cells to enhance antibacterial activity and immunomodulatory cytokine secretion. *Vet. Surg.* **50**, 858–871 (2021).

20. Linde, P. *et al.* Innate immune pathway activation to modulate mesenchymal stromal cell (MSC) interactions with synovium and cartilage. *Front. Bioeng. Biotechnol.* **13**, 1605148 (2025).

21. Wheat, W. *et al.* Activation of upper respiratory tract mucosal innate immune responses in cats by liposomal toll-like receptor ligand complexes delivered topically. *J. Vet. Intern. Med.* **33**, 838–845 (2019).

22. Ammons, D. T. *et al.* Reprogramming the canine glioma microenvironment with tumor vaccination plus oral losartan and propranolol induces objective responses. *Cancer Res. Commun.* **2**, 1657–1667 (2022).

23. Wotman, K. L., Chow, L., Martabano, B., Pezzanite, L. M. & Dow, S. Novel ocular immunotherapy induces tumor regression in an equine model of ocular surface squamous neoplasia. *Cancer Immunol. Immunother.* **72**, 1185–1198 (2023).

24. Lappin, M. *et al.* Nanoparticle ocular immunotherapy for herpesvirus surface eye infections evaluated in cat infection model. *PLoS One* **18**, e0279462 (2023).

25. Pezzanite, L. M. *et al.* Targeted transcriptomic analysis of synovial tissues from horses with septic arthritis treated with immune-activated mesenchymal stromal cells reveals induction of T-cell response pathways. *J. Am. Vet. Med. Assoc.* **262**, S73–S82 (2024).

26. Mikami, T., Miyashita, H., Takatsuka, S., Kuroki, Y. & Matsushima, N. Molecular evolution of vertebrate Toll-like receptors: evolutionary rate difference between their leucine-rich repeats

and their TIR domains. *Gene* **503**, 235–243 (2012).

27. Leulier, F. & Lemaitre, B. Toll-like receptors--taking an evolutionary approach. *Nat. Rev. Genet.* **9**, 165–178 (2008).

28. Hopfner, K.-P. & Hornung, V. Molecular mechanisms and cellular functions of cGAS-STING signalling. *Nat. Rev. Mol. Cell Biol.* **21**, 501–521 (2020).

29. Johnson, B. Z., Stevenson, A. W., Prêle, C. M., Fear, M. W. & Wood, F. M. The role of IL-6 in skin fibrosis and cutaneous wound healing. *Biomedicines* **8**, 101 (2020).

30. Waterman, R. S., Tomchuck, S. L., Henkle, S. L. & Betancourt, A. M. A new mesenchymal stem cell (MSC) paradigm: polarization into a pro-inflammatory MSC1 or an Immunosuppressive MSC2 phenotype. *PLoS One* **5**, e10088 (2010).

31. Court, A. C. *et al.* Mitochondrial transfer from MSCs to T cells induces Treg differentiation and restricts inflammatory response. *EMBO Rep.* **21**, e48052 (2020).

32. Copp, G., Robb, K. P. & Viswanathan, S. Culture-expanded mesenchymal stromal cell therapy: does it work in knee osteoarthritis? A pathway to clinical success. *Cell. Mol. Immunol.* **20**, 626–650 (2023).

33. Dumitru, C. A., Hemeda, H., Jakob, M., Lang, S. & Brandau, S. Stimulation of mesenchymal stromal cells (MSCs) via TLR3 reveals a novel mechanism of autocrine priming. *FASEB J.* **28**, 3856–3866 (2014).

34. Rashedi, I., Gómez-Aristizábal, A., Wang, X.-H., Viswanathan, S. & Keating, A. TLR3 or TLR4 activation enhances mesenchymal stromal cell-mediated Treg induction via Notch signaling. *Stem Cells* **35**, 265–275 (2017).

35. Davies, L. C., Heldring, N., Kadri, N. & Le Blanc, K. Mesenchymal stromal cell secretion of programmed death-1 ligands regulates T cell mediated immunosuppression. *Stem Cells* **35**, 766–776 (2017).

36. Syn, N. L., Teng, M. W. L., Mok, T. S. K. & Soo, R. A. De-novo and acquired resistance to immune checkpoint targeting. *Lancet Oncol.* **18**, e731–e741 (2017).

37. Chow, L. *et al.* Antibacterial activity of human mesenchymal stem cells mediated directly by constitutively secreted factors and indirectly by activation of innate immune effector cells. *Stem Cells Transl. Med.* **9**, 235–249 (2020).

38. Tolstova, T. *et al.* The effect of TLR3 priming conditions on MSC immunosuppressive properties. *Stem Cell Res. Ther.* **14**, 344 (2023).

39. Donnelly, C. R. *et al.* STING controls nociception via type I interferon signalling in sensory neurons. *Nature* **591**, 275–280 (2021).

40. Donnelly, C. R., Chen, O. & Ji, R.-R. How do sensory neurons sense danger signals? *Trends Neurosci.* **43**, 822–838 (2020).

41. Sun, C., Wu, G., Zhang, Z., Cao, R. & Cui, S. Protein tyrosine phosphatase receptor type D regulates neuropathic pain after nerve injury via the STING-IFN-I pathway. *Front. Mol. Neurosci.* **15**, 859166 (2022).

42. Wang, K. *et al.* STING suppresses bone cancer pain via immune and neuronal modulation. *Nat. Commun.* **12**, 4558 (2021).

43. Ishikawa, H. & Barber, G. N. STING is an endoplasmic reticulum adaptor that facilitates innate immune signalling. *Nature* **455**, 674–678 (2008).

44. Liu, C.-C. *et al.* Interferon alpha inhibits spinal cord synaptic and nociceptive transmission via neuronal-glial interactions. *Sci. Rep.* **6**, 34356 (2016).

45. Gao, Q. *et al.* Bone marrow mesenchymal stromal cells: Identification, classification, and differentiation. *Front. Cell Dev. Biol.* **9**, 787118 (2021).

46. Li, C.-Y. *et al.* Comparative analysis of human mesenchymal stem cells from bone marrow and adipose tissue under xeno-free conditions for cell therapy. *Stem Cell Res. Ther.* **6**, 55 (2015).

47. Cornelissen, A. S., Maijenburg, M. W., Nolte, M. A. & Voermans, C. Organ-specific migration of mesenchymal stromal cells: Who, when, where and why? *Immunol. Lett.* **168**, 159–169 (2015).

48. Ouryazdanpanah, N., Dabiri, S., Derakhshani, A., Vahidi, R. & Farsinejad, A. Peripheral blood-derived mesenchymal stem cells: Growth factor-free isolation, molecular characterization and differentiation. *Iran. J. Pathol.* **13**, 461–466 (2018).

49. Krawczenko, A. & Klimczak, A. Adipose tissue-derived mesenchymal stem/stromal cells and their contribution to angiogenic processes in tissue regeneration. *Int. J. Mol. Sci.* **23**, 2425 (2022).

50. Melief, S. M., Zwaginga, J. J., Fibbe, W. E. & Roelofs, H. Adipose tissue-derived multipotent stromal cells have a higher immunomodulatory capacity than their bone marrow-derived counterparts. *Stem Cells Transl. Med.* **2**, 455–463 (2013).

51. Long, H. *et al.* Prevalence trends of site-specific osteoarthritis from 1990 to 2019: Findings from the Global Burden of Disease Study 2019. *Arthritis Rheumatol.* **74**, 1172–1183 (2022).

52. Ankrum, J. A., Ong, J. F. & Karp, J. M. Mesenchymal stem cells: immune evasive, not immune privileged. *Nat. Biotechnol.* **32**, 252–260 (2014).

53. Jo, C. H. *et al.* Intra-articular injection of mesenchymal stem cells for the treatment of osteoarthritis of the knee: a proof-of-concept clinical trial: IA injection of MSCs for knee osteoarthritis. *Stem Cells* **32**, 1254–1266 (2014).

54. Song, Y. *et al.* Human adipose-derived mesenchymal stem cells for osteoarthritis: a pilot study with long-term follow-up and repeated injections. *Regen. Med.* **13**, 295–307 (2018).

55. Pers, Y.-M. *et al.* Adipose mesenchymal stromal cell-based therapy for severe osteoarthritis of the knee: A phase I dose-escalation trial: ASCs for severe OA of the knee. *Stem Cells Transl. Med.* **5**, 847–856 (2016).

56. Lu, L. *et al.* Intra-articular injections of allogeneic human adipose-derived mesenchymal progenitor cells in patients with symptomatic bilateral knee osteoarthritis: a Phase I pilot study. *Regen. Med.* **15**, 1625–1636 (2020).

57. Kuah, D. *et al.* Safety, tolerability and efficacy of intra-articular Progenza in knee osteoarthritis: a randomized double-blind placebo-controlled single ascending dose study. *J. Transl. Med.* **16**, 49 (2018).

58. Xie, R.-H., Gong, S.-G., Song, J., Wu, P.-P. & Hu, W.-L. Effect of mesenchymal stromal cells transplantation on the outcomes of patients with knee osteoarthritis: A systematic review and meta-analysis. *J. Orthop. Res.* **42**, 753–768 (2024).

59. Zhao, J. *et al.* Combination of mesenchymal stem cells (MSCs) and platelet-rich plasma (PRP) in the treatment of knee osteoarthritis: a meta-analysis of randomised controlled trials. *BMJ Open* **12**, e061008 (2022).

60. Cao, M. *et al.* Efficacy and safety of mesenchymal stem cells in knee osteoarthritis: a systematic review and meta-analysis of randomized controlled trials. *Stem Cell Res. Ther.* **16**, 122 (2025).

61. Lee, W.-S., Kim, H. J., Kim, K.-I., Kim, G. B. & Jin, W. Intra-articular injection of autologous adipose tissue-derived mesenchymal stem cells for the treatment of knee osteoarthritis: A phase IIb, randomized, placebo-controlled clinical trial. *Stem Cells Transl. Med.* **8**, 504–511 (2019).

62. Lu, L. *et al.* Treatment of knee osteoarthritis with intra-articular injection of autologous adipose-derived mesenchymal progenitor cells: a prospective, randomized, double-blind, active-controlled, phase IIb clinical trial. *Stem Cell Res. Ther.* **10**, 143 (2019).

63. Kim, Y. S. *et al.* Comparative matched-pair cohort analysis of the short-term clinical outcomes of mesenchymal stem cells versus hyaluronic acid treatments through intra-articular

injections for knee osteoarthritis. *J. Exp. Orthop.* **7**, 90 (2020).

64. Freitag, J. *et al.* Adipose-derived mesenchymal stem cell therapy in the treatment of knee osteoarthritis: a randomized controlled trial. *Regen. Med.* **14**, 213–230 (2019).

65. Koh, Y.-G. & Choi, Y.-J. Infrapatellar fat pad-derived mesenchymal stem cell therapy for knee osteoarthritis. *Knee* **19**, 902–907 (2012).

66. Spasovski, D. *et al.* Intra-articular injection of autologous adipose-derived mesenchymal stem cells in the treatment of knee osteoarthritis. *J. Gene Med.* **20**, e3002 (2018).

67. Dell'Isola, A., Allan, R., Smith, S. L., Marreiros, S. S. P. & Steultjens, M. Identification of clinical phenotypes in knee osteoarthritis: a systematic review of the literature. *BMC Musculoskelet. Disord.* **17**, 425 (2016).

68. Walmsley, J. R., Phillips, T. J. & Townsend, H. G. G. Meniscal tears in horses: an evaluation of clinical signs and arthroscopic treatment of 80 cases. *Equine Vet. J.* **35**, 402–406 (2003).

69. Cohen, J. M., Richardson, D. W., McKnight, A. L., Ross, M. W. & Boston, R. C. Long-term outcome in 44 horses with stifle lameness after arthroscopic exploration and debridement. *Vet. Surg.* **38**, 543–551 (2009).

70. Armitage, A. J., Miller, J. M., Sparks, T. H., Georgiou, A. E., & Reid, J. (2022). Efficacy of autologous mesenchymal stromal cell treatment for chronic degenerative musculoskeletal conditions in dogs: A retrospective study. *Frontiers in Veterinary Science*, *9*, 1014687. https://doi.org/10.3389/fvets.2022.1014687

71. Harman, R., Carlson, K., Gaynor, J., Gustafson, S., Dhupa, S., Clement, K., Hoelzler, M., McCarthy, T., Schwartz, P., & Adams, C. (2016). A prospective, randomized, masked, and placebo-controlled efficacy study of intraarticular allogeneic adipose stem cells for the treatment of osteoarthritis in dogs. *Frontiers in Veterinary Science*, *3*, 81. https://doi.org/10.3389/fvets.2016.00081

72. Barrachina, L., Remacha, A. R., Romero, A., Vitoria, A., Albareda, J., Prades, M., Roca, M., Zaragoza, P., Vázquez, F. J., & Rodellar, C. (2018). Assessment of effectiveness and safety of repeat administration of proinflammatory primed allogeneic mesenchymal stem cells in an equine model of chemically induced osteoarthritis. *BMC Veterinary Research*, *14*(1), 241. https://doi.org/10.1186/s12917-018-1556-3

73. Ferris, D. J., Frisbie, D. D., Kisiday, J. D., McIlwraith, C. W., Hague, B. A., Major, M. D., Schneider, R. K., Zubrod, C. J., Kawcak, C. E., & Goodrich, L. R. (2014). Clinical outcome after intra-articular administration of bone marrow derived mesenchymal stem cells in 33 horses with stifle injury: Intra-articular administered bone marrow derived mesenchymal stem cells. *Veterinary Surgery: VS*, *43*(3), 255–265. https://doi.org/10.1111/j.1532-950X.2014.12100.x

74. Joswig, A.-J., Mitchell, A., Cummings, K. J., Levine, G. J., Gregory, C. A., Smith, R., 3rd, & Watts, A. E. (2017). Repeated intra-articular injection of allogeneic mesenchymal stem cells

causes an adverse response compared to autologous cells in the equine model. *Stem Cell Research & Therapy*, *8*(1), 42. https://doi.org/10.1186/s13287-017-0503-8

75. Kearney, C. M., Khatab, S., van Buul, G. M., Plomp, S. G. M., Korthagen, N. M., Labberté, M. C., Goodrich, L. R., Kisiday, J. D., Van Weeren, P. R., van Osch, G. J. V. M., & Brama, P. A. J. (2022). Treatment effects of intra-articular allogenic mesenchymal stem cell secretome in an equine model of joint inflammation. *Frontiers in Veterinary Science*, *9*, 907616. https://doi.org/10.3389/fvets.2022.907616

76. Kriston-Pál, É., Haracska, L., Cooper, P., Kiss-Tóth, E., Szukacsov, V., & Monostori, É. (2020). A regenerative approach to canine osteoarthritis using allogeneic, adipose-derived mesenchymal stem cells. Safety results of a long-term follow-up. *Frontiers in Veterinary Science*, *7*, 510. https://doi.org/10.3389/fvets.2020.00510

77. Lei, J., Chen, X., Xie, H., Dai, Y., Chen, Z., & Xu, L. (2025). Therapeutic efficacy of intra-articular injection of human adipose-derived mesenchymal stem cells in a sheep model of knee osteoarthritis. *Stem Cell Research & Therapy*, *16*(1), 24. https://doi.org/10.1186/s13287-025-04143-6

78. Yun, S., Ku, S.-K., & Kwon, Y.-S. (2016). Adipose-derived mesenchymal stem cells and platelet-rich plasma synergistically ameliorate the surgical-induced osteoarthritis in Beagle dogs. *Journal of Orthopaedic Surgery and Research*, *11*(1), 9. https://doi.org/10.1186/s13018-016-0342-9

79. Maki, C. B., Beck, A., Wallis, C.-B. C. C., Choo, J., Ramos, T., Tong, R., Borjesson, D. L., & Izadyar, F. (2020). Intra-articular administration of allogeneic adipose derived MSCs reduces pain and lameness in dogs with hip osteoarthritis: A double blinded, randomized, placebo controlled pilot study. *Frontiers in Veterinary Science*, *7*, 570. https://doi.org/10.3389/fvets.2020.00570

80. Luque, R. M., Henderson, B., McCorkell, T. C., Alizadeh, A. H., Russell, K. A., Koch, T. G., & Koenig, J. (2025). Treatment outcomes for equine osteoarthritis with mesenchymal stromal cells and hyaluronic acid. *Equine Veterinary Journal*, *57*(5), 1245–1254. https://doi.org/10.1111/evj.14531

81. Delling, U., Brehm, W., Ludewig, E., Winter, K., & Jülke, H. (2015). Longitudinal evaluation of effects of intra-articular mesenchymal stromal cell administration for the treatment of osteoarthritis in an ovine model. *Cell Transplantation*, *24*(11), 2391–2407. https://doi.org/10.3727/096368915X686193

82. Muir, P., Hans, E. C., Racette, M., Volstad, N., Sample, S. J., Heaton, C., Holzman, G., Schaefer, S. L., Bloom, D. D., Bleedorn, J. A., Hao, Z., Amene, E., Suresh, M., & Hematti, P. (2016). Autologous bone marrow-derived mesenchymal stem cells modulate molecular markers of inflammation in dogs with cruciate ligament rupture. *PloS One*, *11*(8), e0159095. https://doi.org/10.1371/journal.pone.0159095

83. Beerts, C., Broeckx, S. Y., Depuydt, E., Tack, L., Van Hecke, L., Chiers, K., Van Brantegem, L., Braun, G., Hellmann, K., de Bouvre, N., Van Bruaene, N., De Ryck, T., Duchateau, L., Van Ryssen, B., Peremans, K., Saunders, J. H., Verhoeven, G., Pauwelyn, G., & Spaas, J. H. (2023). Low-dose xenogeneic mesenchymal stem cells target canine osteoarthritis through systemic immunomodulation and homing. *Arthritis Research & Therapy*, *25*(1), 190. https://doi.org/10.1186/s13075-023-03168-7

84. Li, X., Jian, X., Yan, Z., Liu, H., & Zhang, L. (2025). Multiple intra-articular injections of adipose-derived mesenchymal stem cells for canine osteoarthritis treatment. *Cells (Basel, Switzerland)*, *14*(5), 323. https://doi.org/10.3390/cells14050323

CHAPTER 2: Innate immune pathway activated mesenchymal stromal cells improve function and histologic outcomes in a rodent osteoarthritis model

2.1 Summary

We used a mouse osteoarthritis (OA) model to evaluate whether immune activation of MSC, using two different agonists of innate immune pathways (TLR3 and cGAS-STING pathways) could improve joint function and chondroprotection compared to non-activated MSC. The impact of MSC injections on animal gait, joint chondroprotection, and joint transcriptome responses was evaluated. We found that activation of MSC by either TLR3 or cGAS-STING pathways significantly improved functional outcomes and joint integrity, compared to treatment with non-activated MSC, with early evidence of superiority of the cGAS-STING pathway activated MSC. We conclude that immune activation of MSC via innate immune pathways such as those associated with strong interferon responses can improve outcomes following intra-articular injection in OA.

2.2 Introduction

Osteoarthritis (OA) is a progressive, degenerative, condition that affects over 550 million people worldwide – a 113% increase since 1990. The prevalence has doubled in the US over the last ten years with an economic impact of $136 billion annually[1,2]. Despite this high prevalence, there remains a lack of effective treatment options that improve quality of life without risk of adverse effects, with current therapies including nonsteroidal anti-inflammatories, intra-articular injections, or arthroscopic debridement and cartilage resurfacing techniques. Cellular therapies to treat OA have emerged as an option in both human and veterinary orthopedics with mixed results reported in terms of efficacy[3-15]. A recent metanalysis of human randomized MSC trials concluded that overall MSC treatment reduced joint inflammation, improved pain scores, and

preserved cartilage integrity, suggesting that MSC cellular therapy is beneficial. Nonetheless, challenges remain, including the use of MSC with greater potency for their intended task, greater uniformity of MSC sources and propagation, as well as improved credentialing of MSC functional properties that correlate with better outcomes[16]. Heterogeneity within stromal cell populations has been proposed to be partially responsible for the observed variability in therapeutic responses, particularly in the context of variably inflamed recipient environments such as that seen in OA[17]. Pre-activation, or 'inflammatory licensing', of mesenchymal stromal cells (MSCs) through priming with their respective ligands has been proposed as a means to generate a homogenous population of immunomodulatory MSCs - thereby potentially improving the consistency of MSC therapy and response to treatment[18-21]. With the lifetime likelihood to develop symptomatic knee OA currently at 45% and increasing, the need to develop improved strategies towards disease-modification is critical[22].

Expression of pattern recognition receptors (PRRs), specialized proteins that detect exogenous pathogens and endogenous ligands, represent a key link between the immune system and sensory nervous system in response to inflammation or injury, such as that described in OA[23]. The PRR family includes Toll-like receptors (TLR) (*e.g.,* nucleotide oligomerization domain-like receptors, C-type lectin receptors, RIG-I-like receptors, and retinoic acid-inducible gene I receptors) and cytosolic DNA sensors (*e.g.,* STimulator of Interferon Genes or STING). The STING receptor, also known as cGAS-STING, as Cyclic GMP-AMP synthase (cGAS), is the primary enzyme to induce STING pathway signaling. In response to tissue injury, PRRs on immune cells are activated to initiate their respective downstream inflammatory response. Activation of both STING and TLR3 results in production of type I interferons (IFN-Is) (IFN-α, IFN-β, and IFN-κ) in immune cells and sensory neurons following tissue injury or infection[24-28],

which has been demonstrated to have the potential to be both inflammatory or antinociceptive depending on the disease process[23,28]. In the context of specifically enhancing therapeutic efficacy of immunomodulatory MSC therapy, previous studies have demonstrated that stimulation of MSC with TLR ligands enhanced their immunomodulatory properties, including cytokine secretion of monocyte chemoattractant protein-1 (MCP-1) and IL-8 *in vitro* resulting in resolution of inflammation and reduced bioburden associated with musculoskeletal infection in animal models[29-31]. However, to the authors' knowledge, comparison of these two PRRs to activate and enhance MSC therapy as a means to treat OA has not been previously evaluated.

Therefore, we built upon this previous work to evaluate and compare activation of MSCs via TLR3 pathway and with the cGAS-STING pathway in the context of intra-articular treatment of OA. The overall objective of this work was to determine whether priming of MSC therapy with agonists of the endosomal TLR3 pathway or the cytoplasmic STING pathway improved the efficacy of MSC intra-articular therapy in a rodent destabilization of the medial meniscus (DMM) model of OA. Our analysis revealed significant improvements in post-operative voluntary movement parameters and histological outcomes with STING pathway activated MSC and improved histological outcomes with TLR3 pathway activated MSC. Bulk RNA sequencing analyses indicated that IFN related pathways were upregulated in the joints of mice treated with either TLR3-activated MSC or STING-pathway activated MSC, with substantially more interferon pathways being upregulated in the STING-pathway MSC treated animals.

Overall, this work provides key insights into the transcriptomic, structural, and synovial responses to intra-articular treatment with immune activated MSC, suggesting that activation of TLR3 pathways or STING pathways in MSC prior to injection can activate multiple IFN

pathways, and that stimulation of IFN pathways in MSC may be a uniquely effective method of licensing MSC for orthopedic applications.

2.3 Materials and Methods

This study was approved by the Institutional Animal Care and Use Committee at Colorado State University (IACUC protocol #3134) and conducted according to the national guidelines under which the institution operates and the NIH Guidelines for the Care and Use of Laboratory Animals (8^{th} edition).

Animals **–** Studies were performed using 12-week-old male C57BL/6Nci mice (Charles River Laboratories, Wilmington, MA, USA). Mice (n=10 per group) were randomly assigned to receive surgery followed by either 1) needle insertion alone, 2) non-activated MSCs, 3) pIC-activated MSCs (TLR3), or 4) 2'3' c-GAMP activated MSC (STING pathway), for a total of 40 mice. Activity monitoring was performed weekly on all mice in each group. At end term, five mice per group were assessed for histologic scoring of joint tissues, while the remaining five mice were processed for transcriptomic analyses of joint tissues. Mice were housed together in the Laboratory Animal Resources building in groups of five in solid bottom cages with corncob bedding and allowed ad libitum water and standard rodent chow. Mice were assessed by a veterinarian daily and body weights were monitored weekly. At the conclusion of the study, mice were euthanized via CO_2 inhalation with confirmation by cervical dislocation. All animals were included in the final analyses. Study overview is provided in Figure 1.

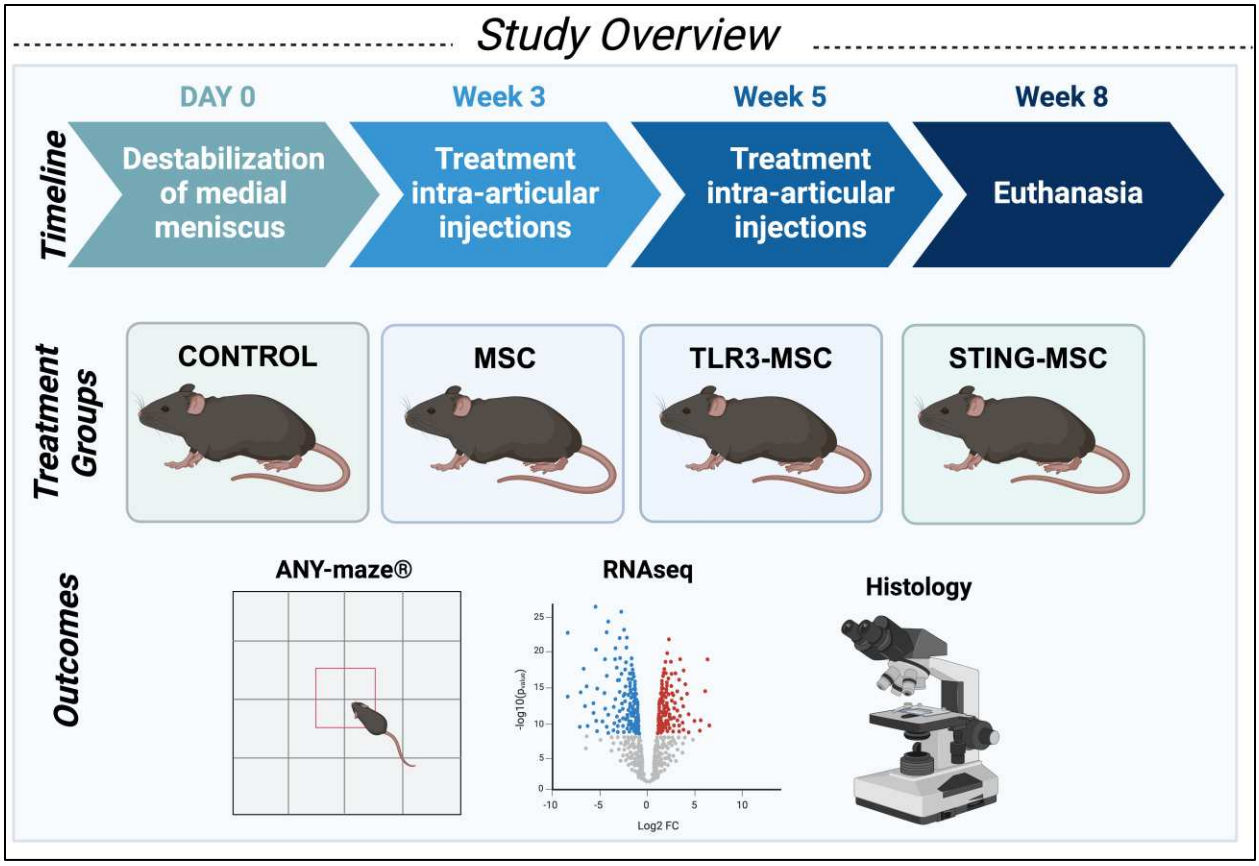

Figure 1. Schematic overview of study design. Studies were performed using 12-week-old male C57BL/6Nci mice (Charles River Laboratories, Wilmington, MA, United States). Mice (n = 10 per group for a total of forty mice) received unilateral destabilization of the medial meniscus surgery in the right knee and were randomly assigned to receive either control treatment (intra-articular needle insertion alone), non-activated MSC, PIC-activated MSC, or STING-activated MSC for two treatments at weeks three and five postoperatively. Activity monitoring was performed weekly on all mice in each group. At end term, five mice per group were assessed for histologic scoring and joint tissues from the remaining five mice were processed for transcriptomic analyses of joint tissues.

Stromal cell preparation – Age-matched male C57BL/6Nci mice served as adipose MSC (adMSC) donors. Murine adMSC was generated from abdominal and inguinal adipose tissue that was aseptically collected immediately following euthanasia via CO_2 inhalation and cervical dislocation. The adipose tissue was isolated, pooled, and cultured as previously described[32,33]. Cells generated were plastic-adherent and displayed typical adMSC morphology and expansion properties[33]. AdMSCs were expanded in culture in complete growth media (Dulbecco modified

eagle medium (DMEM), 10% fetal bovine serum (FBS), penicillin (100 U/mL), streptomycin (100 μg/mL), and 1 mol/lL HEPES) until injection. At weeks 3 and 5, MSC were trypsinized, counted, and a portion activated with the TLR3 agonist polyinosinic-polycytidylic acid (pIC) or stimulator of IFN genes (STING) (10μg/mL, $1x10^6$ cells/mL) in growth media for 2h. Cells were washed 3 times with sterile PBS and prepared at a concentration of 2.5 $x10^7$ cells per mL in PBS.

Destabilization of the medial meniscus model of osteoarthritis - Osteoarthritis was induced in in the right femorotibial joint (knee) of mice at time 0 (week 0) using established methods of destabilization of the medial meniscus (DMM) in the right hindlimb[34]. Mice were induced under general anesthesia using isoflurane (1-5%, to effect) and the right femorotibial joint (knee) was clipped and aseptically prepared in routine fashion. Briefly, to induce OA, a medial parapatellar arthrotomy using a #11 scalpel blade was performed and the infrapatellar fat pad (IFP) temporarily repositioned laterally to allow access to the anterior medial meniscotibial ligament. This ligament was severed using the #11 scalpel blade. The IFP was repositioned, and the surgical incision closed in simple interrupted fashion using 6-0 monofilament absorbable suture. Mice were administered buprenorphine SR (slow release) 0.6-0.8 mg/kg subcutaneously under anesthesia at time of surgery.

Intra-articular administration of adMSCs – Intra-articular injections of MSC were performed at weeks three and five following DMM operation. For injections, mice were induced under general anesthesia using 3% isoflurane with oxygen, followed by 1-1.5% isoflurane to maintain plane of anesthesia. The right (operated) femorotibial joint was aseptically prepared in routine fashion and injected with $2.5x10^5$ murine adipose-derived MSC or pIC- or STING-activated MSC suspended in 10 μL phosphate buffered saline (PBS), or controls of needle insertion alone. Injections were performed with #27 needle and Hamilton syringe.

Activity monitoring to assess osteoarthritis severity - Mice were monitored prior to injury and for eight weeks following surgery using individual cage monitoring to determine general animal behavior and mobility. Cage monitoring was performed for 10 minutes weekly during the experimental time-course. Mice were placed in their primary enclosure / resident cage with their environmental enrichment hut for the duration of the assessment. Prior to taking the baseline measurement, mice were acclimated to the system over one week - after which two baseline measurements were collected immediately before the start of the study. Training and data collection occurred during the same time of day (8am to 12pm) and involved the same handlers throughout the course of the study to minimize circadian rhythm cycle variations. The video analysis software used (ANY-maze^{TM}, Wood Dale, IL, USA) automatically collected mobility parameters including total distance traveled, time mobile, mean speed, maximum speed, time in hut, and entries to the top of the hut. Parameters of interest were assessed both cross-sectionally amongst groups normalized to preoperative baseline and longitudinally over time.

Transcriptomic sequencing of joint tissues – Mouse femorotibial (knee) tissues (n=5 biological replicates per treatment group of 10 mice) were removed immediately following euthanasia, minced, and stored in RLT lysis buffer (Qiagen) at -80°C. RNA was extracted by first using TRIzol Reagent (Invitrogen, Waltham, MA) following manufactures instructions, with a 1:3 RLT lysis buffer to TRIzol ratio. RNA precipitate pellet was then cleaned and concentrated using RNeasy MinElute Cleanup Kit (Qiagen Germantown, MD), according to manufacturer's instructions and sent to Novogene Corporation Inc. (Sacramento, CA) for bulk RNA sequencing. RNA quality was determined by bioanalyzer (Agilent Technologies, Santa Clara, CA). RIN (RNA integrity number) was determined to be >7.5 for all samples. For bulk RNA sequencing, mRNA was enriched using oligo (dT) beads, followed by cDNA library generation using TruSeq

RNA Library Prep Kit (Illumina, San Diego, CA). Sequencing was performed on Illumina Novaseq 6000 machine using 150 bp paired end reads.

Joint histology – At eight weeks after surgery, femorotibial (knee) joints (n=5 biological replicates per treatment group of 10 mice) were fixed in 10% neutral buffered formalin for 24 hours, then decalcified in ethylenediamine tetra-acetic acid (EDTA) and paraffin embedded. Coronal sections (5 μm) were taken from the center of the medial tibial plateau and stained with toluidine blue. Histological grading of joint tissues was performed using an established criteria for OA by two blinded, independent individuals trained in using this scoring method via consensus. In brief, joint tissues were semi-quantitatively graded for osteoarthritic damage including cartilage fibrillation, cartilage loss including clefts/erosions and calcification, synovitis, and proteoglycan content for the whole joint and medial and lateral joint compartments[35].

Data analysis – The experimental sample size was calculated by a-priori power analysis using GPower Version 3.1.1, using pilot gait data (stride length) obtained using this injury model in mice as the primary outcome measure for calculating group sizes. Cross-sectional activity monitoring data was normalized to baseline values and compared using repeated-measures analysis of variance (ANOVA) with Tukey's correction. Longitudinal data were compared using repeated measures ANOVA and Dunnett's correction, comparing each timepoint to baseline values. Histological scoring at end-term was evaluated using a one-way non-parametric ANOVA (Kruskal-Wallis test) with Dunn's multiple comparisons test. Statistical analysis was performed using GraphPad Prism v9.3.1 (GraphPad Software Inc., La Jolla, CA, USA). The significance for enclosure monitoring and histological outcomes was assessed at $p<0.1$ as described[36]. Sequence data were analyzed on Partek Flow software, version 10.0 (Partek Inc. Chesterfield, MO). First,

Raw data were filtered by removing reads containing adapters and reads containing N > 10% and for Phred scores > 30. Filtered reads were then aligned with STAR 2.7.3a using GRCm39 Genome Reference. Aligned reads were annotated and counted using HT-seq with Ensembl 108. Differentially expressed genes were identified using DEseq2[37]. Biological interpretations included gene ontology and gene set enrichment analysis (GSEA), which were performed using GSEA (https://www.gsea-msigdb.org/gsea/index.jsp).

2.4 Results

Comparison of functional impact of treatment via activity monitoring – We assessed functional improvement with treatment over time using the ANY-maze overhead cage monitoring software. When cross-sectional data was normalized to pre-DMM surgery baseline values, mice treated with STING pathway activated MSC exhibited greater adjusted time mobile compared to MSC treated mice (p=0.04) or control (p=0.07) at week 8 (Figure 2A, B). In addition, mice treated with STING-MSC spent less time in their security huts relative to baseline compared to MSC treated mice (p=0.09) at week 8 (Figure 2C, D), and fewer hut entries relative to baseline compared to control at week 4 (p=0.04) or TLR3-pathway activated MSC treated mice at week 6 (p=0.1) (Figure 2E, F). There were no significant differences between TLR3 MSC treated mice compared to needle or MSC alone. There were no significant findings in longitudinal data for within group (*e.g.,* time) differences (Figure 2 significant findings, Supplemental Document 1, additional non-significant findings).

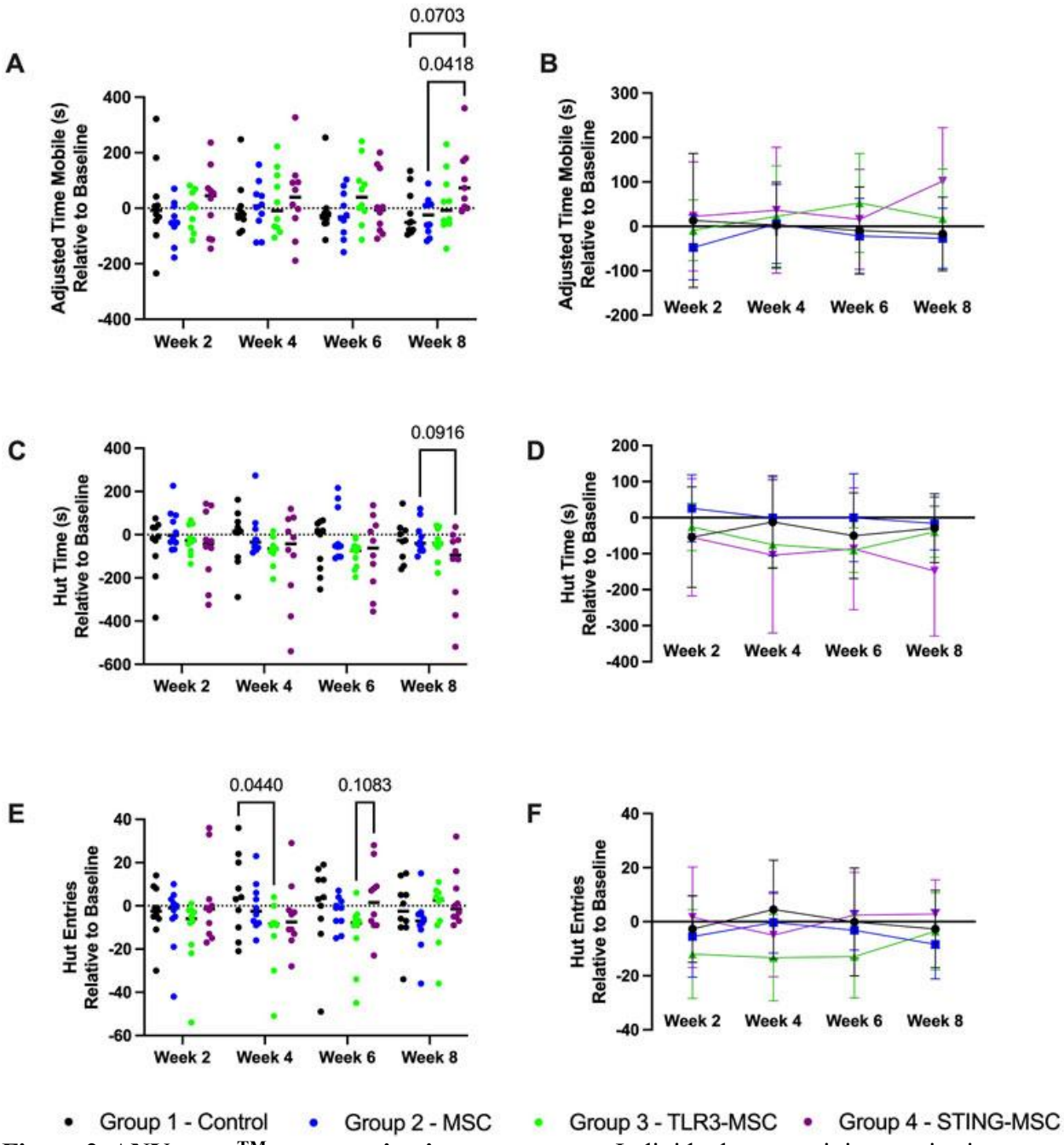

Figure 2. ANY-maze™ cage monitoring parameters. Individual cage activity monitoring was performed following DMM surgery on the right hind limb of mice and two intra-articular treatments administered depending on group. Parameters of interest are shown over time and between groups for distance traveled (m) (A,B), head distance traveled (m) (C,D), time mobile (s) (E,F), adjusted time mobile (s) (G,H) relative to baseline. Significant differences noted, with p value noted as <0.1 and significant differences labeled.
TLR = Toll-Like receptor; STING = Stimulator of Interferon Genes; DMM = destabilization of medial meniscus; m = meters; s = seconds.

Joint immune transcriptome responses to intra-articular therapy – To further understand how intra-articular injection affected the overall immune transcriptome of the joint, mice were treated by intra-articular injection of activated or non-activated MSC, and 24h later RNA was extracted from harvested joint tissues and analyzed via bulk RNA sequencing. Comparisons between the transcriptome of stifle (knee) joints that were treated with STING-pathway activated -MSC compared to MSC, TLR3-pathway activated-MSC vs. MSC, and STING pathway activated -MSC vs. TLR3 pathway activated-MSC were performed and described below. Additional comparisons between each treatment group to control needle insertion alone are provided in Supplemental Document 2.

Comparison of knee joint tissues from STING-pathway activated-MSC to MSC treated animals demonstrated significant upregulation of 24 genes and downregulation of 103 genes (significance defined as fold change ≥ 2 or ≤ -2 or P value ≤ 0.05) (Figure 3A). Differential gene expression (list of genes, description, unadjusted p-value and fold-change of top 20) for upregulated (Figure 3B) and downregulated (Figure 3C) genes in differential analysis results from STING pathway activated-MSC vs. MSC treated joints. Pathway analyses show the top 15 upregulated (Figure 3D) and downregulated (Figure 3E) pathways.

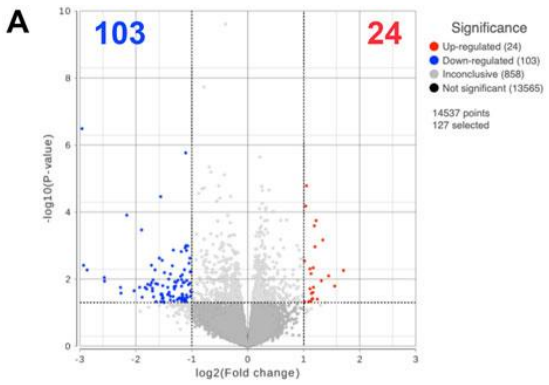

B

Gene name	Description	FDR (STING-MSC vs MSC)	Log2(Ratio) (STING-MSC vs MSC)
Adamts19	A disintegrin and metalloproteinase with thrombospondin motifs 19	3.95E-01	1.71
Themis3	Protein THEMIS3	5.96E-01	1.55
Slc6a18	Sodium-dependent neutral amino acid transporter B(0)AT3	4.71E-01	1.44
Fgfbp1	Fibroblast growth factor-binding protein 1	1.64E-01	1.34
Tph1	Tryptophan 5-hydroxylase 1	5.28E-01	1.31
Cxcl10	Interferon gamma-induced protein 10	7.61E-01	1.24
F830016B08Rik	Interferon-gamma-inducible GTPase Ifgga4 protein	7.80E-02	1.22
Mybph	Myosin-binding protein H	2.13E-01	1.20
Rasd2	GTP-binding protein Rhes	9.93E-02	1.19
Ccl22	C-C motif chemokine 22	6.13E-01	1.17
Tmc3	Transmembrane channel-like protein 3	3.75E-01	1.17
B930094E09Rik	RIKEN cDNA B930094E09 gene (Fragment)	6.91E-01	1.16
Rbm44	RNA-binding protein 44	7.60E-01	1.15
Mrgprb1	Mas-related G-protein coupled receptor member B1	7.60E-01	1.15
Timd4	T-cell immunoglobulin and mucin domain-containing protein 4	6.94E-01	1.14
Cdc34b	Cell division cycle 34B	4.36E-01	1.13
Vmn1r4	Vomeronasal type-1 receptor	7.82E-01	1.13
Actc1	Actin, alpha cardiac muscle 1	6.29E-01	1.11
Cyp2c23	Cytochrome P450 2C44	3.83E-01	1.11
Shisal1	Protein shisa-like-1	7.84E-01	1.09

C

Gene name	Description	FDR step up (STING-MSC vs MSC)	Log2(Ratio) (STING-MSC vs MSC)
Fosb	Protein FosB	1.58E-03	-2.96
Tnfaip6	Tumor necrosis factor-inducible gene 6 protein	3.48E-01	-2.93
Gldn	Gliomedin	3.89E-01	-2.87
Tnr	Tenascin-R	4.97E-01	-2.56
Crabp2	Cellular retinoic acid-binding protein 2	5.31E-01	-2.56
Crlf1	Cytokine receptor-like factor 1	6.13E-01	-2.27
C1qtnf3	Complement C1q tumor necrosis factor-related protein 3	6.92E-01	-2.27
Gabrb1	Gamma-aminobutyric acid receptor subunit beta-1	6.59E-02	-2.16
Adamts16	A disintegrin and metalloproteinase with thrombospondin motifs 16	6.67E-01	-2.03
Lrrc15	Leucine-rich repeat-containing protein 15	6.13E-01	-1.93
Npas2	Neuronal PAS domain-containing protein 2	1.21E-01	-1.90
Mgarp	Protein MGARP	7.37E-01	-1.89
Syna	Syncytin-A	6.13E-01	-1.83
Mmp3	Stromelysin-1	6.29E-01	-1.81
Kcnd3	Potassium voltage-gated channel subfamily D member 3	5.75E-01	-1.79
Myh13	Myosin, heavy polypeptide 13, skeletal muscle	5.84E-01	-1.74
Slc39a2	Solute carrier family 39 (zinc transporter), member 2	3.48E-01	-1.72
Nfasc	Neurofascin	5.51E-01	-1.72
Snap91	Clathrin coat assembly protein AP180	6.28E-01	-1.70
Frmd5	FERM domain-containing protein 5	6.74E-01	-1.70

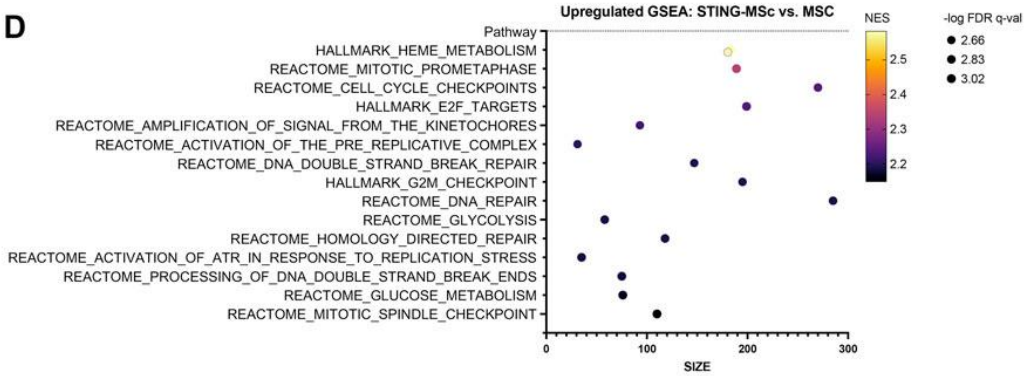

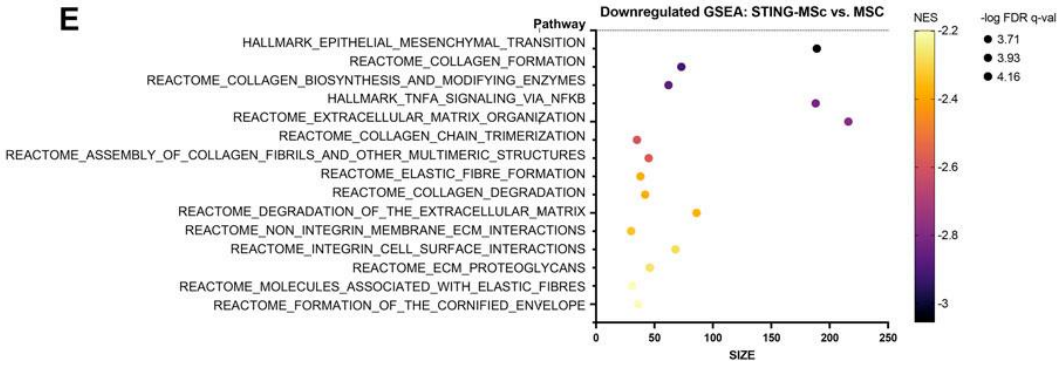

Figure 3. RNA sequencing analysis comparing transcriptomes of joint tissues from mice treated with STING-MSC versus MSC. Volcano plot of transcriptome from $n = 5$ biological replicates of STING-MSC versus MSC treated mouse knee joints **(A)**. X-axis shows fold change and y-axis shows FDR adjusted *p*-value, with significantly upregulated genes shown as red dots

and significantly downregulated genes shows as blue dots. Significance defined as FDR ≤0.05 fold change ≥2 or ≤−2. Differential gene expression (list of genes, description, unadjusted *p*-value and fold-change of top 20) for upregulated **(B)** and downregulated **(C)** genes in differential analysis results from STING-MSC versus MSC treated joints. Pathway analyses of differential gene expression were performed using normalized counts from $n = 5$ biological replicates of mice treated with either STING-MSC or MSC alone, indicating the top upregulated **(D)** and downregulated **(E)** pathways. FC, Fold Change; FDR, false discovery rate; MSC, mesenchymal stromal cells; TLR, Toll-Like receptor; STING, Stimulator of Interferon Genes.

Comparison of knee joint tissues from TLR3 pathway activated-MSC to MSC treated animals demonstrated significant upregulation of 16 genes and downregulation of 26 genes (significance defined as fold change ≥ 2 or ≤ −2 or P value ≤0.05) (Figure 4A). Differential gene expression (list of genes, description, unadjusted p-value and fold-change of top 20) for upregulated (Figure 4B) and downregulated (Figure 4C) genes in differential analysis results from TLR3-MSC vs. MSC treated joints. Pathway analyses highlighted the top 15 upregulated (Figure 4D) and top 15 downregulated (Figure 4E) pathways.

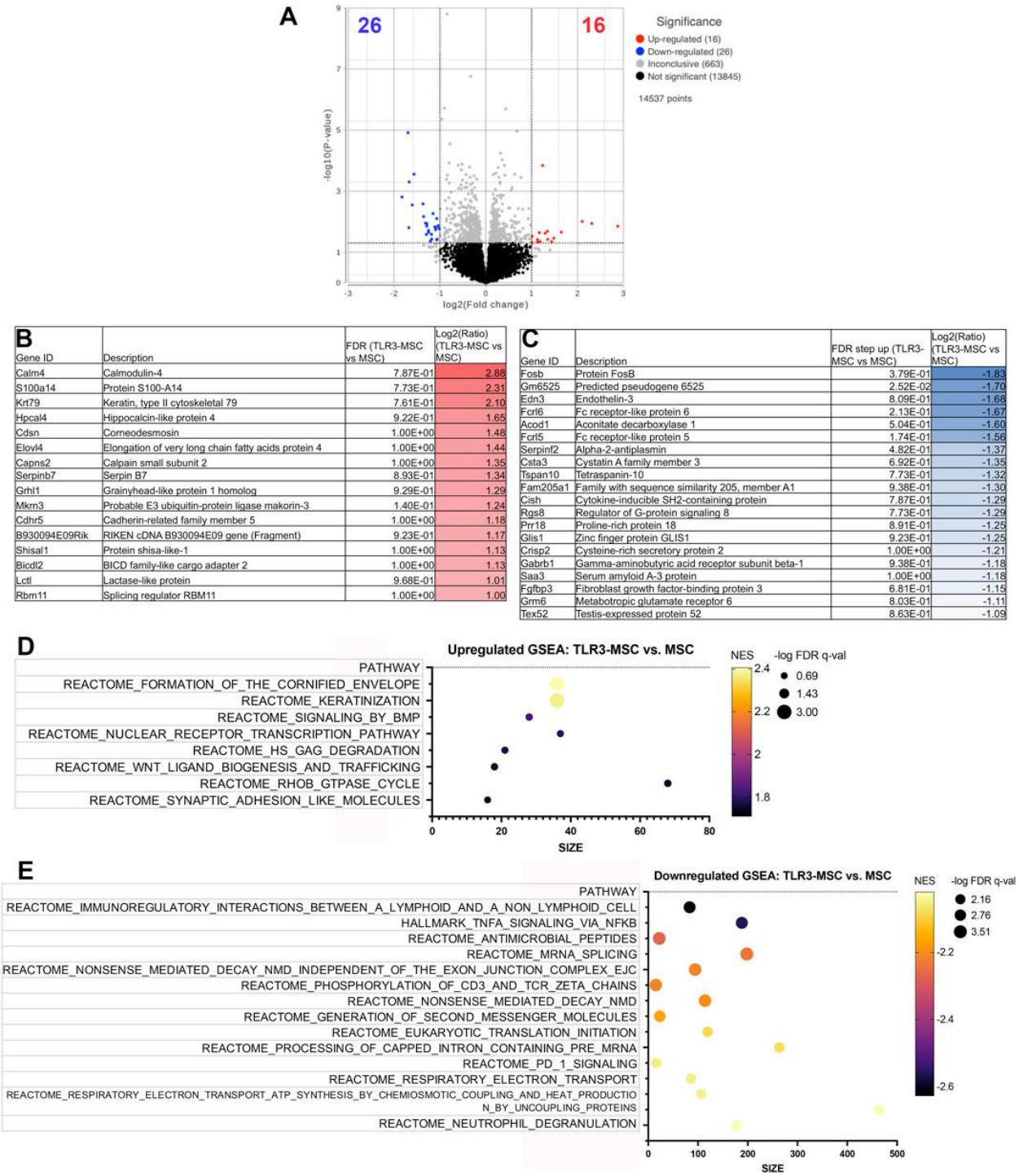

B

Gene ID	Description	FDR (TLR3-MSC vs MSC)	Log2(Ratio) (TLR3-MSC vs MSC)
Calm4	Calmodulin-4	7.87E-01	2.88
S100a14	Protein S100-A14	7.73E-01	2.31
Krt79	Keratin, type II cytoskeletal 79	7.61E-01	2.10
Hpcal4	Hippocalcin-like protein 4	9.22E-01	1.65
Cdsn	Corneodesmosin	1.00E+00	1.48
Elovl4	Elongation of very long chain fatty acids protein 4	1.00E+00	1.44
Capns2	Calpain small subunit 2	1.00E+00	1.35
Serpinb7	Serpin B7	8.93E-01	1.34
Grhl1	Grainyhead-like protein 1 homolog	9.29E-01	1.29
Mkrn3	Probable E3 ubiquitin-protein ligase makorin-3	1.40E-01	1.24
Cdhr5	Cadherin-related family member 5	1.00E+00	1.18
B930094E09Rik	RIKEN cDNA B930094E09 gene (Fragment)	9.23E-01	1.17
Shisal1	Protein shisa-like-1	1.00E+00	1.13
Bicdl2	BICD family-like cargo adapter 2	1.00E+00	1.13
Lctl	Lactase-like protein	9.68E-01	1.01
Rbm11	Splicing regulator RBM11	1.00E+00	1.00

C

Gene ID	Description	FDR step up (TLR3-MSC vs MSC)	Log2(Ratio) (TLR3-MSC vs MSC)
Fosb	Protein FosB	3.79E-01	-1.83
Gm6525	Predicted pseudogene 6525	2.52E-02	-1.70
Edn3	Endothelin-3	8.09E-01	-1.68
Fcrl6	Fc receptor-like protein 6	2.13E-01	-1.67
Acod1	Aconitate decarboxylase 1	5.04E-01	-1.60
Fcrl5	Fc receptor-like protein 5	1.74E-01	-1.56
Serpinf2	Alpha-2-antiplasmin	4.82E-01	-1.37
Csta3	Cystatin A family member 3	6.92E-01	-1.35
Tspan10	Tetraspanin-10	7.73E-01	-1.32
Fam205a1	Family with sequence similarity 205, member A1	9.38E-01	-1.30
Cish	Cytokine-inducible SH2-containing protein	7.87E-01	-1.29
Rgs8	Regulator of G-protein signaling 8	7.73E-01	-1.29
Prr18	Proline-rich protein 18	8.91E-01	-1.25
Glis1	Zinc finger protein GLIS1	9.23E-01	-1.25
Crisp2	Cysteine-rich secretory protein 2	1.00E+00	-1.21
Gabrb1	Gamma-aminobutyric acid receptor subunit beta-1	9.38E-01	-1.18
Saa3	Serum amyloid A-3 protein	1.00E+00	-1.18
Fgfbp3	Fibroblast growth factor-binding protein 3	6.81E-01	-1.15
Grm6	Metabotropic glutamate receptor 6	8.03E-01	-1.11
Tex52	Testis-expressed protein 52	8.63E-01	-1.09

Figure 4. RNA sequencing analysis comparing transcriptomes of joint tissues from mice treated with TLR3-MSC versus MSC. Volcano plot of transcriptome from $n = 5$ biological replicates of TLR3-MSC versus MSC treated mouse knee joints **(A)**. X-axis shows fold change and y-axis shows FDR adjusted *p*-value, with significantly upregulated genes shown as red dots and significantly downregulated genes shows as blue dots. Significance defined as FDR ≤0.05 fold change ≥2 or ≤−2. Differential gene expression (list of genes, description, unadjusted *p*-value and fold-change of top 20) for upregulated **(B)** and downregulated **(C)** genes in differential

analysis results from TLR3-MSC versus MSC treated joints. Pathway analyses of differential gene expression were performed using normalized counts from $n = 5$ biological replicates of mice treated with either TLR3-MSC or MSC alone, indicating the top upregulated **(D)** and downregulated **(E)** pathways. FC, Fold Change; FDR, false discovery rate; MSC, mesenchymal stromal cells; TLR, Toll-Like receptor; STING, Stimulator of Interferon Genes.

Direct comparison of knee joint tissues from STING pathway activated-MSC vs. TLR3 pathway activated-MSC treated animals demonstrated significant upregulation of 15 genes and downregulation of 190 genes (significance defined as fold change ≥ 2 or ≤ -2 or P value ≤ 0.05) (Figure 5A). A Venn diagram of differentially expressed genes for each comparison group is illustrated in Figure 5B. Differential gene expression (list of genes, description, unadjusted p-value and fold-change of top 20) for upregulated (Figure 5C) and downregulated (Figure 5D) genes in differential analysis results from STING-MSC vs. TLR3-MSC treated joints indicating the top 15 upregulated (Figure 5E) and downregulated (Figure 5F) pathways.

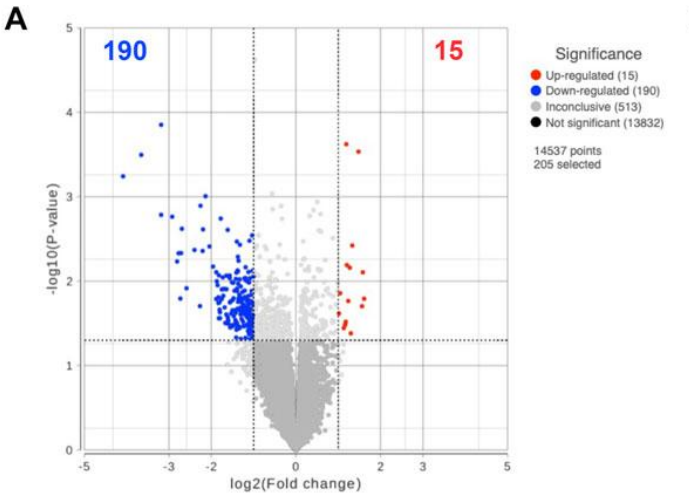

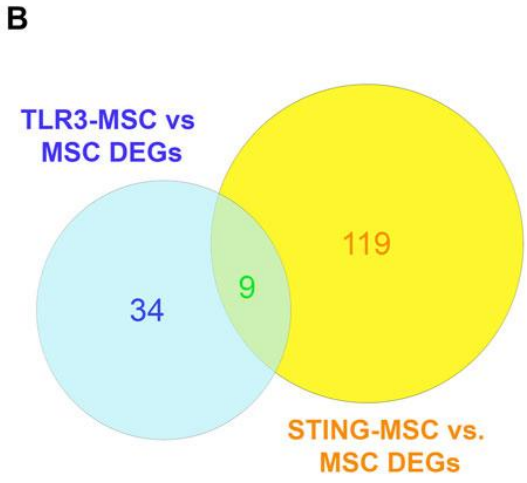

C

Gene name	Description	FDR (STING-MSC vs TLR3-MSC)	Log2(Ratio) (STING-MSC vs TLR3-MSC)
Ppp1r36	Protein phosphatase 1 regulatory subunit 36	9.09E-01	1.61
Ddx43	RNA helicase	9.09E-01	1.58
Adamts13	A disintegrin and metalloproteinase with thrombospondin motifs 13	9.09E-01	1.56
Serpina1b	Alpha-1-antitrypsin 1-2	9.09E-01	1.48
Grm6	Metabotropic glutamate receptor 6	9.09E-01	1.33
Scg3	Secretogranin-3	9.09E-01	1.30
Smim41	Small integral membrane protein 41	9.09E-01	1.27
Rgs8	Regulator of G-protein signaling 8	9.09E-01	1.24
Fcrl5	Fc receptor-like protein 5	9.09E-01	1.20
Syn3	Synapsin-3	9.09E-01	1.19
Slc6a18	Sodium-dependent neutral amino acid transporter B(0)AT3	9.09E-01	1.18
Prr18	Proline-rich protein 18	9.09E-01	1.16
Acod1	Aconitate Decarboxylase 1	9.09E-01	1.13
Cdc34b	Cell division cycle 34B	9.09E-01	1.04
Gbp6	Guanylate-binding protein 6	9.09E-01	1.02
Gm12185	Predicted gene 12185	9.09E-01	0.99
Xlr	X-linked lymphocyte-regulated protein PM1	9.09E-01	0.98
Tgtp2	T-cell-specific guanine nucleotide triphosphate-binding protein 2	9.09E-01	0.95
Gm6525	Predicted pseudogene 6525	9.09E-01	0.95
Cytl1	Cytokine-like 1	9.09E-01	0.90

D

Gene name	Description	FDR (STING-MSC vs TLR3-MSC)	Log2(Ratio) (STING-MSC vs TLR3-MSC)
Calm4	Calmodulin-4	9.09E-01	-4.08
Tnfaip6	Tumor necrosis factor-inducible gene 6 protein	9.09E-01	-3.66
Krt79	Keratin, type II cytoskeletal 79	9.09E-01	-3.19
Crabp2	Cellular retinoic acid-binding protein 2	9.09E-01	-3.19
S100a14	Protein S100-A14	9.09E-01	-2.92
C1qtnf3	Complement C1q tumor necrosis factor-related protein 3	9.09E-01	-2.81
Tnr	Tenascin-R	9.09E-01	-2.77
Cadm2	Cell adhesion molecule 2	9.09E-01	-2.73
Crlf1	Cytokine receptor-like factor 1	9.09E-01	-2.71
Adamts16	A disintegrin and metalloproteinase with thrombospondin motifs 16	9.09E-01	-2.70
Gldn	Gliomedin	9.09E-01	-2.59
Il11	Interleukin-11	9.09E-01	-2.40
Pappa2	Pappalysin 2	9.09E-01	-2.27
Kcnj15	ATP-sensitive inward rectifier potassium channel 15	9.09E-01	-2.25
Steap1	Metalloreductase STEAP1	9.09E-01	-2.21
Snap91	Clathrin coat assembly protein AP180	9.09E-01	-2.20
Hcn1	Potassium sodium hyperpolarization-activated cyclic nucleotide-gated channel 1	9.09E-01	-2.14
Pcdhgc5	Pcdhgc5 protein	9.09E-01	-2.04
Sv2c	Synaptic vesicle glycoprotein 2C	9.09E-01	-1.96
Timp1	Metalloproteinase inhibitor 1	9.09E-01	-1.88

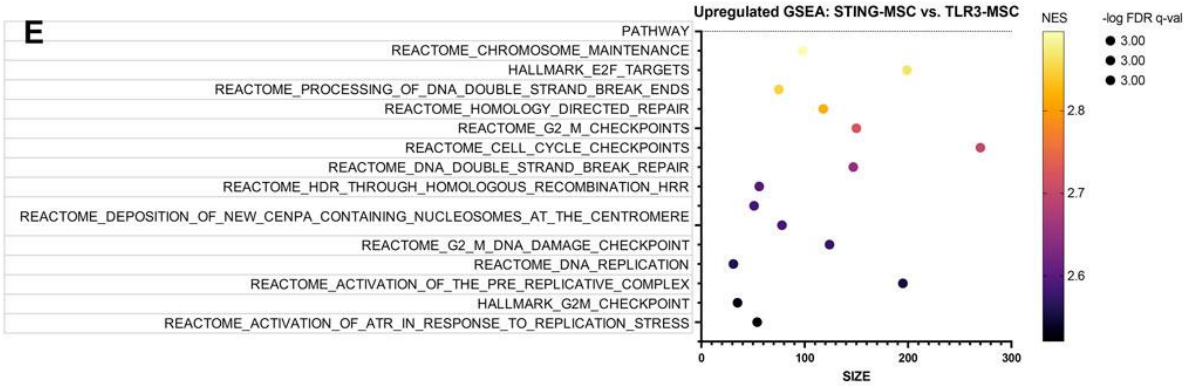

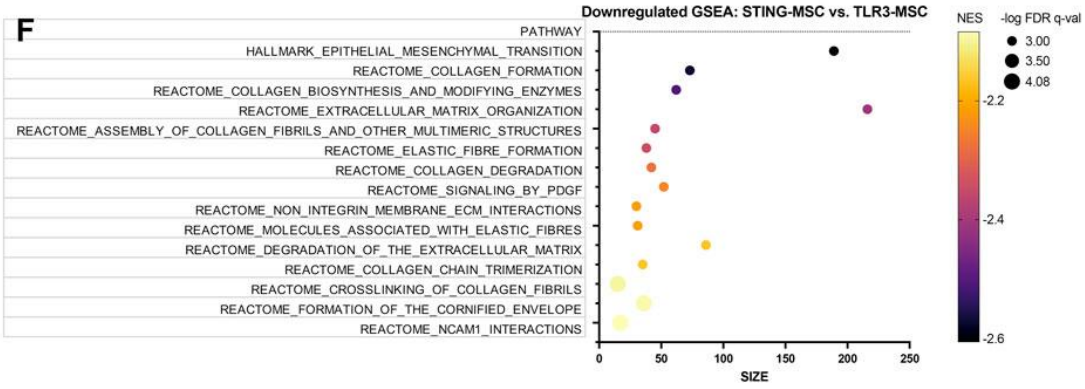

Figure 5. RNA sequencing analysis comparing transcriptomes of joint tissues from mice treated with STING-MSC versus TLR3-MSC. Volcano plot of transcriptome from $n = 5$ biological replicates of TLR3-MSC versus MSC treated mouse knee joints **(A)**. X-axis shows fold change and y-axis shows FDR adjusted *p*-value, with significantly upregulated genes shown as red dots and significantly downregulated genes shown as blue dots. Significance defined as FDR ≤0.05 fold change ≥2 or ≤−2. Venn diagram of differentially expressed genes for each comparison group and to resting MSC **(B)**. Differential gene expression (list of genes, description, unadjusted *p*-value and fold-change of top 20) for upregulated **(C)** and downregulated **(D)** genes in differential analysis results from TLR3-MSC versus MSC treated joints. Pathway analyses of differential gene expression were performed using normalized counts from $n = 5$ biological replicates of mice treated with either TLR3-MSC or MSC alone, indicating the top upregulated **(E)** and downregulated **(F)** pathways. FC, Fold Change; FDR, false discovery rate; MSC, mesenchymal stromal cells; TLR, Toll-Like receptor; STING, Stimulator of Interferon Genes.

Impact of treatment on histologic joint scoring – We evaluated the impact of intra-articular treatment on joint pathology according to an updated quantitative joint-wide histopathological scoring system of murine post-traumatic osteoarthritis models. Medial and lateral scores were assigned for synovitis and for the femur and tibia individually, which were combined to obtain the overall medial and lateral scores that were added to achieve the total joint score. In untreated control animals receiving DMM, there was synovitis, fibrillation, clefts in the medial and/or lateral compartments, and, in some instances, osteophytes on the medial aspect of the joint (representative images, Figure 6).

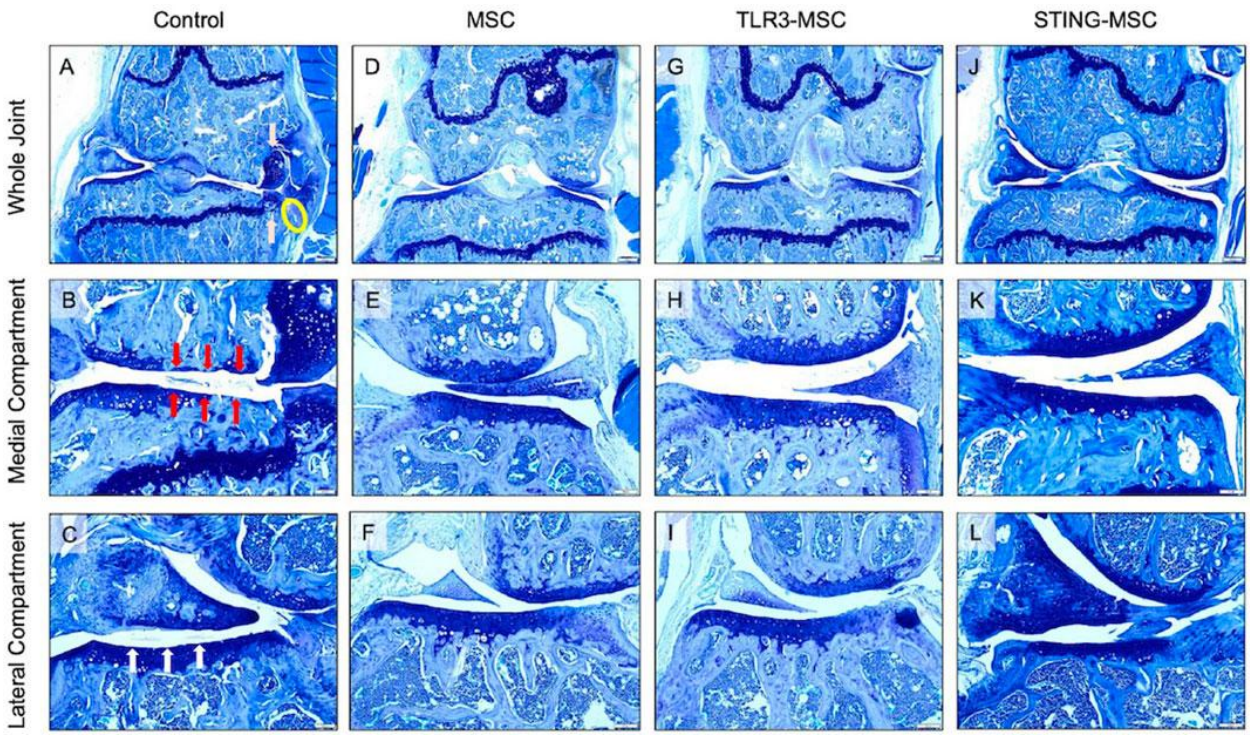

Figure 6. Histologic representative images of mouse knees at endterm. Toluidine blue photomicrographs from (left to right) control (needle insertion alone), MSC, TLR3-MSC, and STING-MSC treated (right) limbs. Low magnification (×4) images of whole knee joints from (left to right) control **(A)**, MSC **(D)**, TLR3-MSC **(G)**, and STING-MSC **(J)** treated joints. Higher magnification (×10) images presented for evaluation of the medial compartment of (left to right) control **(B)**, MSC **(E)**, TLR3-MSC **(H)**, and STING-MSC **(K)** treated joints. Additional higher magnification image for evaluation of the lateral compartment for control **(C)**, MSC **(F)**, TLR3-MSC **(I)** and STING-MSC **(L)** treated joints. **(A,D,G,J)** 4x, scale bar = 200 μm; **(B,C,E,F,H,I,K,L)** 10x, scale bar = 20 μm. Pink arrows represent mostly cartilagenous osteophytes. The yellow circle indicates synovitis. Red arrows highlight areas of cartilage loss to below the calcified layer. White arrows outline a roughened cartilage surface, as well as fibrillation. MSC, mesenchymal stromal cells; TLR, Toll-Like receptor; STING, Stimulator of Interferon Genes.

Overall joint scores (p=0.0003, p=0.05) and medial compartment scores (p=0.0003, p=0.05) were improved in STING-MSC treated joints compared to control and MSC-treated, respectively (Figure 7A,B). Lateral compartment scores were also improved in STING-MSC treated vs. control joints (p=0.001) (Figure 7C). Overall joint and medial compartment scores (p=0.05, p=0.05) were improved in TLR3-MSC treated joints compared to control joints.

Additional scored and individual OARSI parameters for tibia, femur, and synovium in the medial (Figure 7D-F) and lateral compartments (Figure 7G-I) are presented.

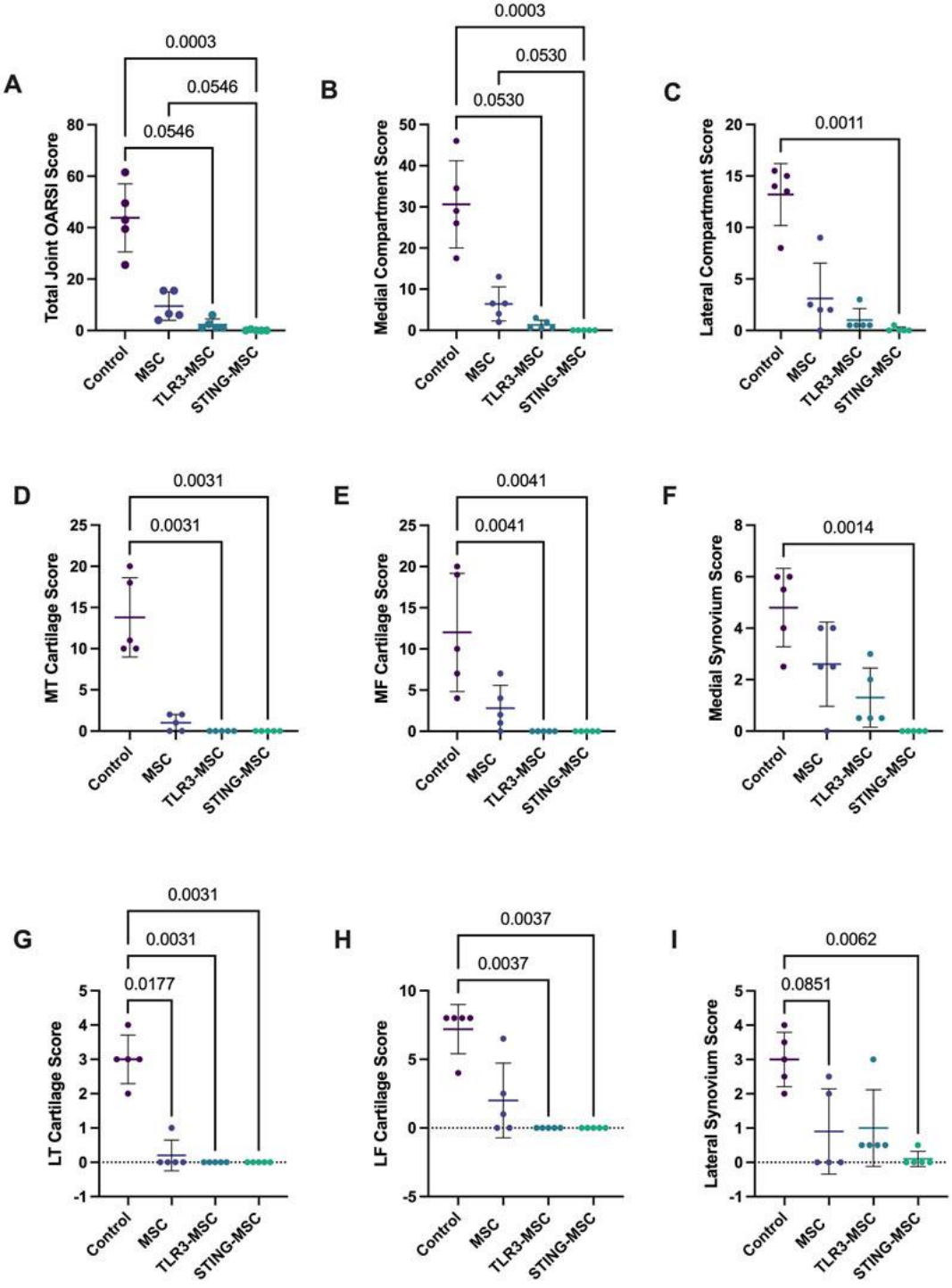

Figure 7. OARSI histopathology scores. Scoring of histology slides was performed following DMM surgery and treatment with control (needle insertion alone), MSC, TLR3-MSC, or

STING-MSC. Parameters listed include whole joint OARSI total score **(A)**, medial compartment total score **(B)**, lateral compartment total score **(C)**, medial tibial cartilage score **(D)**, medial femoral cartilage **(E)**, medial synovium score **(F)**, lateral tibial cartilage score **(G)**, lateral femoral cartilage score **(H)**, lateral synovium score **(I)**. Significant differences noted with p values < 0.05. MSC, mesenchymal stromal cells; TLR, Toll-Like receptor; STING, Stimulator of Interferon Genes.

2.5 Discussion

Intra-articular mesenchymal stromal cell products have demonstrated therapeutic potential in preclinical models of OA previously with varied results reported for efficacy. The findings reported here add to the body of literature regarding the use of regenerative therapies to treat OA, highlighting the potential for STING agonism of MSCs to enhance both functional outcomes and structural joint integrity while promoting transcriptional pathways favoring tissue repair. This was demonstrated via significant improvement in voluntary movement parameters (adjusted time mobile, maximum speed, time spent in hut) and differential gene expression in joint tissues favoring a tissue healing environment with upregulated genes associated with remodeling, cell proliferation and angiogenesis. Importantly, all MSC treated groups also showed improved cartilage integrity and synovial scores compared to control animals.

Pattern recognition receptors (PRRs) play a key role in immune and sensory nervous system regulation of pain and inflammation in injury.[38] Following tissue damage, PRRs on immune cells are activated to initiate an inflammatory response and sensory neurons concurrently sense these signals PRR expression themselves. In this environment, stimulator of IFN genes (STING) has been recognized as a regulator of pain signaling, where activation of STING receptors has been demonstrated to result in production of type I IFNs in immune cells and sensory neurons and subsequently to elicit antinociceptive effects in neuropathic mice[24-27]. Conversely, deletion of the STING gene has been shown to result in mechanical allodynia[24].

While seemingly counterintuitive to induce production of pro-inflammatory mediators associated with further pain propagation, recent evidence indicates that inflammation can contribute to resolution of pain through further induction of counter-regulatory anti-inflammatory mediators[39]. Studies exploring the STING/IFN-1 signaling pathway to alleviate pain have yielded conflicting results, indicating STING agonism and IFN-1 production can be both pro- and anti-inflammatory depending on the context in which they are evaluated. For example, STING agonism has produced antinociceptive effects in the central nervous system while STING agonists or IFN-1 injected peripherally have also elicited nociceptive behaviors suggesting pain induction[28,40-42]. In a rodent model of inflammatory pain, inflammation-induced activation of STING in dorsal root ganglia nociceptors reduced pain-like behaviors[43]. Using a gain-of-function STING mutation model, type I IFN regulation of voltage-gated potassium channels were identified as the mechanism behind this observed reduction in pain[43]. As discussed further below, here we demonstrated enhanced mobility suggesting alleviation of pain, limited structural disease progression in joints evidenced by improved histologic scores, and induction of interferon related genes in synovial tissues of mice with induced post-traumatic osteoarthritis treated with STING-activated MSC. Further investigation into the mechanisms by which induction of inflammatory pathways with STING agonism reduces pain and limits disease progression in the context of OA may expand our approaches to treat chronic persistent musculoskeletal pain in this context.

Loss of mobility and articular associated pain are primary reasons for individuals with OA to seek treatment. Therefore, cage monitoring, or ‘open field testing’ of functional activity which we performed here can offer insights as to voluntary behavior and mobility differences relative to baseline as an indication of pain following injury. In this study, by eight weeks post-DMM surgery, mice injected with two doses of STING-MSC demonstrated increased activity,

evidenced by greater adjusted time mobile and less time in their security huts, implying potential differences in clinical or pain responses between groups. Additionally, STING-MSC treated animals exhibited the greatest number of entries to the top of their hut compared to other treatment groups, which reached significance compared to TLR-MSC treated mice at week 6. In this hindlimb injury model, this may indicate an increased willingness to climb, use and propel off the injured to enter the top of the hut, potentially indicating earlier return to full hind limb function. These findings support previous studies in humans where intra-articular cellular based therapies have been reported to decrease pain and improve functionality in knee OA, resulting in increased physical wellness overall[44,45].

When comparing differentially expressed genes and transcriptomic pathway analyses between treatment groups, treatment of joints with STING pathway activated MSC resulted in upregulation of gene pathways associated with tissue remodeling, cell motility and invasion, cell proliferation and angiogenesis and downregulation of genes associated with inflammatory cytokine production and epidermal barrier formation. Several gene signatures emerged as being potentially particularly relevant to how these two immune pathways (TLR3 and STING pathways) might be functioning to improve joint function. The one common denominator between the two pathways is strong stimulation of interferon pathways, including all 3 major pathways (type I, type II, and type III IFN pathways).[38] As discussed, IFN-related genes have been previously implicated in the resolution of inflammatory pain[37], although the role of type I IFNs in this regard remains controversial with reports supporting both pro- and anti-nociceptive actions of IFN-α and IFN-β.[46] Other potential functions of upregulated IFN pathways in slowing joint degeneration include stimulation of counter-regulatory immune pathways (*e.g.,* IDO pathway, PD-L1 and other checkpoint molecule expression, expansion of Tregs, recruitment of

immune suppressive monocytes), all of which may contribute to reducing joint inflammation and preserving cartilage integrity, and suppression of deleterious vascular responses by suppressing abnormal angiogenesis[38]. Importantly, a recent publication also highlighted the role of IFN-g in stimulating cartilage regeneration[47]. Other IFN-regulated pathways may also be involved in improved joint function following injection of activated MSCs. For example, alterations in tryptophan metabolism have been previously associated with occurrence, and development of OA[48]. In joints of STING pathway activated-MSC treated mice, one of the most upregulated genes was tryptophan 5-hydroxylase, an enzyme essential to synthesis of the neurotransmitter, serotonin. Tryptophan metabolite disturbances have been associated with erosive hand osteoarthritis in people[49] and conversely, supplementation of tryptophan metabolites including 5-hydroxytryptophan have been shown to suppress inflammation and arthritis through suppression of pro-inflammatory mediator production in a rodent inflammatory collagen-induced arthritis model[50]. These findings provide further mechanistic insight as to possible mode of action through which STING and TLR3 pathway activated-MSC may be exerting a therapeutic effect in early post-traumatic OA, relating differential gene expression on the cellular level to improvement seen functionally and structurally on histology. Thus, there is precedent for multiple different IFN pathways being critically involved in reducing joint inflammation, improving mobility, and cartilage integrity.

Histopathology remains the gold standard in animal models to assess structural disease in OA pathology characterized by progressive articular cartilage degradation and osteophyte development[51-53]. In small animal (*i.e.,* rodent) species, evaluation of the entire joint in a single plane allows simultaneous examination of the entire joint, including pathological changes in cartilage degradation, synovial inflammation and fibrosis, meniscal tearing and bone remodeling

including marginal osteophytes or enthesiophytes and subchondral sclerosis. Multiple scoring systems have been reported for histopathological evaluation of the mouse knee OA[54-60], with the destabilization of the medial meniscus (DMM) model presented here representing a reproducible animal model that allows longitudinal evaluation of disease. Haubruck *et al.* further developed a semi-quantitative mouse-OA histopathology scoring system to grade cartilage as well as synovium, meniscus, cruciate ligaments, subchondral bone and marginal osteophytes/enthesiophytes, demonstrating evaluation of a single slide allowed reproducible grading of histopathological changes in joint tissues in this model and reduced scoring time without compromising sensitivity and specificity of results[35]. Using this scoring system, here we notably demonstrated significant improvement in total joint and medial compartment scores with STING pathway activated-MSC treatment compared to control (needle insertion alone) and non-activated MSC, as well as improvement in the lateral compartment between STING pathway activated-MSC to control. When medial and lateral compartments were examined separately, we further demonstrated significant improvement between STING pathway activated-MSC versus control for both medial and lateral tibial and femoral cartilage and synovium scores. TLR3 pathway activated-MSC therapy also resulted in improvement, albeit to a lesser extent compared to STING pathway activated-MSC in overall joint and medial compartment scores compared to needle insertion alone. As animal models remain the foundation for development of therapeutic interventions for human OA with histopathology considered the gold standard for assessment, these findings underscore the potential for immune activated cellular therapy, particularly STING pathway-activated MSC, to mitigate structural disease progression.

Limitations to this study include the relatively short study duration (eight weeks), although this has been reported and considered typical for this model of OA previously. The

mouse DMM model was selected as the first *in vivo* model to initially screen the immune-licensed MSC treatment described due to the low cost of working with rodent models, high reproducibility of the model, fewer/more localized cartilage defects compared to other rodent models (*e.g.,* anterior cruciate ligament transection) making it easier to assess treatment effect, and slower disease progression that more closely mimics human OA, allowing for relatively consistent evaluation of pain-associated behaviors[35,66,67]. Although significant differences in gait parameters and histopathologic findings were seen between treatment groups by eight weeks postoperatively, additional information may have been gained by allowing OA to progress for a more prolonged period. Additionally, mice in this study were operated and evaluated following skeletal maturity at 12 weeks of age which would simulate post-traumatic OA in an early adult population (*i.e.,* mid-twenties); however, it is recognized that knee OA in humans frequently occurs in middle age to elderly patients and further evaluation of this treatment strategy at later age time points would be valuable. The lack of sham-operated controls is acknowledged as a study limitation; however, this work was designed to specifically assess acute changes following cell injection and impact of activation procedures rather than further delineating the DMM model.

Furthermore, this study evaluated outcomes following two MSC injections at three- and five-weeks post-injury, the timing of which was based upon initial pilot studies (not shown). The MSC used in this study underwent minor phenotypic characterization and it is acknowledged that more detailed MSC phenotyping may be required to sufficiently replicate these data due to heterogeneity in MSC populations and potential variation in isolation protocols between laboratories. Further assessment of injection number, timing of injection(s) during the temporal course of disease progression and dose with an expanded examination of control groups may

demonstrate greater improvement and/or provide further information as to the effect of the immune-licensed cellular products. Addition of treatment groups injecting the MSC secretome or extracellular vesicles (EVs) derived from of these immune-activated MSCs were not within the scope of this study; however, evaluation of the impact of immune licensing on immunosuppressive function of EVs or secreted products generated under different culture methods (*e.g.,* 3D vs. 2D monolayer culture) represent future directions of this work. Finally, the use of fetal bovine serum (FBS) in growth media during isolation, culture, and expansion of MSC before immune licensing is acknowledged as a limitation; while the use of FBS in preclinical models is accepted, evaluation of alternate serum-free sources is warranted prior to future translational applications. The findings herein warrant further investigation in additional studies designed to elucidate more specific mechanisms underlying the effect and expanding to large animal models of OA.

In summary, these findings provide key insights into the functional, transcriptomic, and histologic synovial response to intra-articular immune activated (pIC or 2'3'-cGAMP) activated MSC therapy. Notably, all three MSC therapeutic approaches improved histologic outcomes in this model, while STING-pathway activated-MSC treatment and TLR3-pathway activated MSC resulted in further improvement in key functional parameters and induced transcriptomic changes promoting tissue repair. These findings provide further mechanistic insight as to possible mode of action through which STING and TLR3 pathway activated-MSC may be exerting a therapeutic effect in early post-traumatic OA, relating differential gene expression on the cellular level to improvement seen functionally and structurally on histology. Thus, there is a precedent for multiple different IFN pathways being critically involved in reducing joint inflammation and improving mobility and cartilage integrity. These findings suggest that pre-

activation of MSC with stimuli that induce strong IFN responses could be a successful strategy to improve the overall effectiveness of cellular therapy for OA.

References

1. Yelin E, Weinstein S, King T. The burden of musculoskeletal diseases in the United States. Semin Arthritis Rheum. *2016;*46:259-260.

2. Cui A, Li H, Wang D., et al. Global, regional prevalence, incidence and risk factors of knee osteoarthritis in population-based studies. EClinicalMedicine, 2020;29-30:100587.

3. Mezey E, Nemeth K. Mesenchymal stem cells and infectious diseases: smarter than drugs. Immunol Lett. 2015;168:208-14.

4. Cortes-Araya Y, Amilon K, Rink BE, et al. Comparison of antibacterial and immunological properties of mesenchymal stem/stromal cells from equine bone marrow, endometrium, and adipose tissue. Stem Cells Dev 2018;27:1518-25.

5. Ghannam S, Bouffi C, Djouad F, et al. Immunosuppression by mesenchymal stem cells: mechanisms and clinical applications. Stem Cell Res Ther 2018;1:2.

6. Kwon DG, Kim MK, Jeon YS, et al. State of the Art: The immunomodulatory role of MSCs for osteoarthritis. Int J Mol Sci 2022;23:1618.

7. Chahla J, Dean CS, Moatshe G, et al. Concentrated Bone Marrow Aspirate for the Treatment of Chondral Injuries and Osteoarthritis of the Knee: A Systematic Review of Outcomes. Orthop J Sports Med 2016;4:2325967115625481.

8. Harrell CR, Markovic BS, Fellabaum C, et al. Mesenchymal stem cell-based therapy of osteoarthritis: Current knowledge and future perspectives. Biomed Pharmacother 2019;109:2318-26.

9. Iijima H, Isho T, Kuroki H, et al. Effectiveness of mesenchymal stem cells for treating patients with knee osteoarthritis: a meta-analysis toward the establishment of effective regenerative rehabilitation. NPJ Regen Med 2018;3:15.

10. Li X, Wang M, Jing X, et al. Bone Marrow- and Adipose Tissue-Derived Mesenchymal Stem Cells: Characterization, Differentiation, and Applications in Cartilage Tissue Engineering. Crit Rev Eukaryot Gene Expr 2018;28:285-310.

11. Piuzzi NS, Khlopas A, Newman JM, et al. Bone Marrow Cellular Therapies: Novel Therapy for Knee Osteoarthritis. J Knee Surg 2018;31:22-6.

12. Şahin Ş, Tuncel SA, Salimi K, et al. Advanced Injectable Alternatives for Osteoarthritis. Adv Exp Med Biol 2018;1077:183-96.

13. Shah K, Zhao AG, Sumer H. New Approaches to Treat Osteoarthritis with Mesenchymal Stem Cells. Stem Cells Int 2018;2018:5373294.

14. Southworth TM, Naveen NB, Nwachukwu BU, et al. Orthobiologics for Focal Articular Cartilage Defects. Clin Sports Med 2019;38:109-22.

15. Xing D, Wang Q, Yang Z, et al. Mesenchymal stem cells injections for knee osteoarthritis: a systematic overview. Rheumatol Int 2018;38:1399-411.

16. Copp G, Robb KP, Viswanathan S. Culture-expanded mesenchymal stromal cell therapy: does it work in knee osteoarthritis? A pathway to clinical success. Cell & Mol Immunol. 2023;20:626-650.

17. Cassano JM, Schnabel, Goodale MB, et al. Inflammatory licensed equine MSCs are chondroprotective and exhibit enhanced immunomodulation in an inflammatory environment. Stem Cell Res Ther 2018;9:82.

18. Szabó E, Fajka-Boja R, Kriston-Pál É, et al. Licensing by inflammatory cytokines abolishes heterogeneity of immunosuppressive function of mesenchymal stem cell population. Stem Cells Dev. 2015;24:2171–80.

19. Krampera M. Mesenchymal stromal cell 'licensing': a multistep process. Leuk Off J Leuk Soc Am Leuk Res Fund UK. 2011;25:1408–14.

20. Polchert D, Sobinsky J, Douglas G, et al. IFN- gamma activation of mesenchymal stem cells for treatment and prevention of graft versus host disease. Eur J Immunol. 2008;38:1745–55.

21. Waterman RS, Morgenweck J, Nossaman BD, et al. Anti-inflammatory mesenchymal stem cells (MSC2) attenuate symptoms of painful diabetic peripheral neuropathy. Stem Cells Transl Med. 2012;1:557–65.

22. Murphy L, Schwartz TA, Helmick CG, et al. Lifetime risk of symptomatic knee osteoarthritis. Arthritis Rheum. 2008;59:1207-1213.

23. Donnelly CRC, et al. How do sensory neurons sense danger signals? Trends Neurosci. 2020;43(10):822-838.

24. Donnelly CRJ, Chen O, Ji R. STING controls nociception via type I interferon signaling in sensory neurons. Nature. 2021;591(7849):275-280.

25. Sun C, Wu G, Zhang Z, et al. Protein tyrosine phosphatase receptor type D regulates neuropathic pain after nerve injury via the STING-IFN-I pathway. Front Mol Neurosci. 2022;15:859166.

26. Wang K, Donnelly CR, Jiang C, et al. STING suppresses bone cancer pain via immune and neuronal modulation. Nat Commun. 2021;12(1):4558.

27. Ishikawa, HB, Glen N. STING is an endoplasmic reticulum adaptor that facilitates innnate immune signalling. Nature. 2008;455(7213):674-678.

28. Liu CC, Gao Y, Luo H, et al. Interferon alpha inhibits spinal cord synaptic and nociceptive transmission via neuronal-glial interactions. Sci Rep. 2016;6:34356.

29. Pezzanite LM, Chow L, Johnson V, et al. Toll-like receptor activation of equine mesenchymal stromal cells to enhance antibacterial activity and immunomodulatory cytokine secretion. Vet Surg 2021;50:858-71.

30. Johnson V, Webb T, Norman A, et al. Activated mesenchymal stem cells interact with antibiotics and host innate immune responses to control chronic bacterial infections. Sci Rep 2017;7:9575.

31. Pezzanite LM, Chow L, Phillips J, et al. TLR-activated mesenchymal stromal cell therapy and antibiotics that multi-drug resistant Staphylococcal septic arthritis in an equine model. Ann Transl Med.

32. Bunnell BA, Flaat M, Gagliardi C, et al. Adipose-derived stem cells: isolation, expansion and differentiation. *Methods.* 2008;45:115-120.

33. Yoshimura K, Shigeura T, Matsumoto D, et al. Characterization of freshly isolated and cultured cells derived from the fatty and fluid portions of liposuction aspirates. *J Cell Physiol.* 2006;208:64-76.

34. Glasson SS, Blanchet TJ, Morris EA. The surgical destabilization of the medial meniscus (DMM) model of osteoarthritis in the 129/SvEv mouse. *Osteo Cartilage.* 2007;15:1061-1069.

35. Haubruck P, Heller R, Blaker CL, et al. Streamlining quantitative joint-wide medial femora-tibial histopathological scoring of mouse post-traumatic knee osteoarthritis models. Osteoarthritis and Cartilage. 2023;31:1602-1611.

36. Jennions MD, Moller AP. A survey of statistical power of research in behavioral ecology and animal behavior. *Behavioral Ecology.* 2003;14:438-45.

37. Love MI, Anders S, Huber W. Analyzing RNA-seq data with DESeq2 2024. Available at https://www.bioconductor.org/packages/release/bioc/vignettes/DESeq2/inst/doc/DESeq2.html.

38. Rodriguez-Palma EJ, Allen HN, Khanna R. STINGing away the pain: the role of interferon-stimulated genes. J Clin Invest. 2024;134(9):e180497. https://doi.org/10.1172/JC180497.

39. Sugimoto MAS, et al. Resolution of inflammation: what controls its onset? Front Immunol. 2016;7:160.

40. Barragan-Iglesias P, Franco-Enzastiga U, Jeevakumar V, et al. Type I interferons act directly on nociceptors to produce pain sensitization: implications for viral infection-induced pain. J Neurosci. 2020;40(18):3517–3532.

41. Fitzgibbon M, Kerr DM, Henry RJ, et al. Endocannabinoid modulation of inflammatory hyperalgesia in the IFN-α mouse model of depression. Brain Behav Immun.2019;82:372–381.

42. Franco-Enzastiga U, Natarajan K, David ET, et al. Vinorelbine causes a neuropathic pain-like state in mice via STING and MNK1 signaling associated with type I interferon induction. iScience. 2024;27(2):108808.

43. Defaye M, Bradaia A, Abdullah NS, et al. Induction of antiviral interferon-stimulated genes by neuronal STING promotes the resolution of pain in mice. J Clin Invest. 2024;134(9):e176474.

44. El-Kadiry AE, Lumbao C, Salame N, et al. Bone marrow aspirate concentrate versus platelet-rich plasma for treating knee osteoarthritis: a one-year non-randomized retrospective comparative study. BMC Musculoskelet Disord 2022;23:23.

45. Anz AW, Hubbard R, Rendos NK, et al. Bone Marrow Aspirate Concentrate Is Equivalent to Platelet-Rich Plasma for the Treatment of Knee Osteoarthritis at 1 Year: A Prospective, Randomized Trial. Orthop J Sports Med 2020;8:2325967119900958.

46. Tan PH, Ji J, Yeh C, et al. Interferons in pain and infections: emerging roles in neuro-immune and neuro-glial interactions. Front Immunol. 2021;12:783725.

47. Kim J, Hong B, Pham T, et al. Interferon-gamma signaling promotes cartilage regeneration after injury. Scientific Reports. 2024;14:8046.

48. Yang J, Zhou P, Xu T, et al. Identification of biomarkers related to tryptophan metabolism in osteoarthritis. Biochemistry and Biophysics Reports. 2024;39:101763.

49. Binvignat M, Emond P, Mifsud F, et al. Serum tryptophan metabolites are associated with erosive hand osteoarthritis and pain: results from the DIGICOD cohort. Osteoarthritis Cartilage. 2023;31:1132-1143.

50. Yang T, Hsu P, Meng M, et al. Supplement of 5-hydroxytryptophan before induction suppresses inflammation and collagen-induced arthritis. Arthritis Res Ther. 2015;17:364.

51. Zaki S, Blaker CL, Little CB. OA foundations – experimental models of osteoarthritis. Osteoarthr Cartil 2022;30:357–80.

52. Newman S, Ahmed H, Rehmatullah N. Radiographic vs. MRI vs. arthroscopic assessment and grading of knee osteoarthritis – are we using appropriate imaging? J Exp Orthop 2022;9:2.

53. Aigner T, Cook JL, Gerwin N, et al. Histopathology atlas of animal model systems - overview of guiding principles. Osteoarthr Cartil 2010;18(Suppl.3):S2–6.

54. Glasson SS, Chambers MG, Van Den Berg WB, et al.The OARSI histopathology initiative - recommendations for histological assessments of osteoarthritis in the mouse. Osteoarthr Cartil 2010;18(Suppl.3):S17–23.

55. Chambers MG, Bayliss MT, Mason RM. Chondrocyte cytokine and growth factor expression in murine osteoarthritis. Osteoarthr Cartil 1997;5:301–8.

56. Little CB, Barai A, Burkhardt D, et al. Matrix metalloproteinase 13-deficient mice are resistant to osteoarthritic cartilage erosion but not chondrocyte hypertrophy or osteophyte development. Arthritis Rheum 2009;60:3723–33.

57. McNulty MA, Loeser RF, Davey C, et al. A comprehensive histological assessment of osteoarthritis lesions in mice. Cartilage 2011;2:354–63.

58. Sampson ER, Beck CA, Ketz J, Canary KL, Hilton MJ, Awad H, et al. Establishment of an index with increased sensitivity for assessing murine arthritis. J Orthop Res 2011;29:1145–51.

59. Pinamont WJ, Yoshioka NK, Young GM, et al. Standardized histomorphometric evaluation of osteoarthritis in a surgical mouse model. J Vis Exp 2020;159:e60991.

60. Armstrong AR, Carlson CS, Rendahl AK, et al. Optimization of histologic grading schemes in spontaneous and surgically induced murine models of osteoarthritis. Osteoarthr Cartil 2021;29 :536-46.

CHAPTER 3: Conclusions and Future Directions

Osteoarthritis causes considerable burden and significant reduction in quality of life for patients in both human and veterinary medicine[1,2]. This combined with the rising global incidence of OA cases in an aging population reveals a critical need for therapeutics that are both symptom and disease modifying and also carry minimal risk of adverse side effects[3]. Cellular therapy with MSCs has revealed promising results to enhance wound repair in multiple *in vitro* and *in vivo* animal models[4–8]. However, a literature review of MSC cellular therapy overall reveals mixed results in terms of efficacy[9]. One proposed cause for the inconsistencies in reported clinical outcomes with MSC therapy has been phenotypic heterogeneity within expanded mesenchymal stromal cell populations. MSCs' phenotype is known to be altered in response to environmental stimuli, which we hypothesized could be clinically advantageous through targeted stimulation with specific ligands. Therefore, we sought to reduce phenotypic heterogeneity and enhance functional capacity of MSC populations through *in vitro* licensing techniques.

Previous studies, including work from this lab, have demonstrated enhanced immunomodulatory tissue repair outcomes with TLR3 receptor stimulated MSCs – TLR3 agonist polyI:C was further compared to cGAS-STING receptor activated cell therapy in this study. The studies reported here support that prior work and demonstrate that intraarticular injections of immune receptor activated MSCs enhance both functional and structural outcomes in murine post-traumatic OA via destabilization of the medial meniscus. These enhanced outcomes were evident in all measured categories, including functional gait monitoring, structural histologic tissue scoring, and differential gene expression within joint associated tissues. To build upon this research, future directions of this work may include 1) expansion to an ovine large animal model,

2) investigation of whether stimulation can be enhanced through concurrent stimulation with alternate ligands in addition to STING, 3) evaluation of the secreted exosomes from MSC rather than whole MSC themselves, and/or 4) incorporation of these strategies together in a slow-release hydrogel or foam formulation (*i.e.,* STING-exosome-MSC infused multifunctional medical hydrogel foam) for human and veterinary clinical usage. Here we expand upon each of these topics in the future directions section.

Experiment 1: Evaluation of activated MSC in a large animal model. Investigation of this cellular technology in a large animal model would be critical prior to application in veterinary clinical settings (e.g., for companion animals such as horses and dogs) and ultimately humans. The optimal animal model for osteoarthritis research is complicated and typically selected based upon the study's objectives. Large animal models, such as ovine models of osteoarthritis, are excellent for their translational relevancy towards humans. This is due to their stifle joint being more comparable to humans than small animal models are, widespread occurrence of naturally occurring OA, low frequency of spontaneous OA, more comparable cartilage healing times to humans than other large animal models, ease of handling, and relatively low cost. Additionally, the overall joint size of sheep allows for the creation of multiple, relatively large, osteochondral defects (6-12mm) in a single joint, as well as possessing cartilage with up to 2mm in thickness, which is a similar size to humans and allows for both full and partial thickness tear models. However, the most considerable hurdle for ovine models is that it takes up to two years for skeletal maturity. Skeletal maturity is important for its translational relevance to humans, as OA typically occurs in the later stages of life with an aged immune system. Additionally, juvenile patients possess more robust stem cell capability, enhanced vascularity, reduced mechanical load due to lighter body weight, diminished immune

inflammatory response, and enhanced regenerative healing responses; with spontaneous healing also being much more likely before skeletal maturity. This is due to animal growth plates being open, which promotes and maintains an environment of constant growth and remodeling for structural tissues.

A proposed initial study would include seven distinct groups: 1) cGAS-STING stimulation treatment groups, 2) TLR3-pIC stimulation treatment group, 3) nonactivated (naïve) MSC treatment groups, 4) STING exosome isolate treatment group, 5) TLR3 exosome isolate treatment group, 6) STING+TLR3 exosome isolate treatment group, and 7) untreated control groups containing needle insertion and saline injection as placebo. To assess this – osteoarthritis will be unilaterally induced in ovine hind stifle (i.e. knee) joints via destabilization of the medial meniscus and subsequently treated with one of the MSC treatment groups or control group. We hypothesize that treatment with both MSC treatment groups will yield improvement in tissue quality and movement parameters, with STING-MSC treatment having an additional relative advantage over resting MSC alone. The study overview is provided in Figure 3.1.

Figure 3.1: Experiment 1. Schematic overview of study design for future directions – Evaluation of activated MSC in a large animal model.

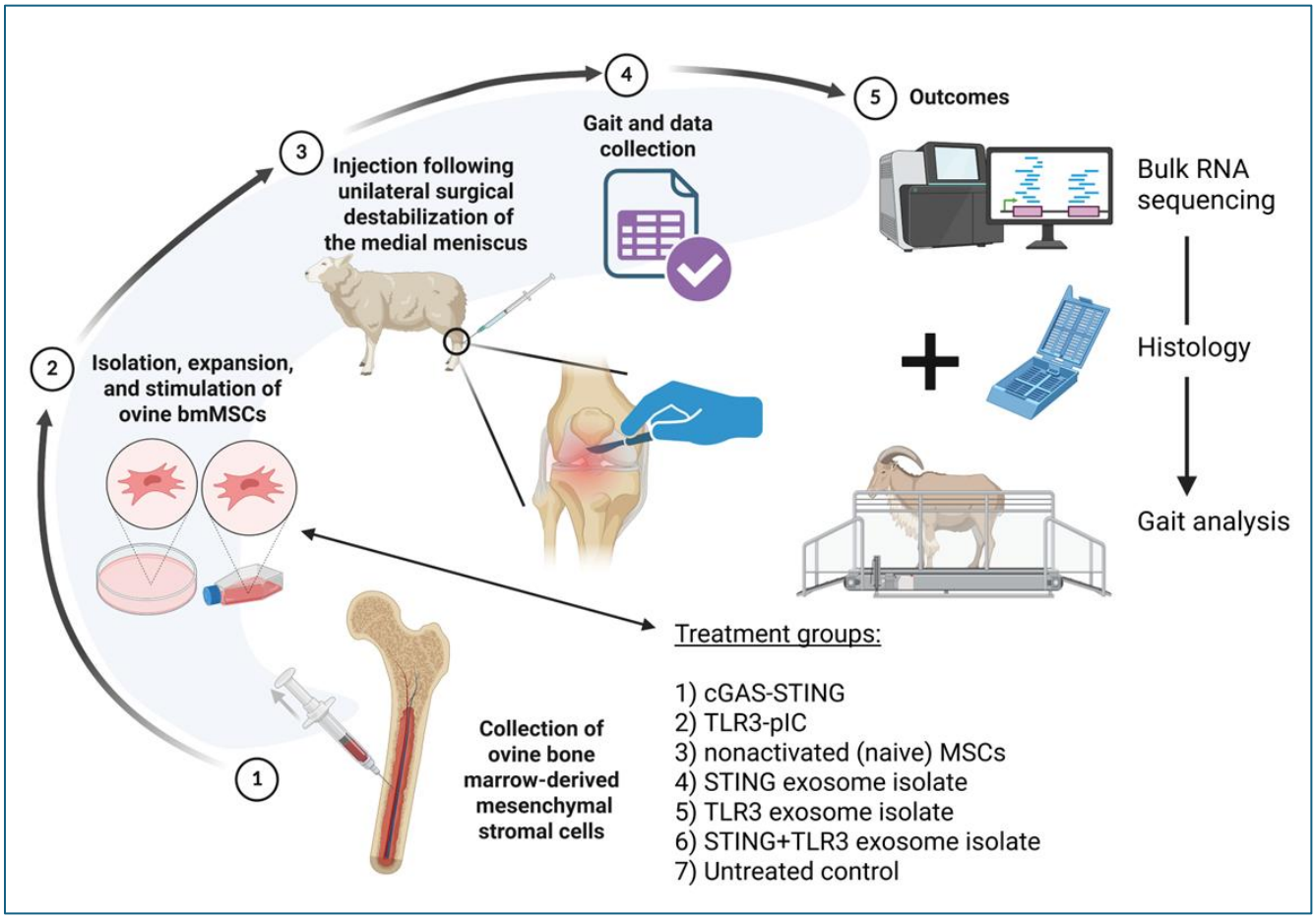

Made using Biorender.com.

Experiment 2: Investigation of alternate/adjunct ligands. The previously mentioned large animal ovine model utilizes treatment groups including a group of MSCs stimulated via their STING receptors to determine if the STING immune receptors yield beneficial clinical outcomes in a large animal ovine model of osteoarthritis. This study, as well as the above-mentioned murine OA study, included stimulation of two receptors each with only one of their respective ligands. This is critically important as the downstream gene expression pathways of MSC receptors such as STING-2'3'-cGAMP and TLR3-pIC are the product of a ligand specific bias – meaning that the secretome of these cells will vary dependent upon which ligand binds to the

receptor[10,11]. The exact number is challenging to quantify, but MSCs express many copies of each immune receptor at a time. However, it is unknown whether activating this receptor pool with more than one of their respective ligands is more advantageous in the context of wound repair. Based on this, we seek to further assess the costimulatory effects from stimulating the MSC's cGAS-STING receptors simultaneously with multiple ligands; as well as costimulation with other MSC receptors, such as TLR3 and TLR9. Whenever this receptor costimulation occurs, it is possible for the downstream products to interfere with each other and cause inhibitory, antagonistic, outcomes towards one or both receptor pathways. However, it is also possible for synergistic effects to occur and create a further enhanced MSC anti-inflammatory and reparative phenotype. Therefore, it is important to elucidate which ligands, receptors, and strategies are most effective for alleviating symptoms of osteoarthritis. This will be done by comparing the *in vitro* secretome of various co-stimulated MSC populations to the secretome of various MSC populations stimulated with only one of a variety of unique ligands – as this would provide greater insights into the modulatory, synergistic, or antagonistic gene pathway interactions influencing the secretome of these MSCs. These STING agonists include two bacterial cyclic dinucleotides (CDNs): 1) 2'3'-cGAMP, 2) 3'3'-cGAMP. Additionally, there are many synthetic agonists for STING, but only the two agonists ADU-S100 and SNX281 possess enough cross reactivity between humans and murine subjects for translational significance. No studies have been published regarding the interactions of these STING agonists with MSCs. Therefore, as these STING agonists have only been utilized in the context of oncology and tumor dynamics, this would be a novel methodology to further elucidate the ideal therapeutic agonism for MSC-STING receptors in the context of wound repair and regenerative medicine. These STING agonists have demonstrated powerful tumor reduction capabilities with nearly identical

mechanisms utilized in wound repair – which includes the enhanced production of potent type I interferons, IFN-β, TNF, and much more as previously mentioned in this thesis. To elucidate the optimal costimulatory grouping, the twelve treatment groups are proposed:

Table 3.2: Summary of proposed STING agonist costimulatory treatment groups.

Group	Agonist Grouping	Assessment
1	Media + cells only	Negative control
2	2'3'-cGAMP	Positive control Bacterial CDN
3	3'3'-cGAMP	Bacterial CDN
4	SNX281	Potent synthetic non-CDN agonist
5	2'3'-cGAMP + 3'3'-cGAMP	Strong + weak bacterial CDNs
6	2'3'-cGAMP + ADU-S100	Traditional STING ligand + potent synthetic CDN ligand
7	2'3'-cGAMP + SNX281	Traditional STING ligand + potent synthetic non-CDN ligand
8	2'3'-cGAMP + CpG-C	Traditional STING ligand + TLR9 ligand
9	2'3'-cGAMP + polyIC	Traditional STING ligand + TLR3 ligand
10	2'3'-cGAMP + CpG-C + polyIC	Traditional STING ligand + TLR9 ligand + TLR3 ligand
11	SNX281 + polyIC	Potent synthetic ligand + TLR3 ligand
12	SNX281 + CpG-C	Potent synthetic ligand + TLR9 ligand

The co-stimulation outcomes will be assessed according to the above grouping pairs. The subsequent secretome produced from these stimulations will be characterized via multiplex assay and western blot. Effective STING stimulation will be confirmed upon detection of IFN-β, CXCL10, and ISG15 – as IFN-β is a hallmark type I interferon produced as a result of STING

stimulation, and CXCL10 and ISG15 confirm IFN-β function as these are only produced following IFN-β stimulation. The secretome will additionally be analyzed for the presence of pro-inflammatory cytokines (IL-6, TNF-α, IL-1β, CCL2), immunomodulatory cytokines (IL-10, TGF-β, PGE2, IDO), and cytokines associated with extracellular matrix maintenance (MMP-13, ADAMTS-5, VEGF, BMP-2, TIMP-1/2). This quantification will determine if further costimulatory testing is warranted or to continue from an *in vitro* model to a rodent *in vivo* model. The study overview is provided in Figure 3.2.

Figure 3.2: Experiment 2. Schematic overview of study design for future directions – Investigation of alternate/adjunct ligands.

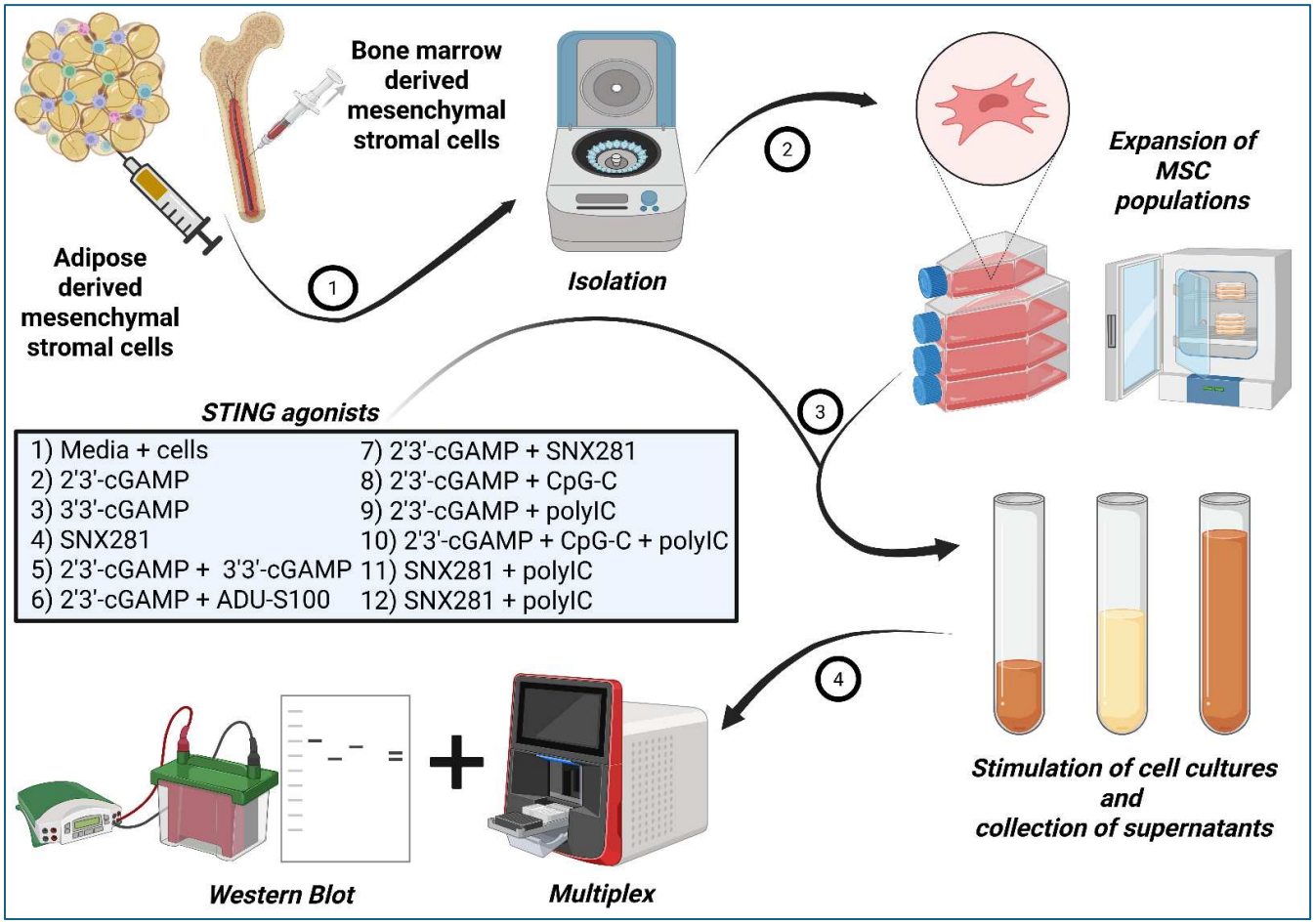

Made using Biorender.com.

Experiment 3: Assessment of secreted exosomes from MSC. Aside from cytokines, chemokines, growth factors, enzymes and antimicrobial peptides, one of the primary secretory products of MSCs and activated MSCs are extracellular vesicles (EVs)[12]. Made from endocytic budding of the cellular membrane – MSC EVs are class of compounds that have a diverse range of biological functions that pertain to the pathology of OA[13,14]. Therefore, we seek to further develop the exosomes secreted by STING-MSCs *in vitro*, with a follow up *in vivo* mouse model study to determine their efficacy as an exosome-based therapeutic for the alleviation of symptoms of osteoarthritis. To analyze this – an *in vitro* model analyzing the extracellular vesicle profile of MSC STING receptors with one or more agonists will be utilized. Extracellular vesicles are secreted by all cells and are notoriously challenging to isolate due to their heterogeneity, shared physical properties, and relatively small particle size[15]. The subsets of EVs can be further characterized by their size, including exosomes (~30-120nm), microvesicles (~100-1000nm), and apoptotic bodies (~500-3000nm)[15]. Isolation protocols for EVs implicate differences dependent upon the source of cells and their intended subsequent usage[15]. Therefore, the bulk *in vivo* characterization of these STING-MSC exosomes will be performed utilizing exosomes isolated from culture media via size exclusion chromatography (SEC), as this will be the technique used in the follow-up murine *in vivo* model. Additionally, this isolation technique is regarded for its high purity and low contamination results compared to other common exosome purification techniques, such as precipitation or ultracentrifugation, as the shear stress from ultracentrifugation can potentially damage the integrity of these exosomes and that is not ideal considering the goal of utilizing the exosomes in animal models of osteoarthritis. Although time consuming and complicated, SEC excels at separating exosomes from the soluble cytokines secreted directly from the MSCs, with minimal stress on the integrity of the exosomes[15,16]. To

assess the cytokine cargo of the isolated exosomes, they will be lysed, and the lysate will undergo a multiple analyte profiling via multiplex bead-based assay to simultaneously probe for a broad spectrum of cytokines. To understand the novel proteomic outcomes of STING-MSC receptor stimulation – an ELISA will be utilized to quantify the exosomal protein cargo compared to naïve control MSC exosomes, as well as detect the presence of contaminating proteins. Additionally, bulk RNA-seq will complement these findings by assessing the presence of and changes in cGAS-STING-MSC exosomal miRNA cargo, which are beyond the scope of this discussion. The study overview is provided in Figure 3.3.

Figure 3.3: Experiment 3. Schematic overview of study design for future directions – Assessment of secreted exosomes from MSCs.

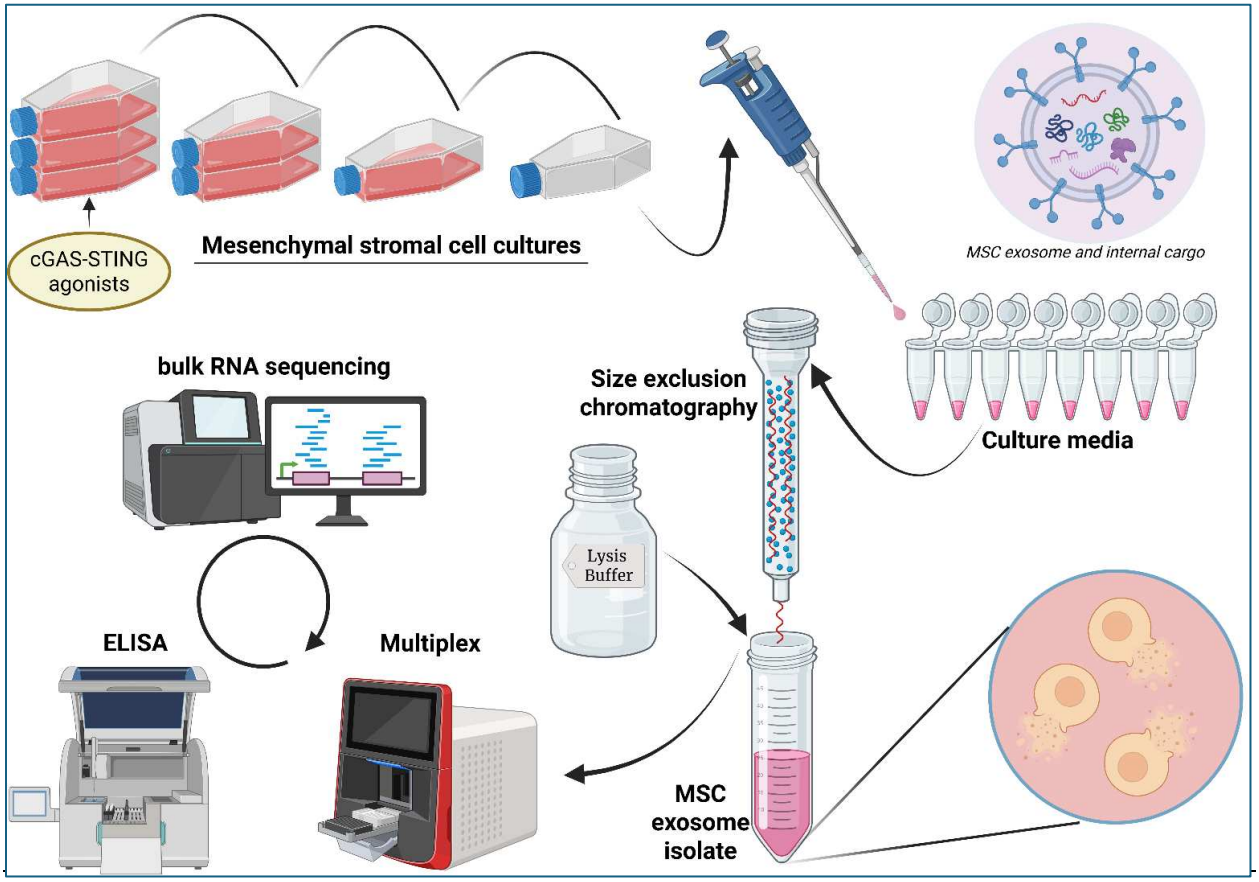

Made using Biorender.com.

Experiment 4: Integration of MSC-derived exosomes in hydrogel delivery devices. We hypothesize that the secretome of at least one of the cGAS-STING costimulated MSCs will produce more EVs, cytokines, and chemokines possessing anti-inflammatory and chondroprotective properties when compared to naïve or the cGAS-STING-MSCs stimulated with a single agonist. The results of this characterization determine which exosomes to investigate for their integration into a multifunctional medical hydrogel foam for usage in an *in vivo* mouse model of osteoarthritis. Upon further development of the hydrogel foam and MSC exosomes from the previously mentioned studies, the continuation study in this segment will involve combining the MF and STING-MSC exosomes to further refine a delivery mechanism for MSCs, their agonists, and their secretory products in an *in vivo* mouse model of osteoarthritis. Osteoarthritis will be induced in the murine stifle joint via destabilization of the medial meniscus. Immediately following surgery – the mice will be treated with one of the five groups: 1) Saline control, 2) MSCs, 3) MF hydrogel, 4) MSCs + exosomes (no MF hydrogel), and 5) MSCs + exosomes (in MF hydrogel). The results will be determined following functional gait analysis, transcriptomics, and histological assessment of the treated limbs. We hypothesize that this MSC and exosome infused hydrogel foam can improve distribution and enhance retention of MSCs and their exosomes within the desired joint spaces. To evaluate the integration and therapeutic potential of MSC-derived exosomes in the MF hydrogel system, in vitro assays will first characterize exosome quality, release kinetics, and bioactivity information. Exosomes will then be analyzed by nanoparticle tracking analysis, flow cytometry, and western blot for detection of specific protein markers – followed by release and stability testing from the hydrogel using fluorescently labeled EVs. Bioactivity of released exosomes will be assessed in

IL-1β-stimulated chondrocytes, fibroblasts, synoviocytes, and macrophage cultures by measuring cytokine suppression, matrix synthesis, and gene expression of well-characterized anabolic markers (COL2A1, ACAN, SOX9, COMP) and catabolic markers (MMP-3, MMP-13, ADAMTS4/5, COX2, IL-1β, TNF, and IL-6). Cellular uptake and viability assays will confirm delivery efficiency and safety. Therapeutic efficacy will be tested *in vivo* in the murine destabilization of the medial meniscus (DMM) osteoarthritis model through functional gait analysis, imaging, and OARSI histological scoring, along with cytokine and transcriptomic profiling of joint tissues. Clinically, the most effective exosome–hydrogel formulation would advance toward GLP safety testing and early-phase clinical evaluation to assess safety, retention, and joint function improvement in patients with osteoarthritis.

The final study in this series of follow-up studies will include combining all these described studies to evaluate the safety and efficacy of utilizing MSC/exosome infused multifunctional medical hydrogel foam in a large animal (ovine) model. Here, the hydrogel will be applied in the same manner as our murine OA studies, which is via intraarticular injection. To do this, we will again induce osteoarthritis via unilateral destabilization of the medial meniscus in ovine hind stifle (knee) joints and subsequently treat with one of the four treatment groups: 1) MSC + STING exosome infused MSC hydrogel, 2) MSC hydrogel, 3) exosome hydrogel, or 4) inert hydrogel. Based upon the results of prior studies to get to this point, we hypothesize that the therapeutically infused hydrogels will significantly improve the functional wound repair outcomes when compared to the inert hydrogels. The study overview is provided in Figure 3.4.

Figure 3.4: Experiment 4. Schematic overview of study design for future directions – Assessment of secreted exosomes from MSCs infused into a medical foam hydrogel in murine and ovine models.

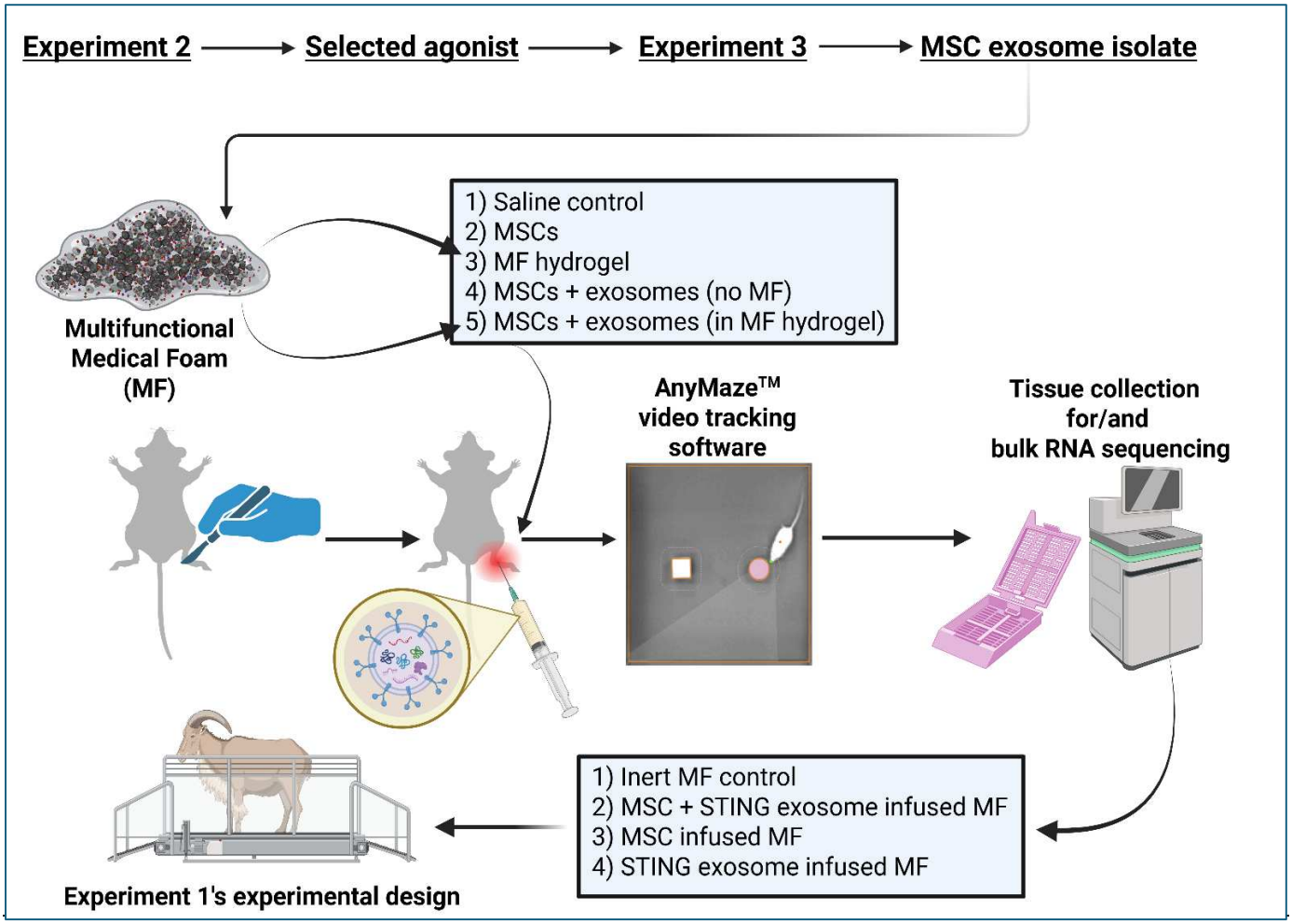

Made using Biorender.com.

Finally, different study directions that would further complement this research and refine these techniques are worthy of mention. Being that these MSCs are incredibly sensitive to all external and internal stimuli, it is important to further develop strategies to induce and promote homogenous populations[17,18]. Additionally, literature suggests that MHC compatibility studies can further improve the results of allogeneic MSC cell therapy, being that MHC mismatch between individuals does theoretically carry the exceedingly rare risk of immune complications,

especially with repeated dosing and chronic inflammation[19]. Lastly, further investigation is warranted to study the effect of different dose timing in respect to OA development (post-OA for example), as well as the differences of male and female treatment responses, as virtually no studies have yet to establish the existence (or non-existence) of different sex responses to MSC cellular therapy. This is important as research has suggested that male and female MSCs have inherently variable phenotypic profiles[20]. Potential sex-based differences in donor attributes or response to MSCs is a growing area of interest among stromal cell research. Studies have found that female MSCs are frequently more resistant to senescence, exhibit enhanced proliferative potential, release more growth factors and less pro-inflammatory cytokines when compared to male MSCs – as a few examples. These differences are commonly believed to be a result of varying levels of hormonal exposure[21]. However, other sex differences among MSCs have also been reported to not be exclusively dependent on sexual hormone exposure[21]. A few examples of this include an increased expression of CXCR4, IDO1, and PGE2 in female MSCs, as well as an increased expression of TNF, IL-1β, and IL-6 in male MSCs[22]. This indicates potential differences in receptor pathway signaling that may affect the therapeutic outcome quality due to observations that female MSCs express higher levels of TLR3 mRNA and that male MSCs express higher levels of TLR4 mRNA, for example. These higher levels of immune receptors suggest different sensitivities to their respective ligands – which can influence the downstream pathway signaling expression. This is important considering our above-mentioned murine OA study utilizing TLR3-pIC and STING-2'3'-cGAMP receptor activated MSCs used only male MSCs donated only to male mice.

In summary, our lab's work on murine osteoarthritis suggests that it has the potential to attenuate bothersome symptoms of osteoarthritis – indicated by the TLR3-pIC-MSC and STING-

2’3’-cGAMP -MSC treated mice demonstrating increased movement and decreased time sheltering in hut compared to the control groups, as well as significant improvements in histological scoring for the treatment groups. Additionally, TLR3-pIC-MSC significantly improved infection resolution in horses inoculated with staphylococcus aureus to induce septic arthritis in the tibiotarsal joint. To build upon these models – we will soon be utilizing an ovine OA model to establish the safety and efficacy of using these STING-2’3’-cGAMP activated MSCs as a treatment for osteoarthritis in a large animal model using the same methodology as the murine model, which is destabilization of the medial meniscus to induce osteoarthritis.

References

1. Abramoff, B. & Caldera, F. E. Osteoarthritis: Pathology, diagnosis, and treatment options. *Med. Clin. North Am.* **104**, 293–311 (2020).

2. Lees, P. Pharmacology of drugs used to treat osteoarthritis in veterinary practice. *Inflammopharmacology* **11**, 385–399 (2003).

3. Ma, W., Chen, H., Yuan, Q., Chen, X. & Li, H. Global, regional, and national epidemiology of osteoarthritis in working-age individuals: insights from the global burden of disease study 1990-2021. *Sci. Rep.* **15**, 7907 (2025).

4. Hu, C. & Li, L. Preconditioning influences mesenchymal stem cell properties in vitro and in vivo. *J. Cell. Mol. Med.* **22**, 1428–1442 (2018).

5. Afflerbach, A.-K., Kiri, M. D., Detinis, T. & Maoz, B. M. Mesenchymal stem cells as a promising cell source for integration in novel in vitro models. *Biomolecules* **10**, 1306 (2020).

6. Pirosa, A. *et al.* Modeling in vitro osteoarthritis phenotypes in a vascularized bone model based on a bone-marrow derived mesenchymal cell line and endothelial cells. *Int. J. Mol. Sci.* **22**, 9581 (2021).

7. Rowland, A. L. *et al.* In vitro MSC function is related to clinical reaction in vivo. *Stem Cell Res. Ther.* **9**, 295 (2018).

8. Tian J.-Y. *et al.* Establishment and evaluation strategy of an in vitro cell model of bone marrow microenvironment injury in mouse acute graft-versus-host disease. *Zhongguo Shi Yan Xue Ye Xue Za Zhi* **32**, 617–624 (2024).

9. Kim, N. & Cho, S.-G. New strategies for overcoming limitations of mesenchymal stem cell-based immune modulation. *Int. J. Stem Cells* **8**, 54–68 (2015).

10. Chen, Y., Lin, J., Zhao, Y., Ma, X. & Yi, H. Toll-like receptor 3 (TLR3) regulation mechanisms and roles in antiviral innate immune responses. *J. Zhejiang Univ. Sci. B* **22**, 609–632 (2021).

11. Zhang, Z. *et al.* Multifaceted functions of STING in human health and disease: from molecular mechanism to targeted strategy. *Signal Transduct. Target. Ther.* **7**, 394 (2022).

12. Tan, F. *et al.* Clinical applications of stem cell-derived exosomes. *Signal Transduct. Target. Ther.* **9**, 17 (2024).

13. Bao, C. & He, C. The role and therapeutic potential of MSC-derived exosomes in osteoarthritis. *Arch. Biochem. Biophys.* **710**, 109002 (2021).

14. Kou, M. *et al.* Mesenchymal stem cell-derived extracellular vesicles for immunomodulation and regeneration: a next generation therapeutic tool? *Cell Death Dis.* **13**, 580 (2022).

15. Dilsiz, N. A comprehensive review on recent advances in exosome isolation and characterization: Toward clinical applications. *Transl. Oncol.* **50**, 102121 (2024).

16. Kim, J. Y. *et al.* Defined MSC exosome with high yield and purity to improve regenerative activity. *J. Tissue Eng.* **12**, 20417314211008624 (2021).

17. Song, Z., Banks, R. W. & Bewick, G. S. Modelling the mechanoreceptor's dynamic behaviour. *J. Anat.* **227**, 243–254 (2015).

18. Li, J. *et al.* The heterogeneity of mesenchymal stem cells: an important issue to be addressed in cell therapy. *Stem Cell Res. Ther.* **14**, 381 (2023).

19. Cequier, A. *et al.* The systemic cellular immune response against allogeneic mesenchymal stem cells is influenced by inflammation, differentiation and MHC compatibility: in vivo study in the horse. *Front. Vet. Sci.* **11**, 1391872 (2024).

20. Maged, G., Abdelsamed, M. A., Wang, H. & Lotfy, A. The potency of mesenchymal stem/stromal cells: does donor sex matter? *Stem Cell Res. Ther.* **15**, 112 (2024).

21. Bianconi, E. *et al.* Sex-specific transcriptome differences in human adipose mesenchymal stem cells. *Genes (Basel)* **11**, 909 (2020).

22. Mckinnirey, F., Herbert, B., Vesey, G. & McCracken, S. Immune modulation via adipose derived Mesenchymal Stem cells is driven by donor sex in vitro. *Sci. Rep.* **11**, 12454 (2021).